DYNAMIC CHANGES IN COLLAGEN ORGANIZATION MODULATE CERVICAL REMODELING DURING PREGNANCY AND PARTURITION: NEW INSIGHTS AND THE POTENTIAL FOR IMPROVED CLINICAL TOOLS TO COMBAT PRETERM BIRTH

APPROVED BY SUPERVISORY COMMITTEE

Mala Mahendroo, Ph.D.

Rolf Brekken Ph.D.

Hiromi Yanagasawa M.D., Ph.D.

Rashmin Savani M.B, Ch.B.

DEDICATION

I wish to dedicate this dissertation to Noah Jacob Rusche, Jackson Roy Gilbert and Kenlee Grace Gilbert. Whose all too short time on this Earth illustrates the critical need for the research herein.

DYNAMIC CHANGES IN COLLAGEN ORGANIZATION MODULATE CERVICAL REMODELING DURING PREGNANCY AND PARTURTION: NEW INSIGHTS AND THE POTENTIAL FOR IMPROVED CLINICAL TOOLS TO COMBAT PRETERM BIRTH

by

MEREDITH LYNNE AKINS

DISSERTATION

Presented to the Faculty of the Graduate School of Biomedical Sciences

The University of Texas Southwestern Medical Center at Dallas

In Partial Fulfillment of the Requirements

For the Degree of

DOCTOR OF PHILOSOPHY

The University of Texas Southwestern Medical Center at Dallas

Dallas, Texas

August, 2011

AKNOWLEDGEMENTS

I would like to thank my mentor, Mala Mahendroo, for allowing me the privilege of becoming her first graduate student. I could not have completed this work without her guidance, knowledge, patience and support. I would also like to thank my committee, Drs. Rolf Brekken, Hiromi Yanagasawa and Rashmin Savani for their optimistic guidance and encouragement during the past five years.

I am very thankful for all the members of the Mahendroo lab, both past and present, for contributing to my scientific education and for their friendship. Above all, I could not have finished this work without the love and support of my family. My husband, my wonderful daughters, my parents and siblings and my in-laws- thank you for always believing in me, your love and support carries me through all my hardships and successes.

DYNAMIC CHANGES IN COLLAGEN ORGANIZATION MODULATE CERVICAL REMODELING DURING PREGNANCY AND PARTURTION: NEW INSIGHTS AND THE POTENTIAL FOR IMPROVED CLINICAL TOOLS TO COMBAT PRETERM BIRTH

MEREDITH LYNNE AKINS, Ph.D.
The University of Texas Southwestern Medical Center at Dallas, 2011

MALA MAHENDROO, Ph.D.

Preterm birth affects approximately 500,000 infants in the United States alone and is the second highest cause of infant morbidity in this country. Obstetricians still do not have reliable tools to diagnose or treat women presenting with premature labor. Understanding mechanisms by which the cervix remodels during term and preterm pregnancy is critical to formulate better methods for detection and treatment of preterm birth. The focus of this study was to identify

how cervical collagen is reorganized throughout pregnancy to allow the cervix to become compliant for parturition. Beginning early in pregnancy a reduction in cervical collagen cross-links as well as a decline in matricellular proteins contribute to the changing cervical extracellular matrix environment. These cumulative changes result in increased collagen fibril diameter, as well as a progressive increase in tissue distensibility and a decline in tissue stiffness. Changes in collagen morphology over pregnancy can be visualized via non-invasive second harmonic generation (SHG). Quantification of specific morphological features such as collagen fiber diameter or porosity reveal progressive changes that allow one to distinguish stages in pregnancy. In addition, analysis of SHG images from two preterm birth models as well as one postterm pregnancy model validate the ability to use quantitative morphological measurements to distinguish normal from abnormal cervical remodeling. These findings suggest SHG technology is a powerful tool that may have potential clinically to predict preterm birth. In closing these studies have identified early and progressive changes in processing and assembly of collagen fibrils as well as changes in other ECM components that likely contribute to the incremental change in cervical tensile strength required for birth.

TABLE OF CONTENTS

PRIOR PUBLICATIONS

Akins, M., Luby-Phelps, K., Bank, R.A., Mahendroo, M. 2011. Cervical Softening During Mouse Pregnancy- Regulated Changes in Collagen Fibril Assembly and Composition of Matricellular Proteins. Biology of Reproduction. 84(5):1053-1062.

Holt, R., Timmons, B.C, Akgul, Y., **Akins, M.,** Mahendroo, M. 2010. The Molecular Mechanisms of Cervical Ripening Differ Between Term and Preterm Birth. Endocrinology. 152(3):1036-1046.

Timmons, B. **Akins, M**. Mahendroo, M. 2010. Cervical Remodeling During Pregnancy and Parturition. Trends in Endocrinology Metabolism. Jun; 21(6):353-361.

Akins, M. Luby-Phelps, K. Mahendroo, M. 2010. Second Harmonic Generation Imaging as a Potential Tool for Staging Pregnancy and Predicting Preterm Birth. Journal of Biomedical Optics. Mar-Apr;15(2):0260201-0260210.

Yousefi, S., Kehtarnavaz, N., **Akins, M.,** Luby-Phelps, K., Mahendroo, M. Distinguishing Different Stages of Mouse Pregnancy using Second Harmonic Generation Images. Conference proceedings : ... Annual International Conference of the IEEE Engineering in Medicine and Biology Society. IEEE Engineering in Medicine and Biology Society. Conference Sept. 2010:5314-5317.

Park, J. Maines, J. **Williams, M**. McKearin, D. 2007. Stonewalling Drosophilla Stem Cell Differentiation by Epigenetic Controls. Development. Apr; 134(8):1471-9.

LIST OF FIGURES

LIST OF TABLES

LIST OF ABBREVIATIONS

5αR1	5-alpha Reductase Type 1
ADAMTS	A Disintegrin-like and Metallopeptidase (Reprolysin Type) with Thrombospondin Type 1 Motif
ANOVA	Analysis of Variance
ART	Assisted Reproductive Technologies
BAPN	Beta-Aminopropionitrile
BMI	Body Mass Index
BMP-1	Bone morphogenic protein -1
C-	Carboxy
Col1a1	Collagen I alpha1
Col3a1	Collagen III alpha1
Col5a1	Collagen V alpha 1
DCN	Decorin
DDR	Discoid Domain Receptor
ECM	Extracellular Matrix
ER	Endoplasmic Reticulum
F/B	Forward to Backward Ratio
F+B	Forward plus Backward (Total Intensity)
FACIT	Fibril-Associated Collagens with Interrupted Triple Helices
GAG	Glycosaminoglycan

HP	Hydroxylysylpyridinolines
HPLC	High Pressure Liquid Chromatography
IL-1	Interleukin 1
IL-6	Interleukin 6
IL-8	Interleukin 8
IVF	In vitro Fertilization
LAP	Latency-Associated Protein
LOX	Lysyl Oxidase
LP	Lysylpyridinolines
LPS	Lipopolysaccharide
LTBP	Latent TGF Beta Binding Protein
MIP2	Macrophage Inflammatory Protein 2-alpha
MMP	Matrix Metalloproteinase
N-	Amino
NIR	Near Infrared
NP	Nonpregnant
PCOLCE	Procollagen C-endopeptidase enhancer protein
PDI	Protein Disulfide Isomerase
PG	Proteoglycan
PLOD	Procollagen-Lysine, 2-Oxoglutarate 5-Dioxygenase
PPROM	Preterm Premature Rupture of Membranes

PTGS2	Prostaglandin-Endoperoxide Synthase 2
QPCR	Quantitative Polymerase Chain Reaction
SERPINH1	Serine (or Cysteine) Peptidase Inhibitor, Clade H, Member 1
SHG	Second Harmonic Generation
SLRP	Small Leucine Rich Proteoglycan
SP-A	Surfactant Protein A
SPARC	Secreted Protein Acidic and Rich in Cysteine
TEM	Transmission Electron Microscopy
TGFβ	Transforming Growth Factor Beta
THBS	Thrombospondin
TLL-1	Tolloid Like Receptor 1
TNC	Tenascin C
TNFα	Tumor Necrosis Factor alpha
WT	Wild Type

Chapter 1 Introduction and Review of Literature

1.1 Overview of Parturition

1.1.1 Introduction

Parturition, the process of birth, is initiated towards the end of the 40-week human pregnancy. It relies on coordinated uterine contractions as well as cervical dilation, in order for successful birth to occur. While the cervix undergoes active tissue remodeling from the beginning of pregnancy, the structural integrity of the cervix remains intact until labor is initiated and cervical dilation takes place. In contrast, the uterus remains dormant until labor signals initiate coordinated contractions. These contractions increase in strength and duration leading to the expulsion of the fetus from the uterus, which then passes through the dilated cervix and birth canal. While parturition has been profusely studied, the exact biochemical events leading to initiation are poorly understood. However, it is known that a complex series of hormonal events from maternal and fetal origin lead to biochemical changes in the cervical and the uterine environment leading to the initiation of parturition.

1.1.2 Biochemical regulation of Parturition

During gestation the progesterone to estrogen ratio remains high. The steroid hormone progesterone is important for maintenance of pregnancy (i.e. uterine quiescence and anti-inflammatory pathways) while high estrogen action promotes uterine contractility and processes involved in labor and birth. In many

mammals, including mouse, serum progesterone drops just prior to birth suggesting that progesterone withdrawal is important in initiating labor (Virgo and Bellward, 1974). This is supported by the fact that parturition is blocked in mice administered progesterone at term and in mice lacking steroid 5-alpha reductase 1, a steroid hormone important in progesterone metabolism (Costa and Csapo, 1959; Csapo and Lloyd-Jacob, 1961; Mahendroo et al., 1996; Mahendroo et al., 1999). In addition, loss of progesterone function by mifepristone, a progesterone receptor antagonist, will cause spontaneous abortions in all mammals studied to date including humans (Cunningham et al., 2010a). In humans, serum progesterone levels and expression of progesterone receptor remain high at the time of birth. Since production of progesterone takes place in the human placenta, levels of progesterone subsequently fall post partum. It is postulated that preceding birth there is a functional drop in progesterone due to changes in progesterone catabolizing enzymes, altered levels of progesterone receptor coactivators and/or changes in the ratio of specific progesterone receptors (Mahendroo et al., 1999; Condon et.al., 2003; Condon et.al. 2006; Andersson et al., 2008; Cunningham et al., 2010a).

Prostaglandins have long been used in the clinic to induce cervical dilation in women who have uterine contractions but lack cervical dilation. Prostaglandins are derived from arachidonic acid via cyclooxygenase enzymes and are involved in wound healing by stimulating pro and anti-inflammatory pathways (Ricciotti

and FitzGerald, 2011). Treatment with prostaglandins will induce labor at all stages of pregnancy (Cunningham et al., 2010a). Prostaglandins also play a role in stimulating uterine contractions and are produced by the myometrium during labor. They are produced in fetal membranes, uterus, placenta, and amniotic fluid. It is present in amniotic fluid during all stages of gestation, but is greatly increased at term (Cunningham et al., 2010a). Studies have shown that the connective tissue of the cervix is similar to that of a normally ripened cervix when given prostaglandin treatment (Uldbjerg et al., 1983; Rath et al., 1993; Feltovich et al., 2005). While prostaglandins can successfully remodel the cervix and cause uterine contractions, it is not clear whether these molecules play a role in normal cervical ripening. For instance, intercourse during pregnancy exposes the cervix to high levels of prostaglandins in semen, however studies fail to link intercourse to cervical ripening or preterm birth (Platz-Christensen et al., 1997; Schaffir, 2006).

The fetus also provides signals to the maternal interface that may cause the initiation of labor. Uterine stretch from fetal growth is postulated to activate labor. Fetal growth in the restricted uterus puts stress on the myometrium causing changes in the gap junction protein connexin-43 and an increase in oxytocin receptors. During fetal lung maturation the fetus produces increasing amounts of a molecule called surfactant protein A (SP-A). Term levels of SP-A have been

shown to promote uterine contractility and prostaglandin synthesis in the uterus acting as possible initiator of labor (Cunningham et al., 2010a).

1.1.3 Conclusion

The exact mechanisms of initiation of labor remain unknown. During gestation many body systems and pathways are utilized to maintain the pregnancy. Due to the complex interactions of hormones, fetal signals, and the maternal reproductive tract, a single initiating switch is unlikely.

1.2 Premature Birth

1.2.1 Introduction

In 2007, 12.7% of all births in the United States were preterm. This represents approximately 500,000 infants born premature each year (Martin, 2011). Preterm birth is defined as birth before 37 weeks of the 40-week gestation. This is further categorized into very preterm birth (less than 32 weeks), moderately preterm (32-34 weeks) and late preterm (34-36 weeks). Infants that are born before 37 weeks of gestation are ill equipped to deal with life outside the womb and suffer from chronic disabilities and increased morbidity (Preterm Birth: Causes, Consequences, and Prevention, 2007). In fact, preterm birth is the 2nd leading cause of infant fatality during the first year of life in the United States (Mathews and MacDorman, 2010). Deaths of premature infants are largely due to systematic organ immaturity and failure (Cunningham et al., 2010c). Large-scale organ immaturity also causes short-term and/or chronic medical conditions in

surviving premature infants. Common complications include respiratory, mental, cardiac and system retardations (Cunningham et al., 2010c). While there has been much improvement in survival of preterm infants, costs of caring for these infants are rising. Due to the high occurrence of medical complications total medical costs of caring for premature infants and their mothers are estimated to be around $26 billion annually or approximately $52,000 per infant (Preterm Birth: Causes, Consequences, and Prevention, 2007).

Although considerable research has been focused on understanding the underlying mechanisms of preterm birth, there is currently an inability to accurately diagnose or predict or treat women at risk for premature labor. Diagnosis and treatment is complicated by the fact that there are many causes and risk factors for preterm birth.

1.2.2 Risk Factors

Causes of preterm birth are broken down into three categories: spontaneous labor, preterm premature rupture of membranes (PPROM) and medically induced. Medically induced preterm birth accounts for 25-30% of all preterm birth, while PPROM and spontaneous preterm birth account for the remaining 70-75% (25% and 45% respectively). Thus, the majority of cases are idiopathic (Meis et al., 1998; Preterm Birth: Causes, Consequences, and Prevention, 2007; Goldenberg et al., 2008).

While direct mechanistic causes of spontaneous preterm birth remain elusive, a variety or risk factors have been identified. Risk factors may provide important clues in unraveling the causes and mechanisms that initiate preterm labor. They can be sorted into the following categories: medical, demographic and lifestyle.

Medical

Previous history of preterm birth is one of the strongest indicators for a subsequent preterm birth. Women with a previous preterm birth have a two-fold higher chance of having a second preterm birth (Spong, 2007). Interpregnancy intervals also play a role in the likelihood of preterm birth. Women who become pregnant less than 6 months after birth are 2-times more likely to deliver preterm. Some studies postulate that the uterine environment still contains immune cells responsible for postpartum repair, which lays a foundation for a weaker uterus and cervix, while others think the nutritional levels of the mother are too depleted to carry another pregnancy to term (Adams et al., 2000; Conde-Agudelo et al., 2006; Goldenberg et al., 2008).

Proper nutrition as well as low and high BMI (body-mass index) are all related to preterm birth outcomes. Women with a low BMI pre-pregnancy have a high incidence of preterm birth (Mercer et al., 1996; Han et al., 2011). Obese women have been shown to have a lower incidence of preterm birth, possibly due to increased nutrition for the fetus. However, obesity is associated with low birth

weight due to size restriction and a higher risk for pre-eclampsia, which is responsible for 40% of medically-induced preterm birth (Iams, 2003; Preterm Birth: Causes, Consequences, and Prevention, 2007; Goldenberg et al., 2008).

Multiple gestations are a risk factor for preterm birth most likely due by overstretching of the uterus. Sixty percent of twins are premature and 40% of those cases are due to spontaneous preterm labor (Goldenberg et al., 2008). Assisted reproductive technologies (ART) such as in vitro fertilization (IVF) have increased the amount of multiple births in the U.S. In 2008, 3% of all live births were due to ART. Of these, 68.4% were singleton births and 31.6% were two or more fetuses (2008 Assisted Reproductive Technology Success Rates: National Summary and Fertility Clinic Reports, 2010). ART itself is a risk factor for preterm birth. Singleton ART pregnancies have a greater risk for preterm birth then naturally conceived singleton pregnancies. This may be explained partially by the fact that more than 50% of ART is performed on woman over 35, since preterm birth rates are increased in women over 35 (Preterm Birth: Causes, Consequences, and Prevention, 2007)

Infection and the associated inflammatory pathways are undeniably one of the most studied risk factors for preterm birth. Both uterine and lower-genital tract infections are related to preterm birth (Meis et al., 1995; Preterm Birth: Causes, Consequences, and Prevention, 2007). Intrauterine infections are prevalent in women who deliver preterm. Positive cultures of both the fetal membranes and

the amniotic fluid have been found in 70% and 30% of women, respectively, who give birth before 30 weeks (Iams, 2003). The most frequent access point for bacteria into the amniotic cavity arrives via ascension from the vagina (Goldenberg et al., 2008). The most common form of lower- genital infection at both 24 and 28 weeks of pregnancy is bacterial vaginosis. This occurs when the normal flora of the vagina is compromised and switched to gram-negative (anaerobic) bacteria. Bacterial vaginosis is associated with a 2-fold higher risk of preterm birth (Meis et al., 1995). Infection activates inflammatory cascades leading to degradation of fetal membranes (PPROM) as well as contractions of the uterus (Preterm Birth: Causes, Consequences, and Prevention, 2007). Despite an established role of infection in preterm birth, administration of antibiotics has not proven to be an effective therapy (McDonald et al., 2007; Iams et al., 2008).

Preterm birth has been observed to run in families. A large disparity of the occurrence of preterm birth exists between racial groups. Several inheritable diseases have a high risk of preterm birth associated with them including, Ehlers-Danlos Syndrome and osteogenesis imperfecta. All these findings suggest a potential role for genetics in preterm birth (Varner and Esplin, 2005; Goldenberg et al., 2008; Anum et al., 2009a; Anum et al., 2009b). Many studies have tried to evaluate a role for genetic inheritance or gene-environment interactions in preterm birth. While no one gene is likely to be a positive marker for preterm birth,

combinations of genetic and epigenetic screens may one day give a highly correlative screen for people at risk for preterm birth.

A premature shortening of the internal os of the cervix at 24 weeks gestation is a risk factor for preterm birth. Iams *et. al.* used transvaginal ultrasound to investigate cervical length in relation to preterm birth (Iams et al., 1996). The mean cervical length is 34 mm at 24 weeks of gestation. The risk of preterm birth scales proportionally the further you decrease from the mean cervical length. There is a 14-fold higher risk for preterm birth with a cervix that is 13 mm at 24 weeks. Cervical lengths are not predictive when measured before 16 weeks and have a greater positive predictive value in women with a history of preterm birth as compared to nulliparous women (Iams, 2003). While the biological causes of premature cervical shortening are unknown, a short cervix may indicate an incompetent cervix, or a cervix that remodels and dilates too early in pregnancy.

Demographic

There is a large disparity in rates of preterm birth between different ethnicities (Meis et al., 1998; Adams et al., 2000). While the national average of preterm birth is 12.7%, the percentage of preterm births in African American women in the United States is 18.1% while Asians have lowest at percentage at 10.8% (Mathews and MacDorman, 2010). Meis *et. al.* report that being of African decent makes woman over 4 times more likely to have preterm birth (Meis et al.,

1998). There are several explanations for the disproportion of African American preterm birth. One explanation is that African American women have a higher incidence of bacterial vaginosis (Goldenberg et al., 1996a). Several groups have also shown polymorphisms in genes associated in the immune response including cytokines and toll-like receptors in women of African descent (Varner and Esplin, 2005; Anum et al., 2009b).

Poor socioeconomic standing has been linked to a higher incidence of preterm birth (Mercer et al., 1996; Meis et al., 1998). The reasoning behind this finding is largely not understood. One probable cause is less access to prenatal care, which has also been shown to be a risk factor for preterm birth (Mercer et al., 1996). Recent work has shown that minority women living in low socioeconomic neighborhoods had a decline in preterm birth rates when enrolled in a program to assist with proper prenatal care (Leveno et al., 2009). This suggests that the correlation between low economic status and preterm birth rates may have more to do with preventative medicine than actual living condition. More research into the causes of this correlation is required.

Both young and advanced maternal age correlates with an increased risk for preterm birth. Women below 16 or older than 35 years have an increased incidence of preterm birth (Mercer et al., 1996; Meis et al., 1998; Adams et al., 2000).

Lifestyle

Smoking has been linked to an increased incidence of preterm birth. Deitz *et. al*., attributed smoking to the cause of 5-8% of early preterm births and 3-4% of late preterm births in 2002. They also showed a dose response of number of cigarettes smoked per day to poorer pregnancy outcomes and increased infant mortality (Dietz et al., 2010). Smoking is related to several placental abnormalities presumably due to the vasoconstrictor properties of nicotine. Other than preterm birth smoking is associated with an increase risk for fetal growth restriction, low birth weight, and perinatal morbidity (Andres and Day, 2000; Goldenberg et al., 2008). Drug use has also been associated with preterm birth. Some recreational drugs such as methadone and cocaine have been marginally correlated with a higher risk for preterm birth; however, more studies are needed to address these risks (Savitz and Murnane, 2010; Cleary et al., 2011). Despite the numerous studies trying to connect alcohol to preterm birth, alcohol use has not been linked to an increased risk of preterm birth (Meis et al., 1998; Savitz and Murnane, 2010).

These risk factors implicate multiple causes and pathways of preterm birth including: immune responses seen in infections, genetic components and polymorphisms, proper nutrition, stretch capacity of the uterus and competence of the cervix. However, these risk factors can only account for 50% of preterm births with the rest having unknown etiologies. This underlies the fact that

understanding the cause or causes premature birth is an extremely complex problem.

1.2.3 Diagnosis/Treatment/Prevention

Diagnositics

A reduction in preterm birth rates will require more reliable detection and treatment methods. Currently, clinical diagnostics have low positive predictive values and detect risk factors past the point where treatment will be beneficial.

As previously stated, a short cervix is a risk factor for premature birth. Cervical length can easily be measured by sonography or ultrasound (Iams et al., 1996). The probability of experiencing preterm birth rapidly increases as cervical length declines from 30 mm (Iams et al., 1996). Many studies have been carried out confirming the efficacy and prediction value of cervical length (Kagan et al., 2006; Celik et al., 2008). Positive prediction power is much higher in women with a history of previous preterm birth than nulliparous women (de Carvalho et al., 2005). While routine cervical length screening is not currently done in clinic, some studies suggest it may be cost effective when taking to account the extreme cost of premature birth (Werner et al., 2010).

Fetal fibronectin, a glycoprotein produced at the fetal/maternal interface, is a protein of interest as a biomarker for preterm birth. Lockwood first proposed fibronectin as a marker for preterm birth after visualizing fibronectin in cervicovaginal secretions in women who presented with PPROM or preterm labor

(Lockwood et al., 1991). Fibronectin can easily be measured in vaginal secretions, which makes it a great target for diagnostics. Several other studies have correlated high levels of fetal fibronectin with preterm birth especially early (before 28 weeks) preterm birth (Nageotte et al., 1994; Goldenberg et al., 1996b; Goldenberg et al., 2000; Honest et al., 2009). In clinic, tests that are negative for fetal fibronectin are indicative of not going into premature labor. A positive fibronectin test in clinic does not necessarily indicate impending preterm labor. Thus the positive predictive value of this test is low.

Prevention/Treatment

Historically, bed rest is the most prescribed prevention method for women who are deemed at risk for preterm birth (Sosa et al., 2004; Maloni, 2010). However, there is currently no correlation between bed rest and avoidance of preterm birth (Sosa et al., 2004; Spong, 2007).

A cerclage is a drastic invasive procedure that involves stitching the cervix closed to prevent preterm birth. It is used on women that have a short cervix and/or who have a history of cervical insufficiency or mid-trimester losses (Cunningham et al., 2010c). The effectiveness of cerclages has been debated. Several recent studies have shown that cerclages do in fact reduce preterm birth in women that have a short cervix with a history of preterm birth and in women who have had a previous preterm birth (Honest et al., 2009; Owen et al., 2009; Berghella et al., 2011). However, the rate of reduction is only 30% (Berghella et

al., 2011). It is still debated whether or not cerclage is beneficial in women with short cervix alone, or other risk factors for preterm birth. As with any invasive procedure, there are risks associated with cerclage including infection and rupture of membranes, both of which can exacerbate premature labor. From a biomechanical standpoint, it is thought that cerclages may or may not help to strengthen a weak cervix. Most of the force exerted on the uterus is centralized at the internal os, however, most cerclages are placed at the median of the cervix, allowing no structural support where support is needed (House and Socrate, 2006).

Given the rationale that progesterone supports pregnancy, while loss of progesterone function induces parturition, many studies have focused on the efficacy of using progesterone therapies (creams/gels/injections) on women at risk for preterm birth with varying success (Spong, 2007). Because progesterone therapies work to prolong labor in animals that exhibit progesterone withdrawal, it is possible that progesterone may stop the progression of labor in humans that exhibit only a functional withdrawal of progesterone. Meis using progesterone injections and Da Fonseca using progesterone suppository both show that progesterone treatment in woman with previous spontaneous preterm birth is capable of preventing preterm birth. (da Fonseca et al., 2003; Meis et al., 2003). Progesterone therapy has also proved beneficial for women with short cervix (less than 15 mm at 22 weeks of gestations) (Fonseca et al., 2007). Most recently,

Hassan tested the efficacy of a vaginal progesterone gel in women with shortened cervix. 5.7% of women receiving progesterone delivered before 33 weeks of gestation compared to 13% delivery in placebo group. Infants with mothers who received progesterone treatment also had significantly less medical complications (Hassan et al., 2011). Currently, there are no adverse affects to infants associated with progesterone treatment (Spong, 2007). While progesterone therapy appears to be useful in some subsets of preterm birth, it is not effective in all risk groups. Multiple studies show no effect when given to women carrying multiple fetuses (Rouse et al., 2007; Caritis et al., 2009). Also, in women with PPROM, progesterone treatment is unable to prolong gestation (Briery et al., 2011). Given the high levels of circulating progesterone, the mechanism by which progesterone therapy reduces preterm birth remains unclear.

Overall, treatment and prevention are very limited because all causes have not yet been identified. Preterm birth risk is not identified until a woman shows signs of premature labor. Diagnostics must be improved to detect preterm birth risk at an early enough time point for intervention. A deeper understanding of the molecular mechanisms that attribute to preterm birth must also be understood in order to develop specialized treatments that could be administered after early detection in order to reduce the incidence of preterm birth worldwide.

1.2.4 Conclusion

Our understanding of risk factors leading to the initiation of premature labor is incomplete. By understanding the mechanisms that take place during normal pregnancy and through studying animal models of preterm birth, we can better understand how to combat preterm birth, both by early detection and improved treatments.

1.3 Birth and the Cervix

1.3.1 Introduction

While the mechanisms that bring about initiation of birth are not completely clear, it is known that both coordinated uterine contractions and complete cervical dilation are essential to successful birth. In term and preterm birth, cervical remodeling precedes uterine contractions by several weeks in women who will deliver preterm (Iams et al., 1996). Furthermore, during cervical insufficiency, in the absence of uterine contraction, premature birth still occurs (Cunningham et al., 2010b). In the mouse, failure of the cervix to remodel, even in the presence of progressive uterine contractions, prevents birth from occurring (Mahendroo et al., 1999). These observations highlight the importance of properly regulated cervical remodeling during pregnancy and delivery.

1.3.2 Anatomy and Composition of the Cervix

The cervix is a dense region of connective tissue making up the most distal region of the uterus, which opens into the birth canal. While it was once thought

to be simply an extension of the uterus we now know it has a distinct composition and independent actions that play important roles in maintaining pregnancy as well as advancing labor. The connective tissue of the cervix is constantly in flux and reorganizes itself during the menstrual cycle, to aid in fertilization, and during pregnancy, to maintain integrity of the pregnancy but also to prepare for labor and birth (Leppert, 1995; Kershaw et al., 2007; Timmons et al., 2010).

The cervix is made up of an epithelium and dense internal stroma (Figure 1-1). The cervical epithelium serves as a protective barrier against invading microbes and impending infection during pregnancy. The cervical epithelium undergoes extensive proliferation beginning early in pregnancy. Changes in epithelia play important functions in barrier protection and immune surveillance (Timmons et al., 2010). The epithelium is also responsible for producing steroid hormones such as steroid 5α reductase type 1 in the mouse and 17beta-hydroxysteroid dehydrogenase type 2 in the human, which are both responsible for the local progesterone metabolism at the end of pregnancy (Mahendroo et al., 1999; Andersson et al., 2008). The cervical stroma consists mostly of fibroblasts surrounded by a rich extracelluar matrix (ECM) with only 10-15% of the cells consisting of smooth muscle cells (Leppert, 1995). The ECM not only determines the biomechanical properties of the resulting tissue, but also acts as a highway for cell migration and contains signaling cascades that control tissue/cell growth, differentiation, cell death and remodeling. Fibrillar collagens (I and III) are the

most abundant structural protein in the cervix. Collagen in the ECM is supported by a unique blend of elastins, matricellular proteins, proteoglycans, and glycosaminoglycans that interact to control the biomechanical properties of the ECM.

1.3.3 Role of the cervix during pregnancy and parturition

During pregnancy the cervix must undergo extensive remodeling to transform from a rigid impassive structure to a pliable passageway. The transitions the cervix makes during pregnancy can be defined as cervical remodeling and further broken down into four main overlapping stages termed: cervical softening, cervical ripening, dilation and post partum repair (Figure 1-2).

Cervical Softening.

The first phase of cervical remodeling is termed cervical softening. It is commonly defined as the first measurable change in the biomechanical integrity of the cervix. Cervical softening is a phenomenon that has long been known in the obstetrics field and was first described in 1895 (Hegar, 1895). In fact, before modern HCG detection many doctors diagnosed pregnancy by a simple palpitation of the cervix to detect a "softening". Unlike the other phases of cervical remodeling, softening is a slow progressive stage that lasts for the majority of pregnancy. In women cervical softening begins as early as one month after conception and in mice mechanical changes can be measured by day 12 of a 19-day pregnancy (Read et al., 2007). During this phase there is a large

proliferation of cervical epithelial cells, especially in the endocervix (Cunningham et al., 2010a). This increase in epithelia provides greater protection from bacterial invasion. Epithelial cells provide increased cervical mucus and secrete cytokines and chemokines that recruit inflammatory cells and antimicrobial factors which aid in protection of the cervix from bacterial invasion (Timmons et al., 2010). While there are substantial changes in the biomechanical and biochemical properties of the cervix during cervical softening, the cervix must maintain structural integrity to allow for the maturation of the fetus. Read *et. al.* has shown that cervical softening is hallmarked by a measurable change in collagen solubility but no change in collagen content (Read et al., 2007). It is important to note that molecular changes that occur during cervical softening do so in progesterone rich and estrogen poor surroundings (Cunningham et al., 2010a).

Cervical Ripening/Dilation.

Following the slow progressive phase of softening, cervical ripening is a period of rapid changes in the cervix at the end of pregnancy. In women this occurs in the last few weeks of pregnancy and in mice is seen on the last day of gestation (Read et al., 2007; Word et al., 2007). Changes that occur during ripening account for the ability of the cervix to efface and dilate for passage of the term fetus. It is characterized by a dramatic change in tissue consistency, from a soft full tissue to one that is thin and elastic. During cervical ripening in the mouse there is a functional withdrawal of progesterone resulting from a decline in

ovarian progesterone synthesis and increased progesterone metabolism. While circulating levels of progesterone do not decline in humans, a functional progesterone withdrawal resulting from increased local progesterone metabolism and perhaps changes in progesterone receptor isoforms and coactivator expression occurs (Condon et.al., 2003; Condon et.al. 2006; Andersson et al., 2008; Cunningham et al., 2010a). During this time the ECM is severely disrupted, as seen by histology (Yu et al., 1995; Winkler and Rath, 1999). Hyaluronon synthesis and concentration increase dramatically during ripening aiding in inflammatory signaling and ECM disruption (Straach et al., 2005). There is an influx of monocytes into the cervix but no evidence of immune cell activation (Timmons et al., 2009; Timmons et al., 2010). With the onset of uterine contractions the ripened cervix begins to dilate. While these two phases are difficult to distinguish, there is some evidence for the activation of the immune system during dilation (Sakamoto et al., 2004). This coupled with altered mechanical forces resulting from extensive changes in the ECM, allows the cervix to completely efface, dilate and for birth to occur.

Postpartum Repair.

Once birth has occurred, the cervix rapidly initiates programs to return itself to a nonpregnant state. Studies have show that the immune system plays an important role in “cleaning up” after pregnancy (Timmons and Mahendroo, 2007; Timmons et al., 2010).

1.3.4 Conclusion

The cervix is the "purse-strings" of the uterus. Where the uterus is a highly muscular organ, the cervix consists of mainly connective tissue. Changes in tissue integrity and compliance are regulated independently of the uterus. The cervix undergoes a loss in biomechanical strength early in pregnancy, which progressively declines until reaching a maximal loss during cervical ripening and dilation. Tissue strength is rapidly regained during the post partum period.

1.4 Extracellular Matrix and Cervical Integrity

1.4.1 Introduction

Cervical remodeling depends on precise regulation and alterations of a changing ECM to alter the tissue biomechanics of the cervix over the course of pregnancy. The cervix must begin remodeling early to lay the groundwork for impending birth, but must maintain integrity during these early phases, so to not lose the pregnancy. Cervical insufficiency, as previously mentioned, occurs when the cervix ripens prematurely in the absence of uterine contractions resulting in preterm birth. Even in other etiologies of preterm birth, the cervix allows the passage of the fetus too early in pregnancy, suggesting altered regulation of cervical biomechanics. Since the main structural portion of the cervical ECM is fibrillar collagen, many studies have focused on the changes in the biochemical properties of collagen, changes in synthesis, degradation and organization during pregnancy.

1.4.2 Collagen Synthesis, Processing, and Degradation

Collagens are a family of proteins that confer structural integrity to tissues, through their unique triple helical structure. Currently there are 28 distinct collagen molecules known, characterized by their classic glycine-x-y repeat (Gordon and Hahn, 2010). The cervix contains fibrillar collagens I and III and the basement membrane collagen IV. Collagen I is the main collagen of the cervix and makes up 70-80% of collagen in the human cervix with collagen III making up the remaining 20-30% (Maillot and Zimmermann, 1976; Kao and Leslie, 1977).

To form the classic triple helix, the collagen monomers are curled into left-handed helices; three monomers come together to form a triple helix. To form this helix, the left-handed helical monomers wrap around each other to form a right-handed super helix, similar to a strong rope (Prockop and Kivirikko, 1995). Collagens are characterized by a distinct glycine-x-y repeat, with x and y commonly consisting of proline, hydroxyproline and less commonly lysine. The glycine is essential for the triple helical structure of collagen; its size allows it to fit directly into the center of the triple helix further strengthening the molecule. The hydroxyproline is also essential for proper helical form; stabilizing the helix with hydrogen bonds (Prockop and Kivirikko, 1995; Kadler et al., 1996). Lysine residues become important extracellularly in cross-linking, which provides covalent stability for the collagen fibril. Enzymes responsible for synthesizing

collagen both intra and extra-cellularly are summarized in Tables 1-1 and 1-2 respectively.

Fibrillar collagen synthesis is a complex process that takes place both intra- and extra-cellularly (Figure 1-3). The individual collagen monomers are synthesized in a pro-form directly into the endoplasmic reticulum. While in the ER, collagen will interact with as many as 6 chaperone proteins to aid in proper protein folding, including the collagen specific chaperone, SERPINH1 (serine (or cysteine) peptidase inhibitor, clade H, member 1) (Lamande and Bateman, 1999; Hendershot and Bulleid, 2000). The pro-form, or procollagen, has both C and N pro-peptides attached to the triple helical portion of the collagen. In the ER the procollagen monomers are hydroxylated on lysine and proline residues by membrane bound enzymes belonging to the lysyl hydroxylase family (PLOD) and prolyl 4-hydroxylase, respectively (Prockop and Kivirikko, 1995; Myllyharju, 2003). With the aid of the chaperone protein and protein diisomerase (PDI) the procollagens line up on the C-terminus side and assemble into a triple helical structure (Hendershot and Bulleid, 2000). The triple helical procollagen molecule is then bound to collagen specific chaperone SERPINH1. While the exact role of SERPINH1 is still largely undetermined, it is known to be important in the collagen biosynthesis pathway (Nagai et al., 2000; Ishida et al., 2006). Procollagen is transported out of the cell via the Golgi. Once out of the cell, the C and N propeptides are cleaved by specific proteases. Bone morphogenic protein 1

(BMP1) and tolloid-like 1 (TLL1) cleave C propeptides and ADAMTS (a disintegrin-like and metallopeptidase (reprolysin type) with thrombospondin type 1 motif) family members AdamTS2, 3, and 14 cleave N propeptides. Special enhancer proteins, procollagen C-endopeptidase enhancer protein 1 and 2 (PCOLCE 1 & 2), aid in cleavage of the C-propeptide. *In vivo* studies have shown that PCOLCE1 enhances activity of C-propeptide proteases by up to 10-fold. Mice lacking PCOLCE1 also present with abnormal collagen fibrillogenesis. Both PCOLCE1 and PCOLCE 2 have been shown to directly bind procollagen (Steiglitz et al., 2002; Ge et al., 2006). Once, cleaved the soluble procollagen becomes insoluble (Kadler et al., 1987). Collagen molecules then spontaneously self-aggregate to form tightly packed fibrils in a C to N direction, in an entropy driven assembly (Kadler et al., 1987; Kadler et al., 1990a; Kadler et al., 1996). It is important to note that molecules with inappropriate cleavage of the C-propeptide cannot form fibrils, while molecules with N-propeptide still attached can form smaller fibrils, possibly indicating that N-propeptides can in part control fibril diameter (Fleischmajer et al., 1987; Hulmes et al., 1989; Kadler et al., 1990b). Fibrils that are formed in the absence of N-proteinase activity form hieroglyphic-like collagen structures that do not resemble normal collagen fibrils (Watson et al., 1998). Humans that lack N-propeptide cleavage have Ehlers-Danlos syndrome, where collagen forms thin and irregular fibrils and patients exhibit hypermobility of joints and skin fragility.

Collagen fibrils are strengthened within a fiber by covalent crosslinking. The strength of a resulting tissue depends on the type and quantity of crosslinks. Lysyl oxidase (LOX) is an enzyme that converts the lysine and hydroxylysine residues of the collagen molecules into aldehydes; allysine and hydroxyallysine, respectively (Eyre et al., 1984). Crosslinks formed between allysine residues form reducible crosslinks found more commonly in skin, while crosslinks formed via the hydroxyallysine route (pyridinolines) are non-reducible and predominate in tissues such as bone and cartilage (Eyre et al., 1984).

Collagen fibrillogenesis can take place *in vitro* with no aiding factors and in the absence of cells. Depending on the tissue, collagens can differ in length, diameter and spacing. This is likely determined by the microenvironment in which the collagen is being secreted. Specifically, proteoglycans, glycosaminoglycans and matricellular proteins interact with forming and newly formed fibrils and can affect size, shape and organization of the newly laid down collagen matrix (Scott and Orford, 1981; Scott et al., 1981; Scott and Parry, 1992; Yang et al., 2000; Raspanti et al., 2008; Bornstein, 2009). Loss of many of these proteins results in severely altered collagen and ECM properties. For example, targeted deletions of decorin (proteoglycan), SPARC (matricellular protein), and Thrombospondin 2 (matricellular protein), all have distinct effects on collagen fibrillogenesis and subsequently tissue strength (Danielson et al., 1997; Kyriakides et al., 1998a; Kyriakides et al., 1998b; Bradshaw et al., 2003).

Additionally, both collagen III and the N-propeptide of collagen III have been shown to affect the organization and resulting strength of collagen I fibers (Romanic et al., 1991).

Collagen I and III are known to form heterotypic fibrils (Keene et al., 1987a; Keene et al., 1987b). Specifically, type III pNcollagen has been shown through immunogold EM and immunofluorescence to coat collagen I fibrils (Fleischmajer et al., 1990a; Fleischmajer et al., 1990b). pNcollagen III coated collagen I fibrils are thinner than non-coated fibrils and it is suggested that this coating inhibits lateral growth while allowing tip growth. However, this inhibition of lateral growth requires a 1:1 ratio of collagen I to pNcollagen III (Romanic et al., 1991). Collagen III knockout mice show that the presence of collagen III is essential for appropriate collagen I fibrillogenesis especially in the cardiovascular system, as most mice died from the rupture of major vessels (Liu et al., 1997). Other studies show that alterations in the ratio of collagen I to collagen III can affect the organization of the ECM (Lui et al., 2010). Taken together this evidence shows that collagen III has an alternative role of controlling collagen I fibrillogenesis in addition to forming fibrillar collagen III.

Collagen is degraded by specific enzymes called matrix metalloproteases (MMP) and is resistant to degradation by many common proteases such as trypsin, pepsin and papain (Kadler et al., 2007). Humans have 23 different MMPs that act to remodel tissue and aid in wound healing. MMPs are highly

regulated and excreted in a pro-form that must be cleaved for enzyme activity to be present. TIMP or tissue inhibitors of matrix metalloproteases are also present in tissues providing an extra level of regulation to ensure proper remodeling or healing of the ECM (Heaps et al., 2007). Proteoglycans interacting directly with collagen fibrils have been shown to provide protection from collagenases, further illuminating their importance in regulation of the ECM (Geng et al., 2006).

Collagen synthesis is a complex, highly regulated process. Alteration in enzyme activity, concentrations of other ECM components as well as regulation of other collagens can all result in changes in tissue integrity by altering collagen I organization. Thus each tissue holds a unique environment of collagens, proteoglycans, matricellular proteins, and cell to matrix interactions that come together to form a distinct tissue, with its own specific properties.

1.4.3 Cervical ECM during Pregnancy

The cervix contains a unique composition of ECM molecules, which contribute to the complexity of the tissue. The ECM of the cervix must change dramatically to give rise to the extensive changes in biomechanical compliance that occurs during pregnancy. Because infection is known to play a prevalent role in preterm birth, it was postulated that the immune system must play an essential role in degrading cervical collagen for remodeling to occur both during normal pregnancy and infection mediated preterm birth (Liggins, 1981; Minamoto et al., 1987). Many studies have tried to understand the mechanisms of collagen

degradation via the activation of immune cells as the foundation of cervical ripening and subsequent dilation. These studies concluded that an inflammatory-like response initiates cervical ripening by secretion of collagenases by infiltrating immune cells (Kleissl et al., 1978; Uldbjerg et al., 1985; Minamoto et al., 1987; Osmers et al., 1990; Osmers et al., 1991; Rajabi et al., 1991; Osmers et al., 1994; Sennstrom et al., 2000). However, many of these studies were carried out in tissue biopsies of pregnant women collected shortly after birth. In addition to having a small sample sizes, it is difficult to obtain similar regions of cervix. Timing of tissue collection also varies between and within studies, with tissue collection ranging from immediately after birth, during different stages of labor or even *ex vivo* from women who underwent cesarean sections followed by hysterectomies. To separate processes that control cervical ripening, dilation, and post partum repair timing is crucial and may be confounded in these studies. Other studies have looked at immune cells via immunohistochemistry in human samples (Sakamoto et al., 2005). While these studies still fall victim to the timing caveat discussed above they also use antibodies that have been shown to recognize multiple myeloid derived cells and thus cannot be used to identify a specific type of immune cell (Timmons et al., 2010).

Recent work from our group and others has led to a paradigm shift away from the immune response theory of cervical ripening. Work by Timmons *et. al.* in the mouse shows that while monocyte infiltration of the cervix occurs during

ripening there is little activation of myeloid derived immune cells until postpartum repair (Timmons and Mahendroo, 2006; Timmons et al., 2009). Furthermore, expression of pro-inflammatory genes and MMP8, a neutrophil specific collagenase, are not induced during cervical ripening (Timmons et al., 2007; Holt et al., 2011). This correlated with the fact that depletion of neutrophils in the mouse during cervical remodeling has no effect on timing of parturition, suggests that the immune system in rodents plays a role in repair of the cervix rather than aiding in ripening (Timmons and Mahendroo, 2006).

Human studies also provide evidence that the immune system is not required for ripening of the cervix. Studies have shown that IL-8, a cytokine that recruits and activates immune cells, does not increase till after vaginal delivery (Sakamoto et al., 2004). Transcriptome analysis of human cervix has also revealed that inflammation-related genes are not regulated during cervical ripening, but are increased at the time of birth (Hassan et.al., 2006; Hassan et al., 2009).

There has been an increased body of work that supports the theory that changes in the ECM composition and collagen structure accounts for the loss of tensile strength during cervical remodeling. Studies in the rat have revealed that the changes in biomechanical state of the cervical tissue throughout remodeling cannot be explained by increases in collagenase activity alone. MMP treated samples decreased in tissue strength as well as tissue compliance while normal

ripening has an increase in both strength and compliance (Buhimschi et al., 2004). Another study in rat showed that changes in collagen organization could be positively correlated with tensile strength (Feltovich et al., 2005). Collagen solubility has also been shown to decline during pregnancy in mice and in humans (Raub et al., 2007; Myers et al., 2009).

Finally, women with connective tissue disorders have a greater risk for preterm birth. Genetic diseases such as Ehlers-Danlos Syndrome, osteogenisis imperfecta, and Marfan syndrome result in numerous defects in connective tissue. Anum *et. al*. shows that women with these genetic defects in collagen-related genes have an increased incidence of preterm births resulting from PPROM or cervical insufficiency (Anum et al., 2009a). In a study by Warren *et. al.*, 25% of patients that presented with cervical insufficiency had a first-degree relative with cervical insufficiency, furthermore women with cervical insufficiency commonly had polymorphisms in both collagen I and transforming growth factor beta (TGFβ), a growth factor known to regulate ECM remodeling (Warren et al., 2007). This highlights the importance of ECM structure to cervical remodeling.

1.5 Goal of Research

The purpose of the following research is to characterize changes that occur in the cervical extracellular matrix that affect the biomechanical properties of the tissue throughout pregnancy. Here we focus on understanding changes in collagen structure and organization along with changes in ECM components that

can affect collagen strength. Detecting early changes that allow for biomechanical changes during normal pregnancy may help in understanding processes that go awry during preterm birth. Consequently, changes in particular ECM components may serve as potential biomarkers for preterm birth and/or give avenues of therapies to prevent preterm labor.

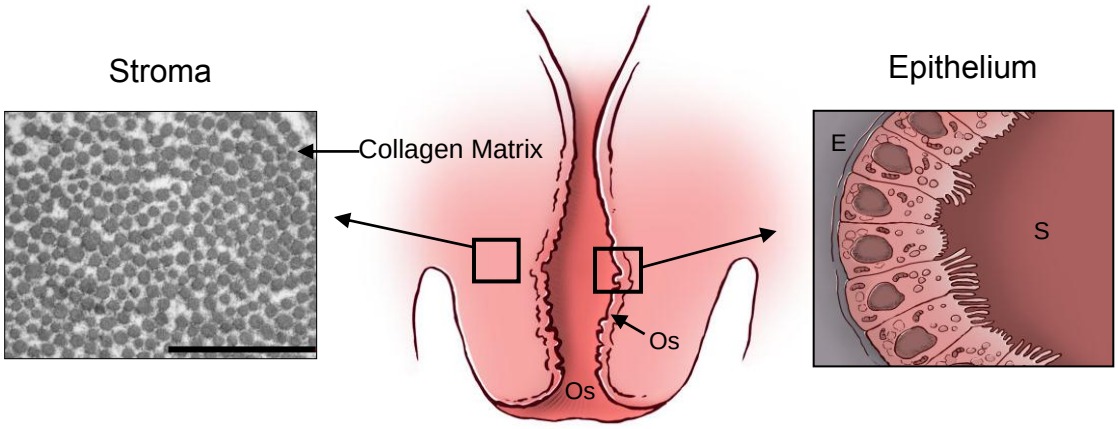

Figure 1-1. Illustration of Cervical Composition. The cervix is a dense connective tissue consisting of a cervical epithelium (squamous) and collagen rich stroma. Modified with permission from Holt (2011) *Endocrinology* 152(3):1036-1046.

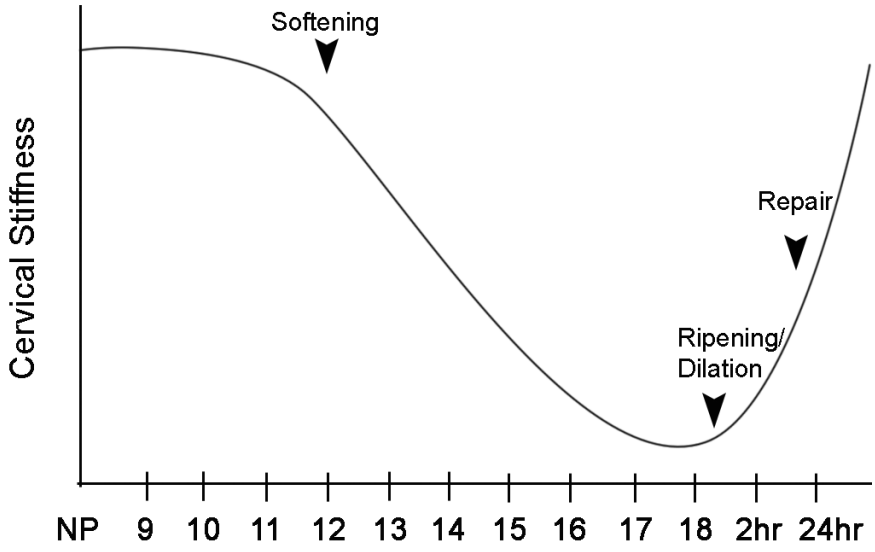

Figure 1-2. Schematic Diagram of Changes in Cervical Compliance through Mouse Pregnancy. Changes in the biomechanical properties of the cervix, described as cervical stiffness, can first be measured on gestation day 12 in the early phase of remodeling, referred to as softening. Thereafter, there is a progressive decline in stiffness, reaching a minimum during ripening and dilation. After birth the tensile strength of the tissue rapidly returns to a non-pregnant state. NP, non-pregnant, 9-18 refers to day of pregnancy and 2 hr and 24 hr refer to hours postpartum. Modified with permission from Akins (2010) *Journal of Biomedical Optics*. 15(2):0260201-02602010.

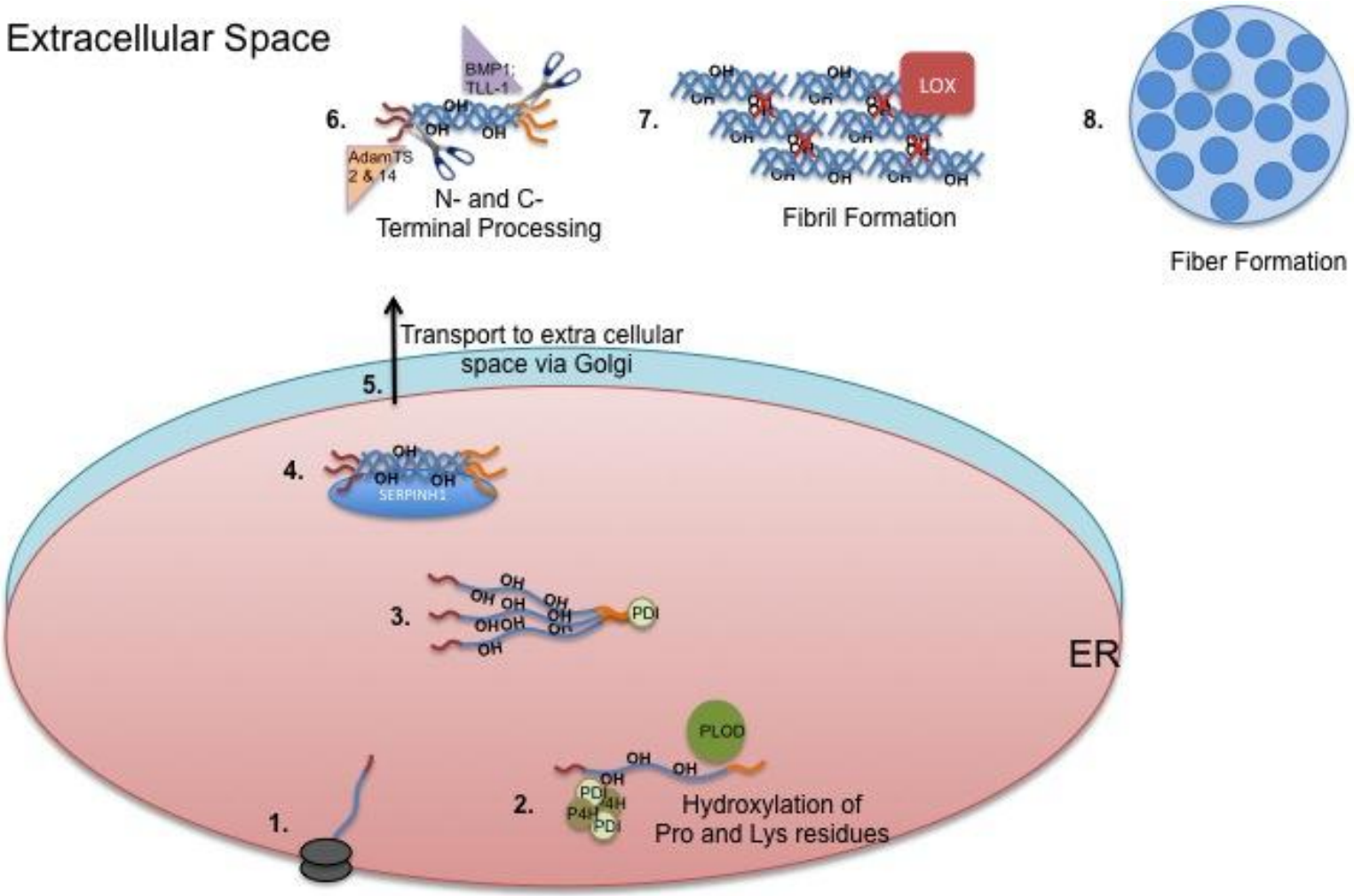
Extracellular Space
6.
BMP1;
TLL-1
AdamTS
2 & 14
N- and C-
Terminal Processing
7.
LOX
Fibril Formation
8.
Fiber Formation
Transport to extra cellular
space via Golgi
5.
4.
SERPINH1
3.
PDI
ER
PLOD
2.
P4H
Hydroxylation of
Pro and Lys residues
1.

Figure 1-3. Schematic of Collagen Synthesis and Fibrillogenesis. 1) Collagen monomers are translated directly into the endoplasmic reticulum. 2) Lysine and proline residues are hydroxylated via PLOD family proteins and Prolyl-4-hydroxylase. 3) PDI assists in lining up 3 collagen monomers at the C-terminus. After alignment, collagen monomers assemble into the triple helix. 4) Collagen specific chaperones (SERPINH1) escort the collagen molecules out of the ER. 5) Collagen is then escorted out of the cell via Golgi and secretory vesicles. 6) Specific enzymes cleave N and C- propeptides from collagen molecules. 7) Collagen molecules self-aggregate into collagen fibrils and are covalently cross-linked via lysyl oxidase enzymes. 8) Representation of mature collagen fiber made up of collagen fibrils.

Table 1-1 INTRACELLUALR ENZYMES IMPORTANT FOR COLLAGEN SYNTHESIS AND FOLDING

Enzyme Name	Function	Importance
Lysyl Hydroxylase	Hydroxylates lysine residue in the Y position.	Hydroxylation sites important for extracellular cross-linking
Prolyl-4-Hydroxlyase	Hydroxylates proline residues in Y position	Essential for proper folding of the triple helix, important in forming stabilizing hydrogen bonds
PDI/proyl-4Hydroxylase Beta Subunit	Disulfide bonds/forming Beta subunit of Prolyl-4 Hydroxylase (not catalytic)	Catalyzing disulfide bonds in the C N terminus, providing stabilization of procollagen monomers to form triple helix/essential in holding the P4H alpha subunits together for proline hydroxylation
Proyl-3-Hydroxylase	Hydroxylates proline residues in X position	
SERPINH1 (HSP47)	Chaperone Protein	Appears to help stabilize collagen triple helix

Table 1-2 EXTRACELLULAR ENZYMES IMPORTANT FOR COLLAGEN PROCESSING

Enzyme Name	Function	
Bone Morphogenic Protein -1	Catalyzes cleavage of C-propeptide	This step decreases collagen solubility by 1000-fold Essential for fibril formation
Tolloid like 1	Catalyzes cleavage of C-propeptide	This step decreases collagen solubility by 1000-fold Essential for fibril formation
AdamTs Family (2,3,14)	Catalyzes cleavage of N-propeptide	Allows for tighter packing of fibrils
Lysyl Oxidase	Catalyzes aldehyde transition of Lysine residues	Cross-links made from pyridinoline aldehydes make the strongest covalent cross-links providing strength to the tissue

Chapter 2- Regulated changes of Cervical ECM during Cervical Softening

2.1 Introduction

The composition and structure of the cervical extracellular matrix (ECM) regulates the ability of the cervix to remain closed and firm during pregnancy and to open and distend at the time of parturition. Greater understanding of the molecular changes within the cervical ECM during pregnancy and parturition will enhance our understanding of this critical physiological process as well as identify mechanisms underlying aberrant remodeling that accompany premature birth. The cervical ECM is secreted by the epithelia and fibroblasts within the cervical tissue and is comprised of five major components: fibrillar collagens, elastin fibers, proteoglycans, hyaluronan and matricellular proteins (Leppert, 1995; Word et al., 2007). Early biochemical modifications result in palpable changes in tissue compliance by the first trimester of pregnancy in women. In mice, quantifiable changes in tissue biomechanics are detectable by mid-pregnancy (Read et al., 2007). This early phase of tissue remodeling, termed cervical softening, is characterized by an increased percentage of soluble collagen and quantifiable changes in collagen fiber microstructure while collagen content remains constant (Read et al., 2007; Akins et al., 2010). Molecular processes that account for changes in collagen solubility and microstructure during cervical softening are not well characterized and are the focus of this study.

Fibrillar collagens type I and III are the main structural proteins of the cervix (Leppert, 1995). While the collagen family includes both fibrillar and non-fibrillar collagens, fibrillar collagens are the primary source of the tensile strength of tissue (Kadler et al., 1996). The load bearing capacity of a tissue is in part determined by collagen type and abundance, post-translational processing of collagen, assembly of collagen into fibrils and fibers, deposition of collagen in the ECM and collagen degradation (Myers et al., 2010). Collagen synthesis is complex. Fibrillar collagen is synthesized in the endoplasmic reticulum (ER) in a pro-form that is folded and assembled into a triple helix, initiated at the C-terminus, with the aid of chaperone proteins (Lamande and Bateman, 1999; Hendershot and Bulleid, 2000). While still in the ER, lysine residues in the procollagen chain are hydroxylated by the enzyme lysyl hydroxylase. Once the procollagen trimer is secreted into the extracellular space, the N and C terminal propeptides are cleaved, and collagen spontaneously aggregates into fibrils, which subsequently assemble into fibers (Leung et al., 1979; Kadler et al., 1990b). Assembly of fibrils from mature collagen molecules involves intermolecular cross-links between lysine residues on adjacent collagen molecules. Some lysine residues are hydroxylated in the ER by the enzyme lysyl hydroxylase and the degree of hydroxylation determines the type of cross-link formed. In turn, the type of cross-link formed determines strength and mechanical stability to the resulting tissue (Eyre et al., 1984; Canty and Kadler, 2005). Collagen cross-

linking is catalyzed by lysyl oxidase (LOX) and occurs between hydroxylated or non-hydroxylated lysine residues in collagen resulting in pyridinoline or nonpyridinoline cross-links respectively (See section 1.4.2 for more comprehensive information on collagen synthesis).

The importance of regulated changes in collagen processing during parturition is supported by numerous reports that preterm birth due to cervical insufficiency and preterm premature rupture of membranes (PPROM) are increased in women with inherited defects in collagen and elastin synthesis or assembly (e.g., Ehlers-Danlos and Marfan syndromes). Recent studies suggest polymorphisms associated with genes important for connective tissue synthesis and metabolism may predispose women to preterm birth due to cervical insufficiency and PPROM (Anum et al., 2009a; Anum et al., 2009b). The activity of the cross-link forming enzyme, LOX, has been reported to decline in the cervix during mouse pregnancy and *Lox* gene expression is regulated in the pregnant mouse cervix (Ozasa et al., 1981; Drewes et al., 2007). These data suggest a progressive decline in the number of collagen cross-links in the mouse cervix over the course of pregnancy.

In addition to collagen synthesis and cross-link formation, the type of fibrillar collagen can affect ECM composition and strength. Studies in collagen III deficient mice indicate that collagen III is essential for normal collagen I fibrillogenesis, and that changes in the ratio of collagen I/III can alter the

mechanical properties of tissue (Liu et al., 1997; Lui et al., 2010). The ratio of type I to III collagen in the human nonpregnant (NP) cervix is reported to be 70 and 30 percent respectively, but it has not been determined if changes in this ratio contribute to changes in cervical tissue compliance during pregnancy (Maillot and Zimmermann, 1976).

ECM matrix architecture and overall tissue strength, is determined by a network of interactions between collagens, proteoglycans and matricellular proteins. Non-collagenous proteins in the cervical ECM, such as proteoglycans and matricellular proteins, can affect matrix organization and consequently tissue strength. Matricellular proteins, such as tenascins, thrombospondins and SPARC (secreted protein acidic and rich in cysteine) are not structural proteins within the ECM but they modulate the functions of structural proteins such as collagen as well as cell functions through interactions with cell surface receptors, proteases and growth factors (Bornstein and Sage, 2002). Targeted gene loss of specific matricellular proteins results in aberrant matrix organization and remodeling (Kyriakides et al., 1998a; Yan and Sage, 1999; Jones and Jones, 2000). In this study we assess changes in relative abundance of fibril collagens I and III, collagen processing, collagen cross-links, matricellular proteins, and collagen ultrastructure, in order to identify early molecular events leading to increased cervical compliance and collagen solubility required for successful birth.

2.2 Results

2.2.1 Expression of type I and III fibril collagen

To observe whether changes in the relative amounts of type I and III fibril collagens could account for the progressive decline in tissue compliance through gestation, mRNA levels for the alpha-1 chain of collagen I and collagen III were determined by QPCR. Collagen I alpha I mRNA levels in the first half of pregnancy were similar to NP but significantly increased in the latter days of gestation ($p<0.01$). Levels declined to NP levels by 24 hours postpartum (Figure 2-1A). Collagen III alpha I mRNA levels were similar to NP throughout gestation. While there was a transient and significant increase in mRNA levels 2 hours postpartum levels quickly declined 24 hours after delivery (Figure 2-1B). Total cervical collagen protein was estimated by hydroxyproline assay of acid hydrolyzed tissue. Collagen levels throughout pregnancy were found to be at similar or elevated levels when compared to NP estrus cervix (Figure 2-1C). Collagen levels were increased significantly compared to NP estrus cervix on gestation days 5, 8, 16, 18 and 24 hours postpartum when normalized to dry weight ($P<0.0001$) (Figure 2-1C).

Two methods were used to estimate the relative abundance and ratio of extractable type I and type III fibril collagen. Dot blots were performed on cervical tissue homogenates extracted in 7M urea and spotted on a nitrocellulose membrane at equal protein loads (Figure 2-1D). Conventional western

immunoblotting could not be used for this assay because the antibodies available to distinguish type I from type III do not work on denatured samples. Extractable collagen I increased approximately two-fold from NP estrus to early pregnancy (day 6) and levels remained constant for the remainder of pregnancy (Figure 2-1E), while there were no significant differences in the extractable collagen III during gestation as compared to NP estrus (Figure 2-1F). Immunofluorescent staining for collagen I and III on cervical tissue showed no change in signal intensity throughout gestation. Overall signal intensity for collagen I was greater than collagen III during pregnancy. The collagen I/collagen III ratio was a factor of 2.4 at all time points. (Figure 2-1G&H). Taken together these results indicate that relative to the nonpregnant cervix, collagen levels are constant or elevated during pregnancy and that the relative abundance of fibrillar type I to III collagen remains unchanged throughout pregnancy.

Intracellular trafficking and folding of procollagen chains requires interaction with ER chaperone proteins, such as SERPINH1 (serine (or cysteine) peptidase inhibitor, clade H, member 1) and protein disulfide isomerase (PDI), as targeted deletion of these genes results in loss of tissue collagen (Nagai et al., 2000). Consistent with constant or elevated collagen content through pregnancy (as seen in Figure 2-1) we observed that protein expression of SERPINH1 and PDI in pregnant and postpartum cervix appears similar or slightly elevated during pregnancy (Figure 2-2).

2.2.2 Collagen Processing

Once secreted from the cell, C- or N- terminal propeptides are cleaved to form mature collagen. Collagen molecules in which the C-propeptide is not cleaved are unable to form fibrils while the inability to cleave the N-propeptide results in formation of irregularly shaped fibrils (Prockop and Kivirikko, 1995; Watson et al., 1998). Both scenarios result in collagen with reduced tensile strength. To examine the possibility that C- or N- terminal propeptide processing may be altered during pregnancy, we determined mRNA levels of enzymes responsible for cleavage of N and C-propeptides from procollagen. The expression of bone morphogenetic protein-1 (*Bmp1*) and tolloid-like 1 (*Tll-1*), which cleave the C-propeptide from the procollagen molecule, were analyzed via QPCR. mRNA levels for *Bmp1* were abundant and constant throughout pregnancy, with small but significant elevations observed on gestation day 18 and during postpartum. There was a trend for reduced *Tll-1* levels during pregnancy though not all time points achieved significance (Figure 2-3 A&B). The procollagen C-endopeptidase enhancer family (Pcolce 1 and 2) reported to enhance the C-proteinase activity of TLL-1 and BMP-1 was also evaluated and mRNA levels of *Pcolce 1* and *2* remained relatively constant throughout gestation when compared to NP (Figure 2-3 D&E). Despite the decrease in expression of *Tll-1*, immunoblots showed increased abundance of the 30 kD C-propeptide

during pregnancy as compared to the NP cervix suggesting C-terminal processing occurs normally (Figure 2-3C).

Three reported AdamTS proteases (a disintegrin-like and metalloprotease domain with thrombospondin type I motifs), ADAMTS2, ADAMTS3 and ADAMTS14, cleave the N-propeptide from the procollagen molecule. Using standard PCR, *AdamTS2* and *14* were found to be present in the cervix, while *AdamTs3* was undetectable (data not shown). QPCR analysis of *AdamTS2* revealed stable expression throughout pregnancy and postpartum (Figure 2-3F). *AdamTS14* expression increased significantly on day 10 of gestation and remained elevated through day 15 ($p<0.01$). Levels dropped on day 18 and remained at NP levels throughout postpartum period (Figure 2-3G). While, an antibody that recognizes the N-propeptide of mouse collagen is available, we were unable to visualize N-propeptide in our system.

2.2.3 Collagen Cross-links

Changes in the type or number of collagen cross-links can affect the tensile strength and solubility of collagen. Hydroxylation of lysine residues by the enzyme lysyl hydroxylase regulates the type of collagen cross-links formed. Expression of three genes that encode lysyl hydroxylase (*Plod 1, 2, 3*) were measured by QPCR (Figure 2-4A). While all three genes were expressed, no appreciable change was seen in *Plod 1* or *Plod* 3 mRNA expression during gestation. In contrast, compared to the NP, *Plod 2* mRNA levels appeared

suppressed throughout gestation, and reached significance on gestation days 9-13. Levels increased 2-fold 2 hours postpartum and returned to NP levels by 24 hours postpartum.

Previous reports of reduced activity of the cross-link forming enzyme, lysyl oxidase along with our observation that *Plod2* is suppressed significantly led us to evaluate the type and degree of lysine cross-links during gestation. Lysylpyridinolines (LP) cross-links derived from one lysine and two hydroxylysines and hydroxylysylpyridinolines (HP) cross-links derived from three hydroxylysines are the stronger pyridinoline cross-links that predominate in rigid connective tissues such as bone, cartilage and tendon. LP and HP cross-links are relatively low in the more flexible connective tissues such as skin where cross-links between lysine predominate (Eyre et al., 1984). Thus, a reduction in LP and HP cross-linking could contribute to increased compliance of the cervix during ripening.

HP and LP cross-links in cervical collagen at time points throughout pregnancy were measured by HPLC. HP cross-links declined significantly from NP estrus levels on day 12 of gestation and remained low throughout gestation and during postpartum repair (Figure 2-4B). LP cross-links also declined by day 14 of gestation and remained low until day 18, increasing after birth (Figure 2-4C).

The progressive decline in LP and HP cross-links as birth approaches likely contributes towards increased solubility of collagen. To evaluate collagen extractability, protein was extracted in 7M urea from NP, gestation days 6 and 8-18, and 4, 12, 24, and 48 hours postpartum cervices and immunoblotting of equal protein loads was used to detect collagen I. Because cross-linked collagen is not readily soluble, these blots cannot assess changes in total collagen, but rather give an estimate of extractable collagen I. Three bands were visible on the western blot: a broad band at ~250 kD that we attribute to procollagen dimers and trimers, a mature collagen monomer band at 140 kD, and an unidentified band at 50 kD that appears in NP and postpartum samples (Figure 2-4D). The 140 kD mature collagen band is not visible in NP samples. During pregnancy this band increased in density, suggesting that mature collagen is more extractable (soluble) during pregnancy. The band declines in density by 4 hours postpartum and is not seen in later postpartum samples. Increased extractability of collagen during pregnancy is consistent with our previous observations of increased collagen solubility as determined by extraction in acetic acid and pepsin and with current data showing a decline in HP and LP collagen cross-links (Figure 2-4)(Read et al., 2007). The 250 kD band appeared by day 11 of pregnancy and remained visible throughout gestation but disappeared postpartum. The presence of this procollagen band suggests an increase in the proportion of newly synthesized but unprocessed collagen.

2.2.4 Matricellular Proteins

Expression of mRNAs encoding the matricellular proteins, *Thbs2* (Thrombospondin 2), *Tnc* (Tenascin C), and *Sparc* were obtained via QPCR (Figure 2-5). *Thbs2* mRNA expression dropped from NP levels by day 8 of gestation and remained low until 2 hours after birth returning to NP levels by 24 hours postpartum (Figure 2-5A). The decline in expression on days 8, 10 and 11 did not achieve significance. Similar to *Thbs2*, tenascin-C mRNA expression declined significantly on day 8 of gestation and remained downregulated for the remainder of pregnancy. *Tnc* mRNA increased 6-fold by 2 hours postpartum and returned to NP levels by 24 hours postpartum (Figure 2-5B). In contrast, there was a trend for increased expression of *Sparc* from gestation day 10 through day 17 though significance was only achieved at gestation days 14 and 17. Relative expression returned to NP levels on day 18 of gestation throughout postpartum (Figure 2-5C).

2.2.5 Collagen Ultrastructure

The observed changes in collagen solubility, type and degree of cross-links as well as matricellular protein composition can affect collagen organization and ultrastructure. Electron micrographs of cervical tissue at day 6 and 18 were taken at 4200X magnification (Figure 2-6). Cellular components and electron dense components of the ECM appeared in close proximity during early pregnancy (Figure 2-6A). In late gestation, collagen fibers were more dispersed

and not associated with cellular components of the tissue (Figure 2-6B) and generally there was a dramatic loss of electron dense ECM. To evaluate changes in collagen ultrastructure, collagen fibril diameters were measured from transmission electron micrographs of cervical tissue during from NP metestrus and gestation days 6, 12, 15 and 18 as described in Methods (Figure 2-7A-E). The mean fibril diameter significantly increased from early to late pregnancy along with a shift in the distribution towards a higher frequency of fibrils with a larger diameter. As early as day 6 there was an increase in fibril diameter of 12.1nm compared to NP metestrus with an additional 20 nm increase from day 6 to day 18 (Figure 2-7F-J).

2.3 Discussion

This study identifies changes in the cervical ECM early in pregnancy that contributes cumulatively to the progressive decline in tensile strength during the cervical softening phase. Most notable are changes in the degree and types of collagen cross-links and a decline in expression of two matricellular proteins, thrombospondin 2 and tenascin-C. The decline in collagen cross-links, as well as decline in expression of THBS2 and TNC must independently or cumulatively result in an increased solubility of collagen during pregnancy as well as the striking changes in collagen fibril ultrastructure.

Based on these observations we propose a model in which mature collagen in the cervical ECM is gradually replaced with less cross-linked collagen

beginning early in gestation. As the less cross-linked collagen becomes more abundant in the ECM tissue compliance begins to increase, eventually reaching a threshold of measurable change. This threshold defines the beginning of cervical softening which in the mouse is measurable by gestation day 12 and tissue stiffness declines progressively thereafter (Read et al., 2007). The decline in LP and HP cross-links correlates with the decline in mRNA expression of *Plod2* as well as the reported decline in activity of lysyl oxidase in the mouse cervix (Ozasa et al., 1981). While the other two lysyl hydroxlylase genes (*Plod1* and *Plod3*) were expressed at normal levels in the mouse cervix, they did not compensate for the decline in *Plod2* expression. It has been suggested that PLOD2 may have greater specificity for hydroxylation of the telopeptide region of collagen; important in formation of pyridinoline cross-links, while the other lysyl hydroxylases may preferentially hydroxylate lysine residues in the triple helical regions of various collagens (van der Slot et al., 2003). Mutations in the *Plod2* gene and a reduction in pyridinoline cross-links have been described in patients with Bruck syndrome, which is characterized, by fragile bones, scoliosis and osteoporosis (Ha-Vinh et al., 2004; Hyry et al., 2009).

In addition to a decline in collagen cross-linking, altered levels of matricellular proteins likely contribute to early changes in tissue compliance as well. In mice, THBS2 appears to regulate cell-matrix adhesion, inhibit angiogenesis and regulate collagen fibril assembly (Kyriakides et al., 1999; Yang

et al., 2000). Loss of THBS2 results in defective cell adhesion of fibroblasts; increased collagen solubility in skin and collagen fibril size is increased while tensile strength is decreased. Wound healing is accelerated in these mice along with increased tissue vascularization (Kyriakides et al., 1999). In addition, THBS2 null mice have a reported acceleration of cervical softening without premature birth (Kokenyesi et al., 2004). Both THBS2 and tenascin-C play an important function in promoting cell migration during wound healing after injury and consistent with this function are upregulated several fold in the cervix at the time of birth and postpartum (Timmons and Mahendroo, 2007). Future studies are required to understand the mechanisms by which THBS2 and tenascin-C contribute to collagen fibril assembly as well as a potential role in tissue vascularization, which is increased in late pregnancy (Mowa et al., 2004).

The early, progressive and cumulative changes in the cervical ECM are supported by the observed increase in collagen fibril diameter as measured in electron micrographs. Increased fibril diameter between gestation days 12, 15 and 18, coincide with biomechanical changes that occur in late pregnancy (Figure 2-8)(Mahendroo et al., 1997; Word et al., 2007). These changes also correlate with quantifiable changes in cervical collagen fiber morphology as determined by second harmonic generation microscopy at the same time points in mouse pregnancy (Akins et al., 2010). The increasing fibril diameter may result from reduced packing of fibrils due to both the decline in HP and LP cross-links as well

as the decline in THBS2 and/or tenascin C expression. The net result is a loss of tensile strength. This is supported by the observation that a reduction in pyridinoline cross-links, or loss of THBS2 in knockout mouse models, lead to an increase in collagen fibril diameter as measured by EM (Kyriakides et al., 1998a; Takaluoma et al., 2007).

A number of genes/proteins important in synthesis, trafficking or processing of collagen were expressed at levels similar to or slightly elevated as compared to nonpregnant cervix (Figures 2-3 & 2-4). The resulting continued production of newly synthesized collagen might ensure that collagen is maintained at a constant level yet allows for a gradual turnover of well cross-linked collagen with poorly cross-linked collagen. Consistent with this hypothesis is the observation that *Sparc* transcripts (Figure 2-5B) and protein (data not shown) are elevated during pregnancy and decline to NP levels by gestation day 18. *Sparc* expression is frequently associated with tissues in which there is a high rate of collagen turnover and SPARC is required for appropriate procollagen processing and deposition of collagen in the ECM. Mice deficient in *Sparc* have reduced collagen content and collagen is tethered to the cell surface with reduced fibril aggregation in the ECM (Rentz et al., 2007) (Bradshaw et al., 2003).

This work has identified early pregnancy changes in collagen processing and ECM composition that are likely responsible for the initial increase in tissue compliance during cervical softening. In contrast to the accelerated changes that

occur during cervical ripening and dilation at the end of pregnancy, these early changes occur in an environment rich in progesterone and relatively low estrogen. Future studies are required to identify steroid and peptide hormones that may regulate collagen cross-link formation and *Thbs2* and *Tnc* expression. These studies not only enhance our understanding of the progressive physiological changes in normal cervical softening but also identify specific genes/proteins in which mutations or misregulation may account for clinical complications such as cervical insufficiency or result in premature cervical shortening of the cervix, which is a risk factor for preterm birth (Iams et al., 2001; Owen et al., 2001). Future studies will address these important questions and provide necessary understanding required for development of therapies to prevent preterm birth, the leading cause of infant death in the first year of life.

2.4 Materials and Methods

2.4.1 Animal and Tissue Collection

Nonpregnant mice. To assess stage of cycle, vaginal smears were taken and analyzed for characteristic cell structure and immune cell presence specific for each phase of the cycle (Taylor, 1986). Mice were observed through at least one full cycle in order to insure proper cycling prior to tissue collection. In this study the term "NP" refers to data pooled from an equal number of cervices collected in proestus, estrus and metestrus. "NP estrus" or "NP metestrus" refers to cervices assessed at a single stage of the estrus cycle. Pregnant and postpartum mice.

Females were housed overnight with males and separated the following morning. Vaginal plugs were checked at the time of separation; mice with plugs were considered to be day 0 of their pregnancy with birth occurring early on gestation day 19. In general, cervices were collected at noon for all time points from gestation d8-18 except day 18 for which cervices were collected between 6-7 PM in order to collect cervices a few hours prior to onset of labor. Postpartum cervices collected after vaginal birth on gestation d19 were obtained *exactly* 2 or 4 hours after delivery of the first pup or *approximately* 10-12 hours, 24 hours or 48 hours after delivery of the first pup.

Mice used for these studies were of C57B6/129Sv mixed strain. Cervical tissue was dissected out of the reproductive tract and vaginal tissue was carefully removed from cervical tissue. Cervices were flash-frozen in liquid nitrogen immediately following their extraction. All studies were conducted in accordance with the standards of humane animal care described in the National Institutes of Health Guide for the Care and Use of Laboratory Animals using protocols approved by an institutional animal care and research advisory committee (Committee for the Update of the Guide for the Care and Use of Laboratory Animals, 2011).

2.4.2 Quantitative Real-time PCR

Total RNA was extracted from frozen cervical tissue in RNA STAT 60 (Tel-Test Inc., Friendswood TX). RNA was then treated with DNase (New

England Biolabs, Massachusetts) to remove genomic contaminants. cDNA was synthesized and RT-PCR was carried out using the SYBR Green detection system (Applied Biosystems, Carlsbad, California) or using the Taqman Probes system (Applied Biosystems). All gene expression is relative to gestation day 18 levels.

2.4.3 Immunofluorescence

Cervical tissue was collected on day 6, 12, 15, and 18 of gestation and frozen in OCT medium (Tissue Tek, Indiana). Five-micrometer cervical sections were cut from tissue blocks. Sections were fixed for 10 minutes in acetone at -20°C. Tissue was rehydrated in PBS, blocked in 10% normal goat serum (Invitrogen, California, catalog # 01-6201) and incubated with collagen I or collagen III rabbit polyclonal antibodies (Abcam, Cambridge, ab34710 and ab7778). Sections were then washed in PBS and incubated with goat α rabbit IgG antibodies coupled to Alexa 488 (Invitrogen/Molecular Probes, California, A11008). Slides were viewed on a Zeiss LSM510 META NLO confocal microscope using an Acroplan 40x/0.8 W objective lens. Fluorescence signal intensity was measured using ImageJ 1.41k (http://rsbweb.nih.gov/ij/).

2.4.4 Immunoblotting

Collagen was extracted with 7M urea (Sigma, St. Louis), 0.1M sodium phosphate with 1% protease inhibitor (Sigma, St.Louis), overnight at 4°C. The protein concentration was determined by a Bradford protein assay (Pierce, Thermo Scientific, Rockford, Il). Ten micrograms of protein was loaded on a 4-

20% Tris-HCL polyacrylamide gel and electrophoresed at 100V. After overnight transfer to nitrocellulose membrane and Ponceu S (Sigma) staining to assess equal loading of protein, immunoblotting was performed using rabbit polyclonal anti-mouse collagen I (MD Biosciences, St. Paul MN, MD20151).

Protein used in dot blot analysis was extracted as described for immunoblotting. 2.5μg of protein was spotted onto a nitrocellulose membrane and probed with rabbit polyclonal anti-collagen I or rabbit polyclonal anti-collagen III primary antibody (Abcam, Cambridge, ab34710 and ab7778). Secondary antibody for both western and dot blots was donkey anti-rabbit HRP (Jackson ImmunoResearch, Pennsylvania, #711036152). Chemiluminescence was visualized using ECL (GE Healthcare, Buchinghamshire UK). Digital images of the blots were analyzed quantitatively using Multi Gauge software (Fuji Film, Tokyo).

2.5.5 Collagen Content and Cross-links

Frozen cervical tissue was lyophilized, weighed, and then hydrolyzed in 6M HCl at 100°C for 20-22 hours. Collagen cross-links were measured via HPLC as described previously (Bank et al., 1997; Breeveld-Dwarkasing et al., 2003). In brief, cervical samples were lyophilized and then hydrolyzed in 6M HCL at 100°C for 20-22 hours. The samples were then dried and dissolved into 10uM pyridoxine and 2.40 mM homo-arginine in water. Samples were then diluted 1:4 in 0.5% heptafluorobutyric acid in 10% acetonitrile. Cross-links were analyzed

by reverse-phase HPLC and calculated based on internal pyridoxine standards. Hydroxyproline assays were carried out as previously described (Stegemann and Stalder, 1967). Total collagen was calculated using a ratio of 300 hydroxyproline residues per triple helix (Breeveld-Dwarkasing et al., 2003).

2.5.6 Electron Microscopy

Nonpregnant mice in metestrus or pregnant mice at gestation days 6, 12, 15 and 18 were perfused with 1% glutaraldehyde, 2% paraformaldehyde fixative in 0.1M phosphate buffer. Cervical and uterine tissue was removed and fixed in 2.5% glutaraldehyde in 0.1M cacodylate buffer containing 0.1% ruthenium red overnight at 4^0C. Tissue was then cut into 250μm longitudinal sections using a Vibratome Series 3000 Sectioning System (The Vibratome Company, St. Louis). Vaginal and uterine tissue was removed from the cervix and the cervix was rinsed for 30 minutes with cacodylate buffer. The tissue was post-fixed with 1% osmium in 0.1M cacodylate buffer containing 0.1% ruthenium red for 90 minutes. Specimens were dehydrated through a graded series of ethanols (50%, 70%, 95%, 100%) followed by propylene oxide and embedded in Epon. Thin sections were stained with uranyl acetate and lead citrate. Sections were viewed on a TEM Tecnai microscope (FEI Company, Hillsboro, Oregon) and images captured at 4200x or 20500x with a Morada 11 1 megapixel CCD camera.

2.5.7 Collagen Fibril Measurements

Electron microscope images of transversely sectioned collagen fibrils taken at 20,500x were analyzed with Image J 1.41k (http://rsb.info.nih.gov/ij/). An intensity threshold was interactively determined for optimal segmentation of fibril from background. Segmented images were converted to a binary mask, and erode, open, dilation and fill holes binary operations were used to separate merged fibrils. Particles were analyzed using the Particle Analysis function of Image J with parameters set for size, 1000-10000 and circularity 0-1. Ellipses were fit to all particles and the minor angle of the ellipse was taken as the fibril diameter. Ten images from three animals were analyzed for each time point resulting in an n= 8,197 fibrils/day 6; 12,958 fibrils/day 12; 8,362 fibrils/day 15; and 12,161 fibrils/day 18. Due to low contrast ratio of fibrils versus background in NP samples, an n = 516 fibrils was taken from 3 animals, 1 image each.

2.5.8 Statistics

Statistics were performed using Prism software version 5.0b (Graphpad Software, La Jolla, CA). For comparison of QPCR, collagen content and collagen cross-links data, one-way ANOVA was used followed by Dunnet's comparison test using NP or day 8 as the control. Fibril diameter data were analyzed using a one-way ANOVA followed by a Dunn's multiple comparison test.

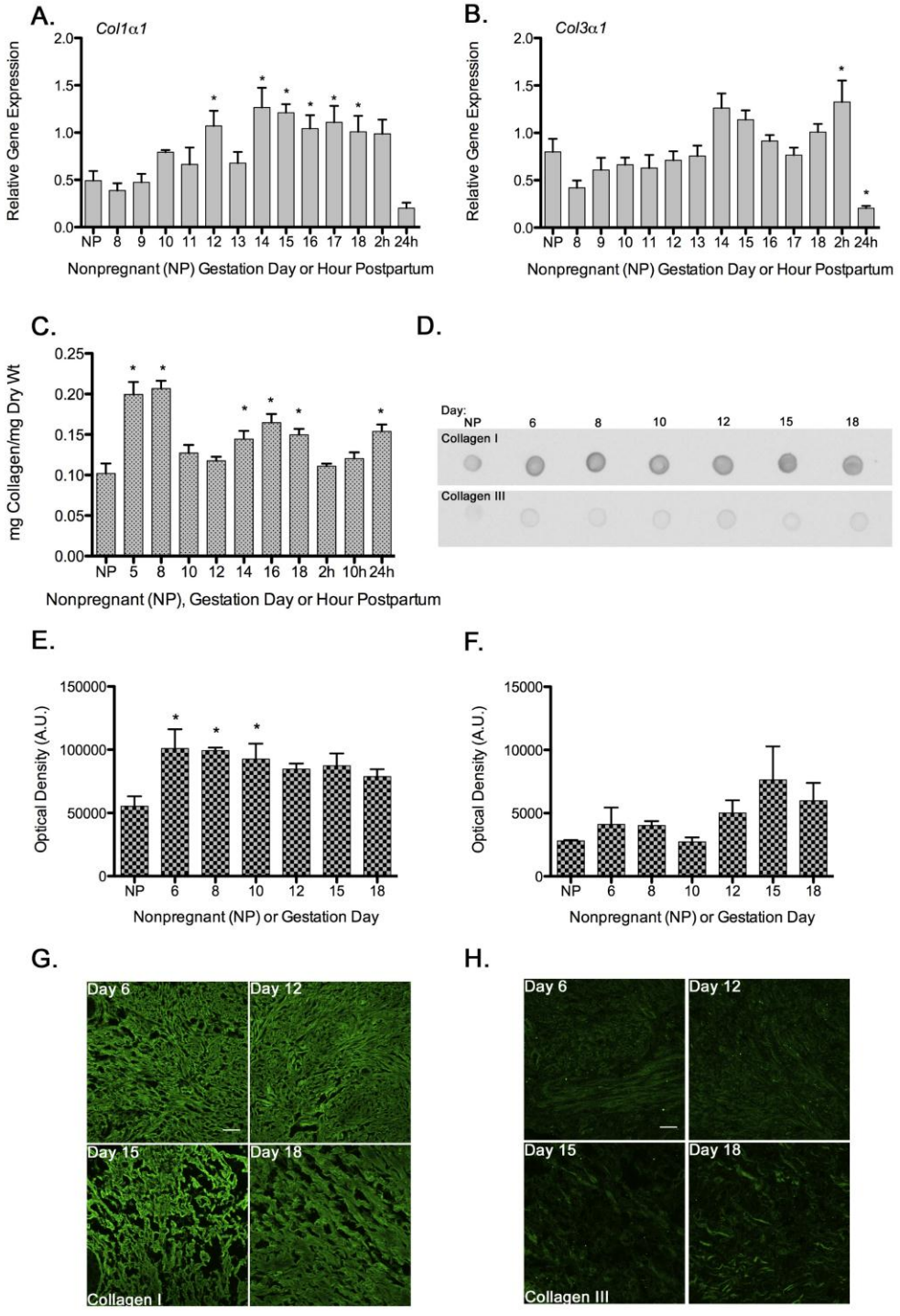
A.
Col1α1
Relative Gene Expression
2.0
1.5
1.0
0.5
0.0
NP 8 9 10 11 12 13 14 15 16 17 18 2h 24h
Nonpregnant (NP) Gestation Day or Hour Postpartum
B.
Col3α1
Relative Gene Expression
2.0
1.5
1.0
0.5
0.0
NP 8 9 10 11 12 13 14 15 16 17 18 2h 24h
Nonpregnant (NP) Gestation Day or Hour Postpartum
C.
mg Collagen/mg Dry Wt
0.25
0.20
0.15
0.10
0.05
0.00
NP 5 8 10 12 14 16 18 2h 10h 24h
Nonpregnant (NP), Gestation Day or Hour Postpartum
D.
Day:
NP 6 8 10 12 15 18
Collagen I
Collagen III
E.
Optical Density (A.U.)
150000
100000
50000
0
NP 6 8 10 12 15 18
Nonpregnant (NP) or Gestation Day
F.
Optical Density (A.U.)
15000
10000
5000
0
NP 6 8 10 12 15 18
Nonpregnant (NP) or Gestation Day
G.
Day 6
Day 12
Day 15
Day 18
Collagen I
H.
Day 6
Day 12
Day 15
Day 18
Collagen III

Figure 2-1. Cervical Collagen Iα1 and IIIα1 Levels Remain Constant during Pregnancy. A) Collagen Iα1 and B) collagen IIIα1 mRNA levels were measured via QPCR using cervices at NP metestrus and days 8, 9, 10, 11, 12, 13, 14, 15, 16, 17, 18, 2 hours postpartum and 24 hours postpartum and normalized to day 18. For NP n=15 cervices, for pregnant and post partum n=4-6 cervices per time-point. * Indicates significance at $p<0.05$. C) The amount of collagen in the cervix was measured through hydroxyproline content. Hydroxyproline assay was carried out in NP estrus, gestation days 5, 8, 10, 12, 14, 16, 18, 2 hours postpartum, 10 hours postpartum and 24 hours postpartum cervices and normalized to dry weight. n=5 cervices per time point. D) Dot blot analysis of Collagen I and Collagen III soluble protein levels in NP estrus, gestation days 6, 8, 10, 12, 15 and 18. E/F) Optical density analysis of E) collagen I and F) collagen III dot blot. n=3 cervices per time point. G/H) Immunofluorescence of G) collagen I and H) collagen III in gestation day 6, 12, 15 and 18 cervical sections. With permission from Akins (2011) *Biology of Reproduction*. 84(5): 1053-62.

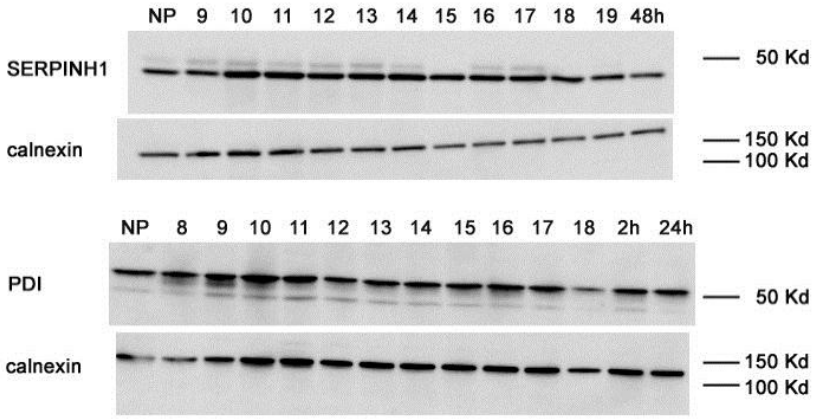

Figure 2-2. Cervical Expression of SERPINH1 and PDI is Constant throughout Pregnancy. Expression of the chaperone protein, SERPINH1 (47 KD) was evaluated in the nonpregnant (NP) cervix and pregnant days 9, 10, 11, 12, 13, 14, 15, 16, 17, 18, 2-4 hours postpartum (labeled as 19) and 48 hours postpartum [Top Panel]. Expression of PDI was measured in NP and days 8, 9, 10, 11, 12, 13, 14, 15, 16, 17, 18, 2 hours postpartum and 24 hours postpartum [Bottom Panel]. Loading control was carried out using rabbit anti-Calnexin. With permission from Akins (2011) *Biology of Reproduction*. 84(5): 1053-62.

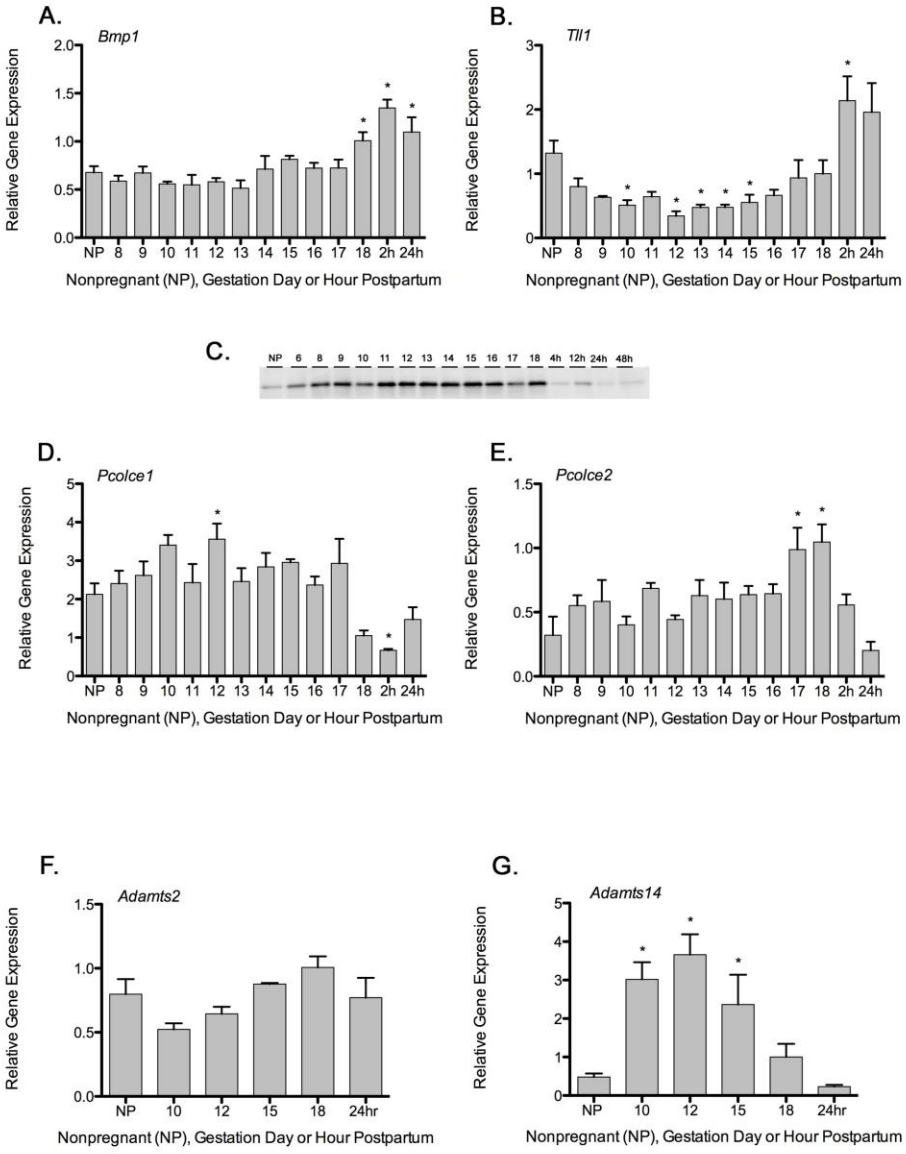
A.
Bmp1
Relative Gene Expression
2.0
1.5
1.0
0.5
0.0
NP 8 9 10 11 12 13 14 15 16 17 18 2h 24h
Nonpregnant (NP), Gestation Day or Hour Postpartum
B.
Tll1
Relative Gene Expression
3
2
1
0
NP 8 9 10 11 12 13 14 15 16 17 18 2h 24h
Nonpregnant (NP), Gestation Day or Hour Postpartum
C.
NP 6 8 9 10 11 12 13 14 15 16 17 18 4h 12h 24h 48h
D.
Pcolce1
Relative Gene Expression
5
4
3
2
1
0
NP 8 9 10 11 12 13 14 15 16 17 18 2h 24h
Nonpregnant (NP), Gestation Day or Hour Postpartum
E.
Pcolce2
Relative Gene Expression
1.5
1.0
0.5
0.0
NP 8 9 10 11 12 13 14 15 16 17 18 2h 24h
Nonpregnant (NP), Gestation Day or Hour Postpartum
F.
Adamts2
Relative Gene Expression
1.5
1.0
0.5
0.0
NP 10 12 15 18 24hr
Nonpregnant (NP), Gestation Day or Hour Postpartum
G.
Adamts14
Relative Gene Expression
5
4
3
2
1
0
NP 10 12 15 18 24hr
Nonpregnant (NP), Gestation Day or Hour Postpartum

Figure 2-3. mRNA Expression of Collagen Processing Proteins. A&B) mRNA expression of C-propeptide collagen processing enzymes *Bmp-1* (A) and *Tll-1* (B) were evaluated in NP, gestation days 8, 9, 10, 11, 12, 13, 14, 15, 16, 17, 18, 2 hours postpartum and 24 hours postpartum and normalized to day 18. For NP n=15 cervices, for pregnant and post partum n=4-6 cervices per time-point. C) C-propeptide was evaluated via Western blot in NP, gestation days 6, 8, 9, 10, 11, 12, 13, 14, 15, 16, 17, 18, 4 hours postpartum, 12 hours postpartum, 24 hours postpartum and 48 hours postpartum cervices. A 30kD band corresponding to the collagen C-propeptide is present. D&E) mRNA expression of C-propetidase enhancing proteins, (D) *Pcolce1* and *Pcolce2* were evaluated at same time points from (A). For NP n=7; for pregnant and postpartum n=4-7 cervices per time point. F) mRNA expression of N-propeptide collagen processing enzyme *AdamTs2* was evaluated at NP, and gestation days 10, 12, 15, 18 and 24hr postpartum postpartum and normalized to day 18. For NP n=15 cervices, for pregnant and post partum n=4-5 cervices per time-point. G) mRNA expression of N-propeptide collagen processing enzyme *AdamTs14* was evaluated at the same time points in (F) . For NP n=15 cervices for pregnant and post partum n= 4-5 cervices per time point. * Indicates significance at $p<0.05$. Modified with permission from Akins (2011) *Biology of Reproduction*. 84(5): 1053-62.

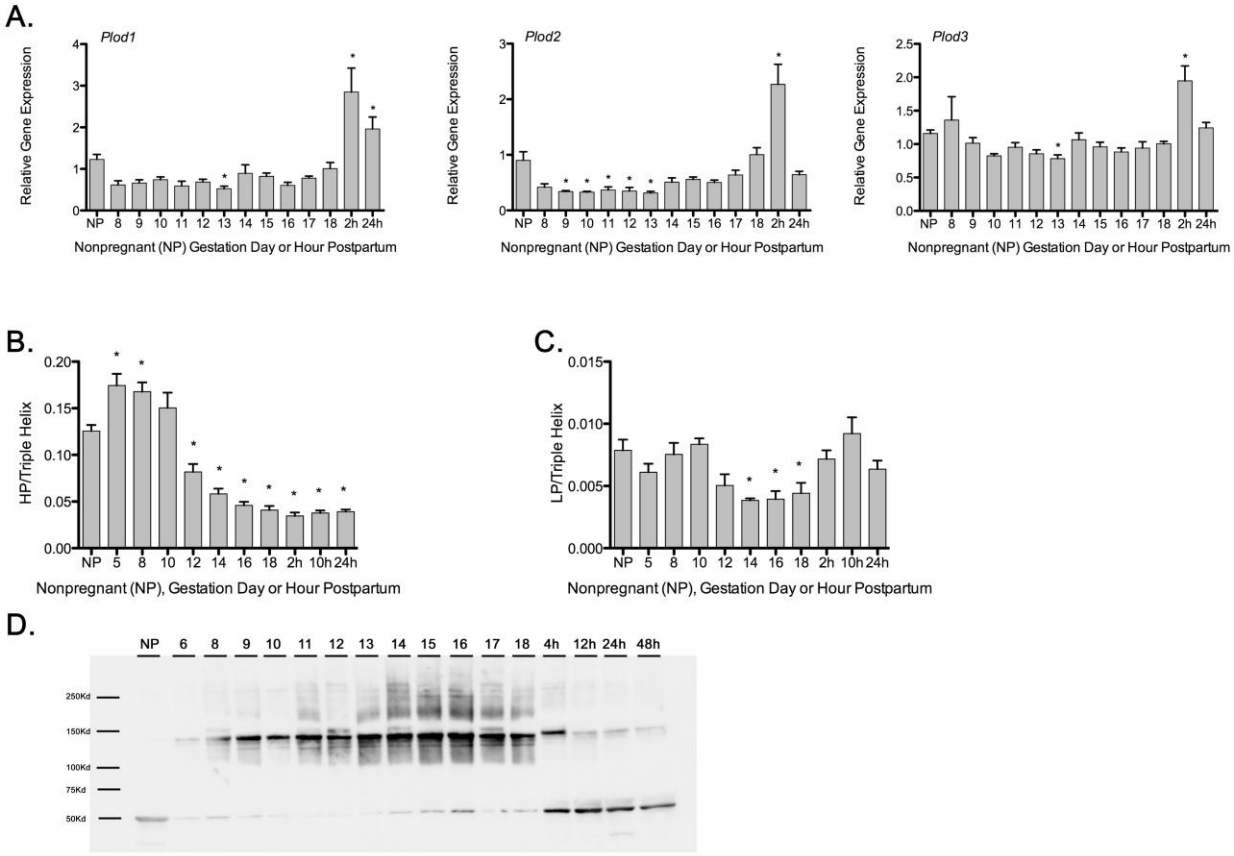
A.
Plod1
Plod2
Plod3
Relative Gene Expression
NP 8 9 10 11 12 13 14 15 16 17 18 2h 24h
Nonpregnant (NP) Gestation Day or Hour Postpartum
B.
HP/Triple Helix
NP 5 8 10 12 14 16 18 2h 10h 24h
Nonpregnant (NP), Gestation Day or Hour Postpartum
C.
LP/Triple Helix
NP 5 8 10 12 14 16 18 2h 10h 24h
Nonpregnant (NP), Gestation Day or Hour Postpartum
D.
NP 6 8 9 10 11 12 13 14 15 16 17 18 4h 12h 24h 48h
250Kd
150Kd
100Kd
75Kd
50Kd

Figure 2-4. Decline in mRNA Expression of *Plod2* Correlates to a Reduction in Pyridinoline Cross-links During Pregnancy and an Increase in Soluble Collagen. A) mRNA levels of the *Plod* family were evaluated in NP, gestation days 8, 9, 10, 11, 12, 13, 14, 15, 16, 17, 18, 2 hours postpartum and 24 hours postpartum and normalized to day 18. For NP n=15 cervices, for pregnant and post partum n=4-6 cervices per time-point. B) HPLC analysis of HP cross-links in NP estrus, gestation days 5, 8, 10, 12, 14, 16, 18, 2 hours postpartum, 10 hours postpartum and 24 hours postpartum cervices. n=5 cervices per time point. C) LP cross-links were evaluated in the same time-points as (B). n=5 cervices per time-point. D) Extractable collagen was assessed in NP, gestation days 6, 8, 9, 10, 11, 12, 13, 14, 15, 16, 17, 18, 4 hours postpartum, 12 hours postpartum, 24 hours postpartum and 48 hours postpartum cervices. Blot was probed with rabbit anti-Collagen I. Bands are present at ~250kD and 140kD representing procollagen and mature collagen, respectively. An unidentified 50kD band is also present in NP and postpartum tissues.* Indicates significance at $p<0.05$. With permission from Akins (2011) *Biology of Reproduction*. 84(5): 1053-62. **Crosslink analysis was performed by Dr. Ruud Bank.**

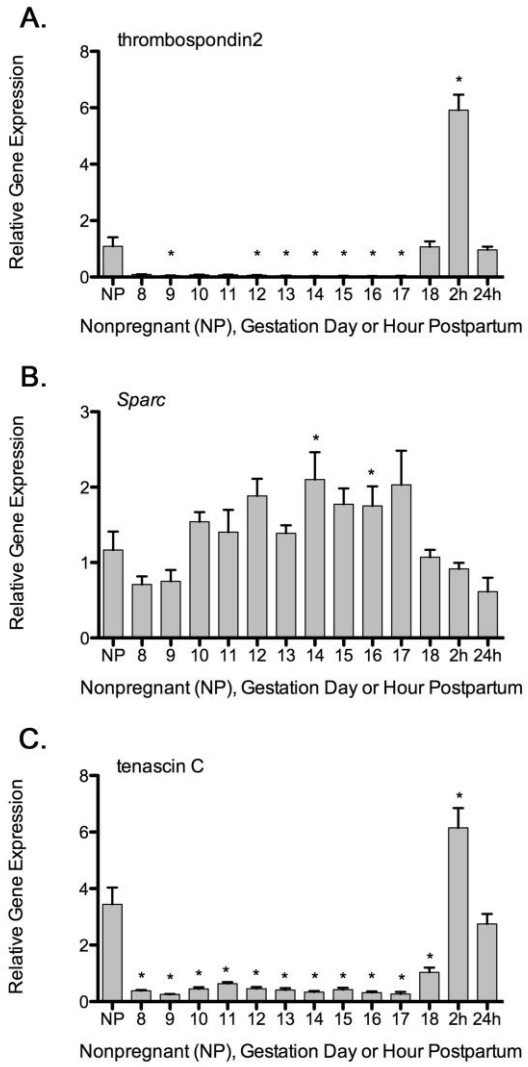

Figure 2-5. Cervical Matricellular Protein Expression during Pregnancy and Parturition. mRNA levels of A) Thrombospondin 2 B) Sparc and C) Tenascin C were analyzed via QPCR on NP, gestation days 8, 9, 10, 11, 12, 13, 14, 15, 16, 17, 18, 2 hours postpartum and 24 hours postpartum and normalized to day 18. For NP n=11 cervices for pregnant and post partum n=5-7 cervices per time-point. * Indicates significance at $p<0.05$. With permission from Akins (2011) *Biology of Reproduction*. 84(5): 1053-62.

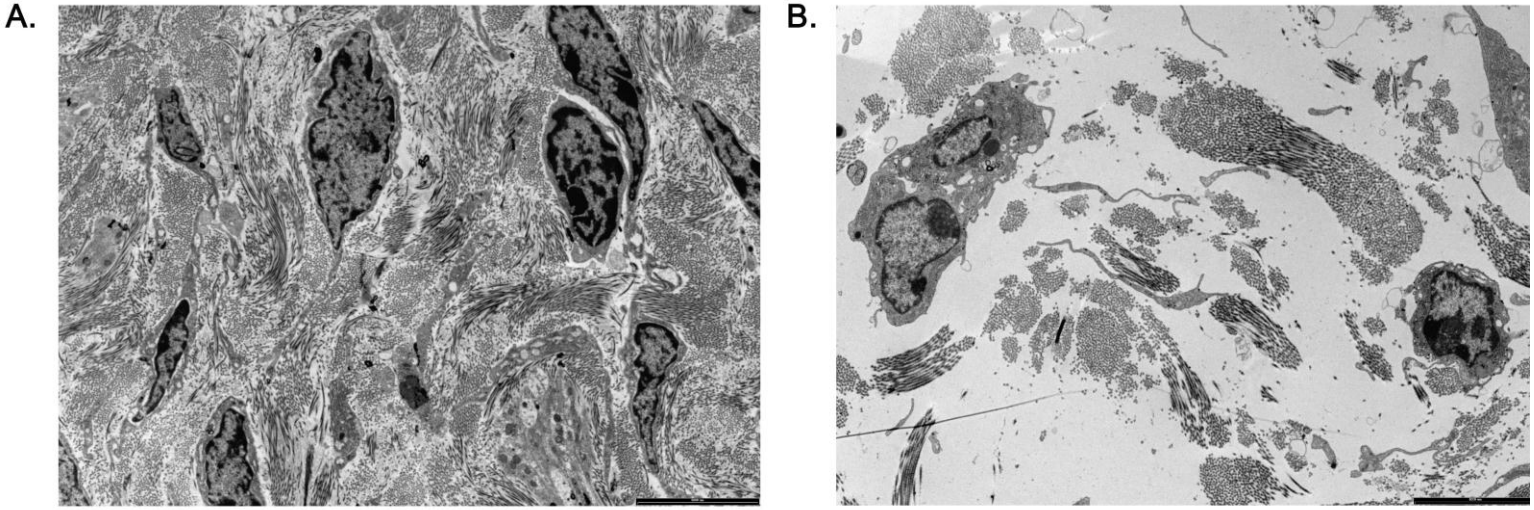

Figure 2-6. Cervical ECM Becomes Dispersed Throughout Pregnancy. Electron micrographs of cervical ECM taken at 4200x on A) Day 6 and B) Day 18 of pregnancy. Bar= 1000nm. With permission from Akins (2011) *Biology of Reproduction*. 84(5): 1053-62.

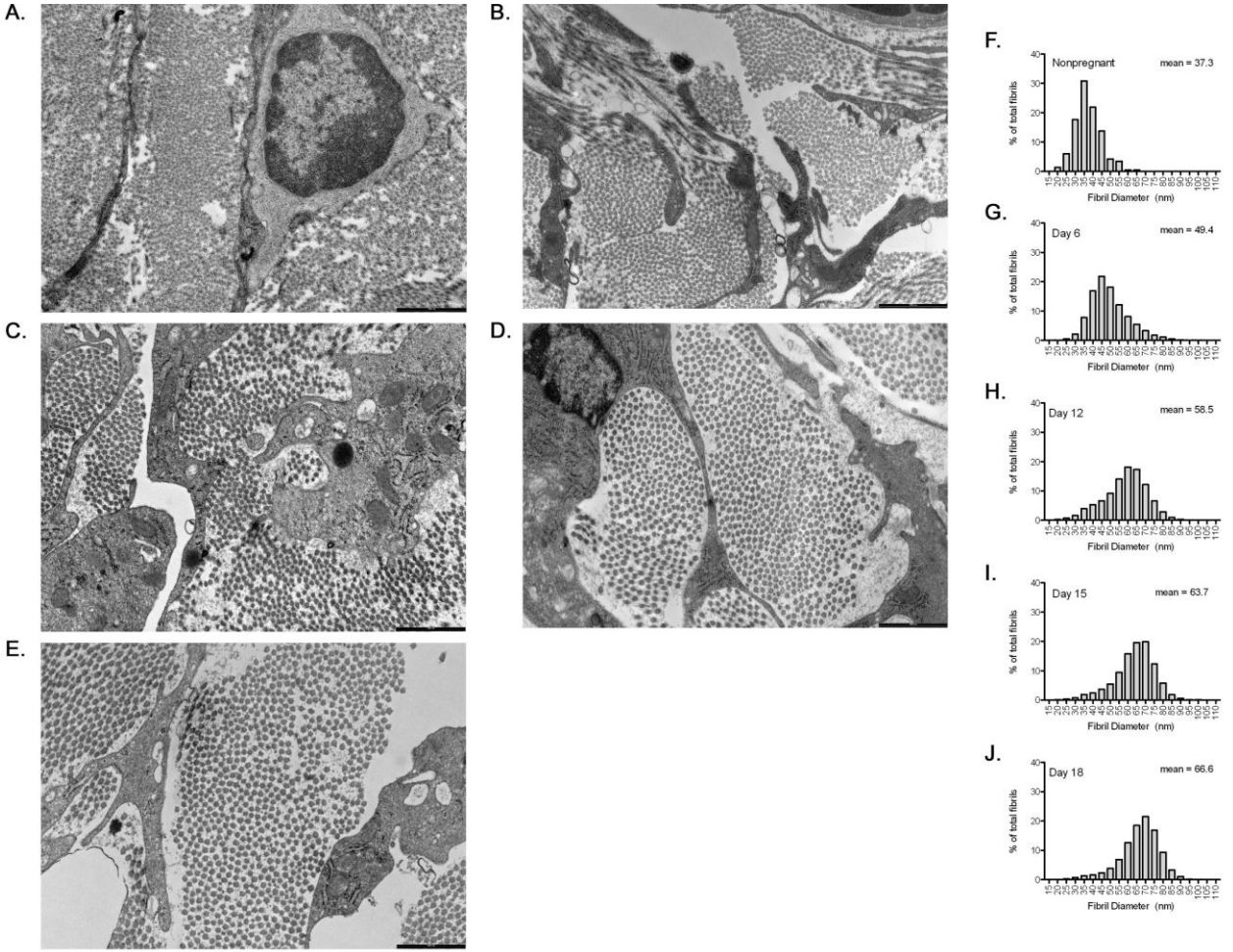
A.
B.
C.
D.
E.
F.
Nonpregnant
mean = 37.3
G.
Day 6
mean = 49.4
H.
Day 12
mean = 58.5
I.
Day 15
mean = 63.7
J.
Day 18
mean = 66.6
% of total fibrils
Fibril Diameter (nm)

Figure 2-7. Collagen Fibrils Increase in Size during Pregnancy. Electron micrographs taken at 20500x of A) NP metestrus, B) day 6, C) day 12, D) day 15, and E) day 18. Bar= 1000nm Analysis of frequency of fibril diameter of F) NP metestrus G) day 6, H) day 12, I) day 15, and J) day 18. n= 8260-13030 fibrils. With permission from Akins (2011) *Biology of Reproduction*. 84(5): 1053-62.

Chapter 3- Role of SLRPs and TGFβ Signaling in Cervical Remodeling

3.1 Introduction

The cervical extracellular matrix is composed of interacting factors that work together to change the biomechanical strength of the tissue. As discussed in the previous chapter, collagen and other collagen-modulating extracellular matrix components are regulated during gestation.

One important component of the ECM that modulates collagen function is proteoglycans (PGs). They consist of a protein core with one or more covalently attached glycosaminoglycan (GAG) chain (Iozzo, 1999). PGs have many diverse functions that include controlling collagen fibrillogenesis and initiating cell signaling cascades that affect cell proliferation, migration and death (Scott and Parry, 1992; Iozzo, 1998). The GAG chains that attach to the protein core are made up of repeating units of disaccharides (heparin sulfate, chondroitin/dermatan sufate or keratin sulfate). GAG chains help control the osmotic properties of a tissue by controlling hydration and equilibrium tension. They may also play a role in cell signaling (Aszodi et al., 2006). Several proteoglycans are expressed in the pregnant cervix including versican, decorin, biglycan, asporin and fibromodulin (Danforth et al., 1974; Norman et al., 1991; Osmers et al., 1993; Westergren-Thorsson et al., 1998; Read et al., 2007). Versican is a large molecular weight proteoglycan that has multiple GAG chains attached to the protein core while

decorin, biglycan, asporin and fibromodulin belong to the small leucine-rich proteoglycans (SLRPs) family of proteoglycans.

SLRPs are a subset of PGs that have small protein cores made up of a number of leucine-rich repeats which can make up 80% of the protein (Iozzo, 1999). These include biglycan, decorin, asporin, fibromodulin and several other related proteins (Kalamajski and Oldberg, 2010). Many SLRPs can bind collagen and have been shown to regulate collagen fibrillogenesis, organization, and accessibility of collagenases to recognition sites on collagen molecule (Aszodi et al., 2006; Geng et al., 2006; Kalamajski and Oldberg, 2010). While it is known that SLRPs interactions in the ECM are important for organization, mechanical strength and signaling, the exact mechanisms are still unknown.

Decorin, a widely studied SLRP, is highly expressed in the cervix (Danforth et al., 1974; Uldbjerg et al., 1983; Norman et al., 1991; Westergren-Thorsson et al., 1998). Collagen molecules, *in vitro,* can self-assemble into fibrils without the addition of any outside, aiding factors. The addition of decorin to this system retards the rate that collagen fibrils assemble and results in thinner collagen fibrils, highlighting decorin's role in controlling fibril size (Vogel and Trotter, 1987). Decorin can bind collagen and is important in lateral fusion of collagen fibrils and maintaining even interfibrillar spacing (Danielson et al., 1997; Reed and Iozzo, 2002). Knockout animals present with skin fragility and collagen

fibrils in skin and tendon appear enlarged with abnormal outlines (Danielson et al., 1997).

Not only do SLRPs play a role in regulating collagen fibril diameter, but they also bind to a number of growth factors and subsequently regulate cell survival, migration and other essential cellular pathways. Decorin, biglycan, fibromodulin and lumican have all been shown to bind and regulate TGFβ (Transforming growth factor beta-1)(Hildebrand et al., 1994). TGFβ is a growth factor that regulates cell death and acts mainly as a growth inhibitor; it has also been implicated in a number of fibrotic diseases and has been shown to be a potent regulator of many ECM genes. TGFβ can upregulate expression of collagens and other supporting ECM proteins as well as increase the expression of collagenase inhibitors. TGFβ also affects expression of integrin receptors, which bind numerous ECM ligands (Heino et al., 1989a; Heino and Massague, 1989b; Riikonen et al., 1995). It has been shown to both increase and decrease integrins in different cell types thus affecting the adhesion of cells to the matrix.

Synthesis involves cleavage of the pro-TGFβ into its two parts: latency-associated protein (LAP) and TGFβ. Even though they are cleaved, the LAP and TGFβ remain associated with one another through non-covalent interactions. This dimer is known as the small-latent TGFβ complex. This complex interacts with the latent TGFβ binding protein (LTBP) to form the large-latent TGFβ

complex (Hyytiainen et al., 2004). TGFβ is secreted from the cell in the large-latent TGFβ complex. After secretion, the LTBP is important for targeting the TGFβ complex to the ECM (Taipale et al., 1994). While entrapped within the LTBP and the LAP in the ECM, TGFβ is unable to signal through any cell surface receptors. In order to signal, the latent TGFβ complex must be activated through cleavage from the LAP and LTBP. Many factors including plasmin, thrombospondins, integrins, pH, and temperature sensitivity can all activate TGFβ (Hyytiainen et al., 2004).

Decorin is known to be an inhibitor of TGFβ activity (Yamaguchi et al., 1990; Border et al., 1992). Studies in the kidney have shown that decorin suppressed TGFβ activity to a similar level as TGFβ blocking antibodies (Border et al., 1992). Decorin and biglycan have been implicated in trapping and sequestering TGFβ in the ECM thus limiting its association to receptors, but without inactivating it completely (Hausser et al., 1994; Aszodi et al., 2006).

Understanding the expression and roles of proteoglycans in modulating cervical collagen structure, fibrillogenesis and cell signaling cascades is a focus of the current study. As described in Chapter 2, collagen fibril diameter increases progressively over the course of pregnancy and is maximal at term. We hypothesized that a decline in decorin at the end of pregnancy may account for the increase in fibril diameter seen at term, and that TGFβ signaling, which would be

depressed by the presence of decorin, is activated during cervical ripening to upregulate ECM proteins and aid in postpartum repair.

3.2 Results

3.2.1 Proteoglycan Expression

Given the ability of small leucine rich proteoglycans to modulate collagen structure, the mRNA expression for decorin, biglycan, fibromodulin, asporin and osteomodulin were quantified by QPCR (Figure 3-1). Decorin, biglycan, and osteomodulin mRNA levels showed no significant changes throughout pregnancy (Figure 3-1A-C). Asporin levels remain constant throughout pregnancy, with a transient upregulation 2 hours postpartum (Figure 3-1D). Fibromodulin levels remain constant throughout gestation and were significantly downregulated postpartum (Figure 3-1E).

3.2.2 Decorin Expression and Cell Location

Decorin mRNA is highly expressed and constant in the cervix during gestation, parturition and postpartum repair (Figure 3-1A). Because decorin function can be regulated by alterations in expression of the protein core as well as changes in the intact proteoglycan containing GAG chains, protein blotting was performed using cervical protein. Three western blots were done for each condition, however, the decorin antibody proved un-strippable, therefore no loading controls were possible. Western blots of decorin with GAG chain attached revealed constant expression of protein that ran as a smear around 100 kD. After

removal of GAG chain by chondroitinase ABC enzyme treatment, the core decorin protein level was constant and resulted in a band that migrates at 40 kD (Figure 3-2). Decorin extracted from skin has a shorter GAG chain as compared to the cervix which migrates at approximately 50-60 kD. (Figure 3-2 Lane 1).

To identify the cell specific expression of decorin transcripts in the cervix, *in situ* hybridization was carried out in day 15 (Figure 3-3A) and day 18 (Figure 3-3B) cervical samples. *In situ* revealed that decorin is produced primarily in the cervical stroma, with minimal expression in the epithelia (Figure 3-3). No change was observed in the amount of mRNA present at these time points.

3.2.3 GAG composition

The GAG chain that is attached to the decorin core protein plays an important role in signaling, binding, and structural support of the tissue (Aszodi et al., 2006). Decorin can contain chondroitin–sulfated, dermatan-sulfated, or hybrid GAG chains. The degree of sulfation, type of GAG chain and length of the GAG chain may affect decorin function. Decorin protein levels are constant during pregnancy; however, GAG chain composition may be altered during pregnancy.

To assess GAG chain composition and length western blotting of protein extracts digested with GAG-specific enzymes were performed. Cervical samples were treated with chondroitinase ABC (cleaves all chondroitin/dermatan chains), chondroitinase AB (cleaves only chondroitin-4-sulfate and chondroitin-6-sulfate

chains), and chondroitinase B (cleaves only dermatan sulfate chains). Samples were then run out on a 4-20% gel to assess changes in size of the enzyme-treated decorin. NP, days 10, 12, 16, 18 and 12 and 24-hours postpartum cervices were assessed. As noted before, there was no difference in expression of untreated decorin in the analyzed time points. NP samples cleaved with chondroitinase ABC or AC showed similar cleavage in both reducing the proteoglycan size from ~100kD to 40kD. The remaining samples were treated only with chondroitinase AC or B. Chondroitinase AC treatment showed the same cleavage as in NP samples chondroitinase AC samples for all other time points. When treated with chondroitinase B decorin ran slightly higher at all time-points. This data indicates that cervical decorin is comprised of hybrid GAG chains containing both chondroitin and dermatan sulfate (Figure 3-4). When first performing these experiments, we believed they would show us the composition of the GAG chains attached to the decorin protein core. However, it became clear that the entire chain was cleaved at the PG:GAG interface, eliminating any information about the percentage of dermatan sulfate to chondroitin 4 or 6-sulfate. While this experiment shows the existence of hybrid chains, the relative composition remains to be elucidated. While decorin can bind to collagen without the GAG chain attached, studies have shown that the ratio of chondroitin sulfate to dermatan sulfate can affect collagen fibril diameter, highlighting the importance

of understanding specific changes in GAG composition in our model (Kuc and Scott, 1997).

3.2.4 Dcn$^{-/-}$ Cervical Phenotype

Decorin knockout mice have abnormal skin collagen fibril circumferences and as well as marked skin fragility (Danielson et al., 1997). A colony of these mice was established in our laboratory in order to investigate the affect of decorin loss on cervical function in pregnancy and labor. Timed mating studies and observation of parturition timing in decorin null mice revealed no variation in gestation length as compared to wild-type mice.

While cervical function appeared normal, assessment of cervical collagen ultrastructure in electron micrographs revealed sporadic fibrils with abnormal morphology (Figure 3-5). The abnormal collagen morphology observed in the nonpregnant *Dcn*$^{-/-}$ mice mouse cervix was similar to our observations in *Dcn*$^{-/-}$ skin and tail samples and is consistent with previous reports in skin and tendon Danielson *et. al.* (Danielson et al., 1997).

3.2.5 Dcn$^{-/-}$ Collagen Solubility

Abnormal morphology of collagen fibers may result in collagen fibers with increased solubility in acetic acid and pepsin. Solubility was measured in cervices collected from NP metestrus *Dcn*$^{-/-}$ mice and compared to WT controls. Collagen solubility was not altered significantly in *Dcn*$^{-/-}$ NP mice as compared to

WT controls (Figure 3-6A). In addition, no change in total collagen content (Figure 3-6B) or water content (Figure 3-6C) was observed in NP *Dcn*$^{-/-}$ mice.

Dcn$^{-/-}$ *SHG*

Morphological changes in collagen I fibers can be assessed via second harmonic generation (SHG) microscopy. (Discussed in more detail in Chapter 4). SHG signal for *Dcn*$^{-/-}$ mice was evaluated at day 15 and day 18 of gestation (Figure 3-7A&B). Fiber diameter (average diameter of collagen I SHG signal) and porosity (area lacking signal within the micrograph image) was quantified. Fiber diameter increased in both forward and backward directions from day 15 to day 18 in null animals (Figure 3-7 C&D). Pore number (Figure 3-7E) declined while size (Figure 3-7F) and spacing (Figure 3-7G) increased. Pore fractional area did not change in the forward direction (Figure 3-7H). All changes in morphological assessment of *Dcn*$^{-/-}$ mice are similar to changes seen between normal gestation days 15 and 18 reported in Chapter 4 (Akins et al., 2010).

3.2.6 Thrombospondin 1 Levels

Thrombospondin 1 is a matricellular protein that is a potent activator of TGFβ (Hyytiainen et al., 2004). Levels of *Thbs1* were seen to increase ~4 fold from day 18 to 12 hours post partum in microarray studies (Timmons and Mahendroo, 2007). To confirm microarray data, QPCR was carried out to assess relative levels of *Thbs1* mRNA during normal gestation in wild type mice. Relative to NP, *Thbs1* expression declines by gestation day 10 and levels remain

low in the cervix for the remainder of pregnancy. At 24 hours postpartum there is a 10-fold upregulation of *Thbs1* (Figure 3-8).

3.2.7 TGFβ Activity

Decorin is known to be an inhibitor of TGFβ signaling and is expressed at high and constant levels throughout pregnancy. *Thbs1*, a potent activator of TGFβ, remains low throughout pregnancy. However, *Thbs1* becomes highly upregulated during postpartum repair, while decorin levels remain at a steady state, thus changing the ratio of inhibitor to activator. We hypothesized that this change in ratio would cause an activation of TGFβ during postpartum repair; when matrix synthesis is upregulated to facilitate repair and recovery to nonpregnant state. In order to assess levels of TGFβ activation during parturition we measured active TGFβ levels in the cervix during pregnancy and parturition. NP, days 12, 15, 18, and 12 and 24 hour postpartum cervices were assessed for activated-TGFβ. Unexpectedly, no change was observed in the amount of TGFβ activation over gestation or during the postpartum period (Figure 3-9). However, at all time points levels of activated TGFβ were very low in cervical tissue; less than 0.2 pg/μg tissue. Even with 300 μg of protein loaded per time point, measurements were consistently at the lower end of the standard curve. It is possible that this assay is not sensitive enough to measure small changes in

local cervical TGFβ levels. Further studies are needed to look at the downstream components of the TGFβ pathway to confirm these results.

3.3 Discussion

Previous studies in both human and animal models report conflicting results with respect to proteoglycans in the pregnant cervix. Several studies report increased decorin concentration with the progression of pregnancy, while others report no change in decorin during pregnancy (Kokenyesi and Woessner, 1990; Norman et al., 1991; Westergren-Thorsson et al., 1998; Leppert et al., 2000). In this study cervical mRNA levels of SLRPs through mouse gestation indicated no change in SLRPs during pregnancy, however some are upregulated in the postpartum period (Figure 3-1).

Experiments summarized in this Chapter looking at expression of decorin mRNA shows high and constant expression throughout pregnancy (and in nonpregnant tissue). Consistent with mRNA expression, western blots also show constant expression of decorin protein in the cervix. Decorin is produced in a pro-form, so it is possible that the active form of decorin changes during pregnancy, however, the expression of *Bmp1* (the enzyme responsible for cleaving pro-decorin) remains constant during gestation suggesting that decorin

activation is not regulated in the cervix during pregnancy (Figure 2-3) (von Marschall and Fisher, 2010).

Decorin GAG chains appear to exist as hybrid GAGs (Figure 3-4). Additional studies are required to determine if changes in the ratio of dermatan to chondroitin sulfate of the decorin GAG chain occur and if these changes modulate cervical function. Studies have shown that the concentration of total GAGs increases during pregnancy and the composition changes as well (Danforth et al., 1974; Osmers et al., 1993). Other GAGs, especially hyaluronan may be responsible for these changes. Measuring GAG composition of individual proteoglycans with more sensitive tools such as FACE (fluorophore assisted carbohydrate electrophoresis) may shine more light on the changes that occur in chain composition (Straach et al., 2005).

Despite increased expression of *Thbs1,* TGFβ levels remained low during postpartum. It is possible that *Thbs1* levels are not high enough relative to decorin to overcome the inhibition TGFβ by decorin. However, it has been shown that THBS2 counteracts activation of TGFβ by THBS1, presumably by competitively binding the TGFβ (Schultz-Cherry et al., 1995). In chapter 2 we show that *Thbs2* levels are highly upregulated during the same time as *Thbs1* activation, which could in part, explain why no increase in active TGFβ is seen in the cervix postpartum. It is also possible that TGFβ activation is seen later in the postpartum period. *Thbs1* levels were not upregulated until 24 hours postpartum,

which is the latest time-point we assessed for TGFβ levels. However, Dailey *et.al.* measured TGFβ mRNA as well as downstream components of the TGFβ pathway in the rat cervix. They found an increase in phosphorylated SMAD2 (mothers against decapentaplegic homolog 2) at term (Dailey et al., 2009). We do not see indication in this study of TGFβ activation before or after term pregnancy, however, due to low levels of TGFβ in the cervix, it is possible that this assay was not sensitive enough to detect small changes in local TGFβ activity. Further studies must be undertaken to validate these results.

Studies from *Dcn*$^{-/-}$ mice have shown that cervical collagen fibril shape is affected by loss of decorin. However, no parturition phenotype was observed, as well as no change in collagen solubility, content or water content. If cervical tissue biomechanics are affected in *Dcn*$^{-/-}$ mice, it suggests that genetic defects leading to reduced decorin synthesis may contribute to cervical insufficiency in women. Further studies are required to test this hypothesis. Direct measurements of cross-links and biomechanical testing of the cervix needs to be performed in these mice to correctly address the contribution decorin plays in structural stability of the cervix. SHG morphological measurements also showed similar patterns to changes seen in WT day 15 and 18. This could be due to the fact that not all collagen fibrils are affected (Figure 3-5). TEM of gestation day 15 and day 18 *Dcn*$^{-/-}$ mice should be carried out to assess the morphological affects of loss of decorin on collagen fibrillogenesis during parturition.

It is possible that other SLRPs such as biglycan are compensating for the loss of decorin in *Dcn*$^{-/-}$ mice. Biglycan is also highly expressed in the cervix and can bind collagen and TGFβ (Figure 3-1B) (Schonherr et al., 1995; Ameye and Young, 2002). However, no compensatory upregulation of biglycan has been observed in *Dcn*$^{-/-}$ mice. Loss of both decorin and biglycan leads to an increase in activated TGFβ in the extracellular matrix (Bi et al., 2005). The decorin/biglycan double knockout mouse has recently been reported to exhibit a preterm birth phenotype. Fetal membranes from these animals are disorganized, suggesting a possible PPROM phenotype. Since decorin and biglycan are produced in the ECM of the uterus, placenta, fetal membranes and the cervix, causation of preterm birth in the decorin/biglycan knock-out mouse has yet to be determined (Calmus et al., 2011). However, these mice highlight the importance of these proteoglycans in parturition.

3.4 Materials and Methods

3.4.1 Animal and Tissue Collection

Females were housed overnight with males and separated the following morning. Vaginal plugs were checked at the time of separation; mice with plugs were considered to be day 0 of their pregnancy with birth occurring early on gestation day 19. In general, cervices were collected at noon for all time points from gestation d8-18 except day 18 for which cervices were collected between 6-

7 PM in order to collect cervices a few hours prior to onset of labor. Postpartum cervices collected after vaginal birth on gestation d19 were obtained *exactly* 2 or 4 hours after delivery of the first pup or *approximately* 10-12 hours, 24 hours or 48 hours after delivery of the first pup.

Mice used for these studies were of C57B6/129Sv mixed strain and mice with exon 2 of the decorin gene disrupted (Danielson et al., 1997). Cervical tissue was dissected out of the reproductive tract and vaginal tissue was removed. Cervices were flash-frozen in liquid nitrogen immediately following their extraction. All studies were conducted in accordance with the standards of humane animal care described in the National Institutes of Health Guide for the Care and Use of Laboratory Animals using protocols approved by an institutional animal care and research advisory committee (Committee for the Update of the Guide for the Care and Use of Laboratory Animals, 2011).

3.4.2. Immunoblotting

Proteoglycans were extracted in 4M guanidine HCL 100mM sodium acetate with 1% protease inhibitor for 48 hours at 4°C. Samples were then dialyzed for 4 hours in 0.1M NaCl 0.1M Tris HCL pH 7.3. Protein concentration was determined by a Bradford protein assay (Pierce, Thermo Scientific, Rockford, Il). To evaluate the core protein without GAG chain, samples were incubated with 1uL Chondroitinase AC, B, or ABC (Seikagaky Corp, Tokyo, Japan) for 2 hours at 37°C. These enzymes cleave chondroitin-4-sulfate and chondroitin-6-sulfate

chains, dermatan sulfate, and all chondroitin/dermatan chains, respectively. Samples then underwent ethanol precipitation at -20°C and protein was resuspended in 0.5M Tris HCL/0.5% SDS. Twenty-five micrograms of protein was loaded on a 4-20% Tris-HCL polyacrylamide gel and electrophoresed at 100V. The gel was transfer to nitrocellulose membrane at 100V for 1.5 hours and Ponceu S (Sigma) staining was used to assess equal loading of protein. Immunoblotting was performed using rabbit polyclonal anti-human decorin (LF-113, Gift from Dr. Larry Fisher, NIH).

3.4.3 In Situ Hybridization

Mice were perfused with 4% paraformaldehyde on day 15 and day 18 of gestation. Cervices were collected, paraffin embedded, and sectioned. *In situ* hybridization was performed as described previously by the Molecular Pathology core at UT Southwestern Medical Center (Shelton et al., 2000). Probes for decorin were labeled with UTP ^{35}S.

3.4.5 Electron Microscopy

Nonpregnant mice in metestrus were perfused with 1% glutaraldehyde, 2% paraformaldehyde fixative in 0.1M phosphate buffer. Cervical and uterine tissue was removed and fixed in 2.5% glutaraldehyde in 0.1M cacodylate buffer containing 0.1% ruthenium red overnight at 4^0C. The cervix was rinsed for 30 minutes with cacodylate buffer. The tissue was post-fixed with 1% osmium in 0.1M cacodylate buffer containing 0.1% ruthenium red for 90 minutes.

Specimens were dehydrated through a graded series of ethanols (50%, 70%, 95%, 100%) followed by propylene oxide and embedded in Epon. Thin sections were stained with uranyl acetate and lead citrate. Sections were viewed on a TEM Tecnai microscope (FEI Company, Hillsboro, Oregon) and images captured at 4200x or 20500x with a Morada 11 1 megapixel CCD camera.

3.4.6 Hydroxyproline Assay

Frozen cervical tissue was lyophilized. Water content was determined by subtracting dry weight from wet weight. Hydroxyproline assay was carried out as described previously (Read et al., 2007). Briefly, samples were reconstituted in 0.5M acetic acid with 1mg/mL pepsin (Sigma) at 4°C for 24 hours. Next samples were centrifuged at 13.4g for 10 minutes to separate supernatant from pellet. Both supernatant (containing soluble collagen) and pellet (containing insoluble collagen) were hydrolyzed in 6M HCl at 100°C for 20-22 hours. Amount of hydroxyproline was measured in both sample via hydroxyproline assay (Stegemann and Stalder, 1967).

3.4.7 Second Harmonic Generation

Cervices of decorin knockout mice were obtained from 3 mice at gestation days 15 and 18. Cervical tissue was snap frozen at liquid nitrogen temperature in OCT (Tissue Tek, Indiana). The entire length of the cervix was cut transversely into 50 µm serial sections. Sections were mounted in 0.1 M PBS on glass slides

under #1.5 glass coverslips (Corning, Corning, NY). Images were collected and analyzed as described in Chapter 4.

3.4.8 ELISA

Cervical tissue was flash frozen and homogenized in RIPA buffer. Homogenates were assessed for protein concentration using BCA Assay. 300ug of cervical protein was immediately measured for active TGFβ levels using TGFβ ELISA Duoset (R&D Systems DY1679, Minneapolis MN). ELISA for active TGFβ was performed using manufacturer's protocol.

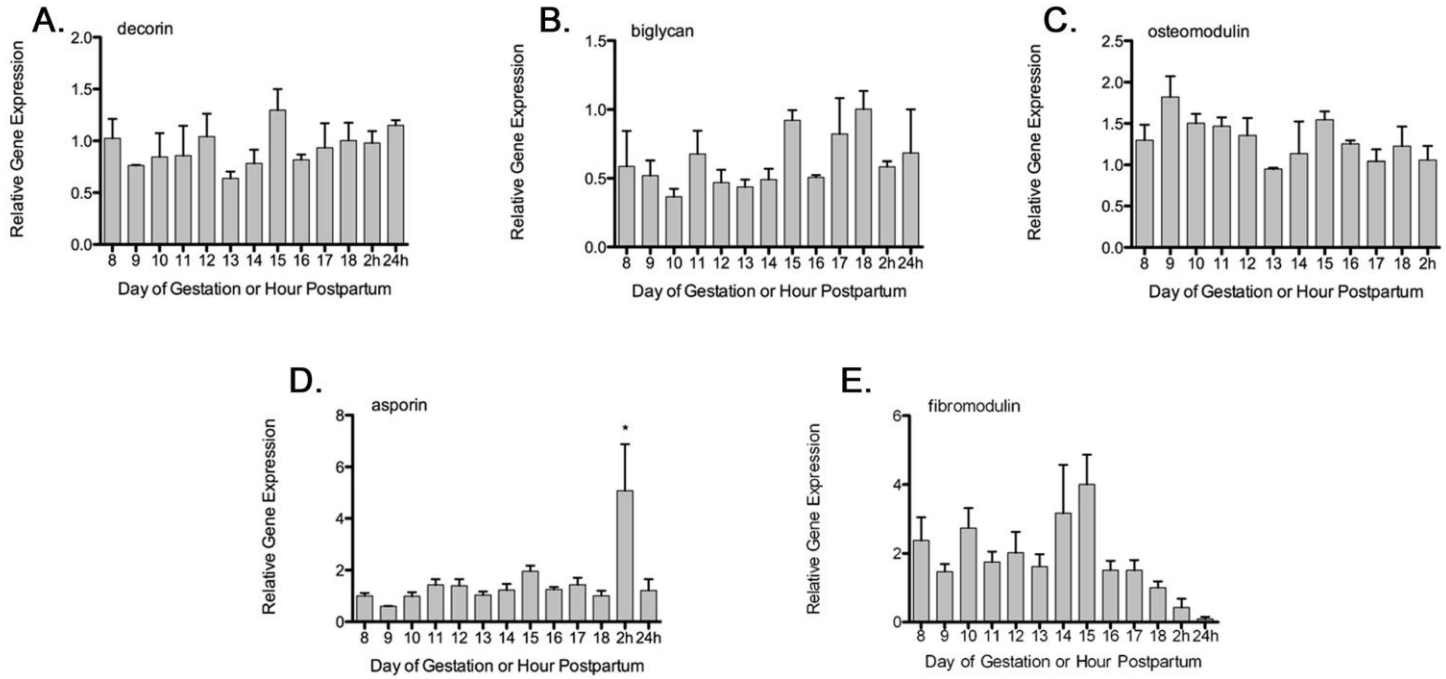

Figure 3-1. Cervical Proteoglycan mRNA Expression during Pregnancy and Parturition. mRNA levels of A) Decorin, B) Biglycan, C) Osteomodulin, D) Asporin, and E) Fibromodulin were determined via QPCR on gestation days 8, 9, 10, 11, 12, 13, 14, 15, 16, 17, 18, 2 hours postpartum and 24 hours postpartum and normalized to day 18. n= 3-6 cervices per time point. * Indicates significance at $p<0.05$. With permission from Akins (2011) *Biology of Reproduction*. 84(5): 1053-62.

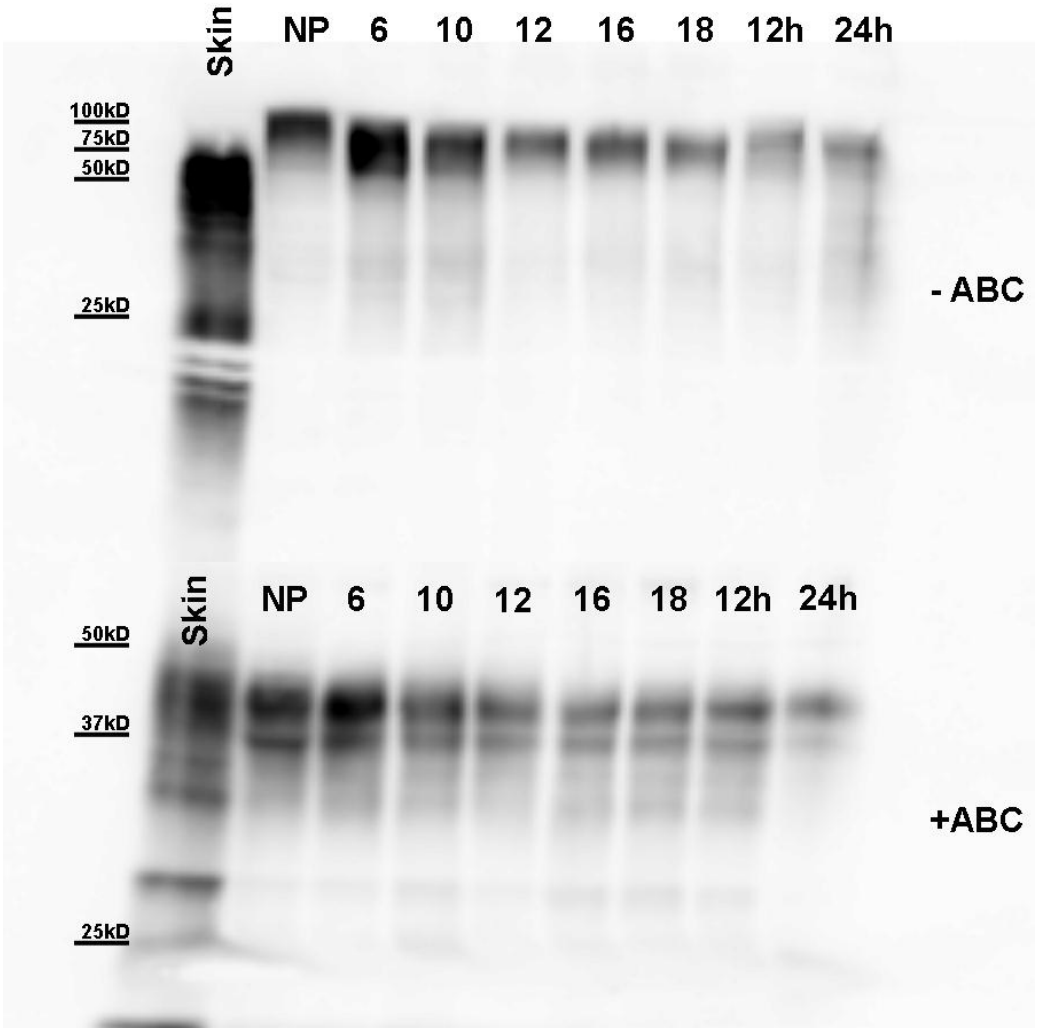

Figure 3-2. Decorin Protein Expression Remains Constant during Parturition. Decorin protein levels were assessed using LF-113 antibody for decorin. Protein was assessed in skin (control), NP cervix, day 6, 10, 12, 16, and 18 of gestation and 12 and 24 hours postpartum. Samples were assessed with or without cleavage of GAG chain by Chondroitinase ABC enzyme. Decorin from the cervix with GAG chain attached runs approximately 100kD while untreated decorin from skin runs approximately 50-60kD (lane 1). After Chondroitinase ABC treatement decorin core protein runs approximately 40 kD. Loading controls were not possible due to decorin antibody's failure to strip. Blots were repeated 3 times.

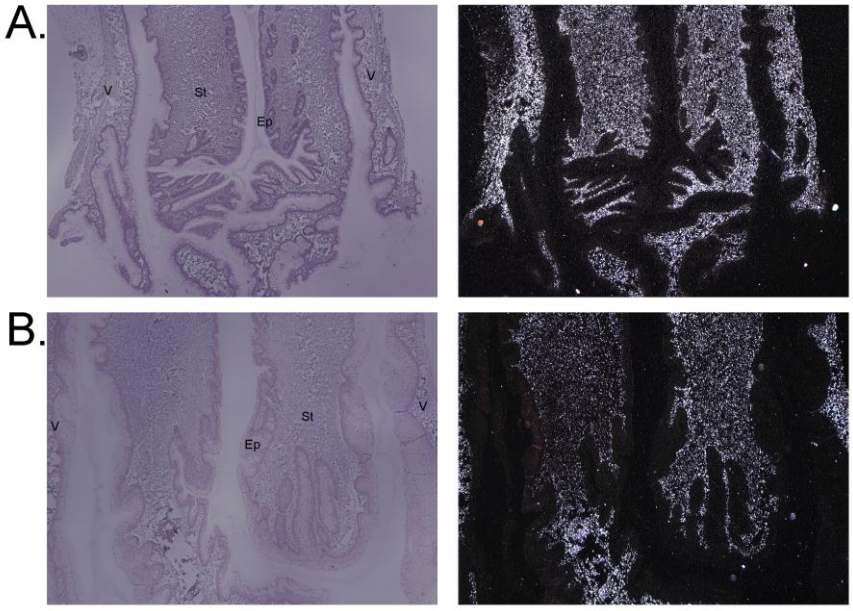

Figure 3-3. Decorin mRNA is Localized to Cervical Stroma. *In situ* hybridization was performed to assess localization and expression of decorin mRNA in cervical tissue at A) day 15 and B) day 18 of gestation. Decorin is localized to the cervical stroma as addressed by silver staining. Brightfield images are in the left and darkfield silver stain is seen on the right. St= stroma, Ep= epithelia, V= vaginal tissue.

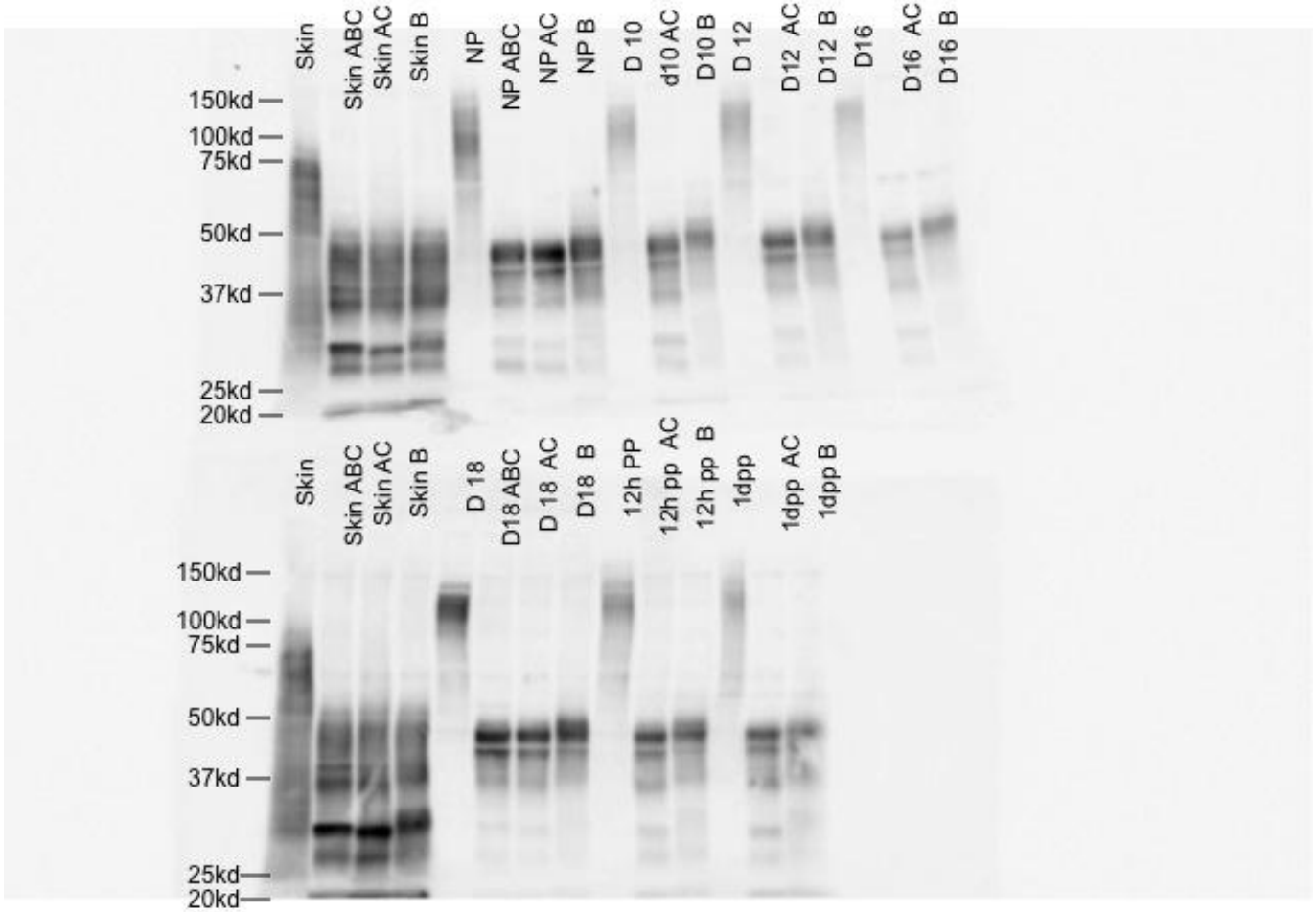
Skin
Skin ABC
Skin AC
Skin B
NP
NP ABC
NP AC
NP B
D 10
d10 AC
D10 B
D 12
D12 AC
D12 B
D16
D16 AC
D16 B
150kd
100kd
75kd
50kd
37kd
25kd
20kd
Skin
Skin ABC
Skin AC
Skin B
D 18
D18 ABC
D 18 AC
D18 B
12h PP
12h pp AC
12h pp B
1dpp
1dpp AC
1dpp B
150kd
100kd
75kd
50kd
37kd
25kd
20kd

Figure 3-4. Characterization of GAG Chain Composition of Decorin. Cervical proteoglycans were incubated with chondroitinase ABC, chondroitinase AC or chondroitinase B. Samples were assessed in skin (control), NP cervix, day 6, 10, 12, 16, and 18 of gestation and 12 and 24 hours postpartum.

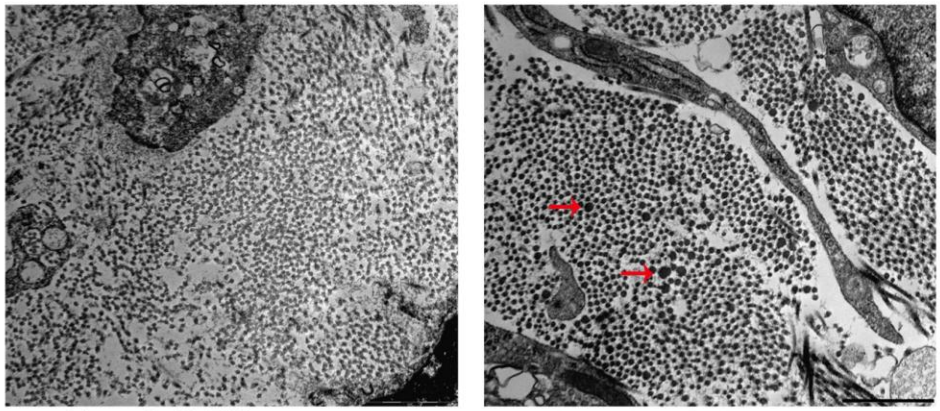

Figure 3-5. Loss of Decorin in the Cervix Causes Abnormal Collagen Fibril Morphology. Electron micrographs of WT (A) and *Dcn*$^{-/-}$ (B) NP metestrus cervical ECM taken at 4200x on A) Da and B) Day 18 of pregnancy. Bar= 1000nm

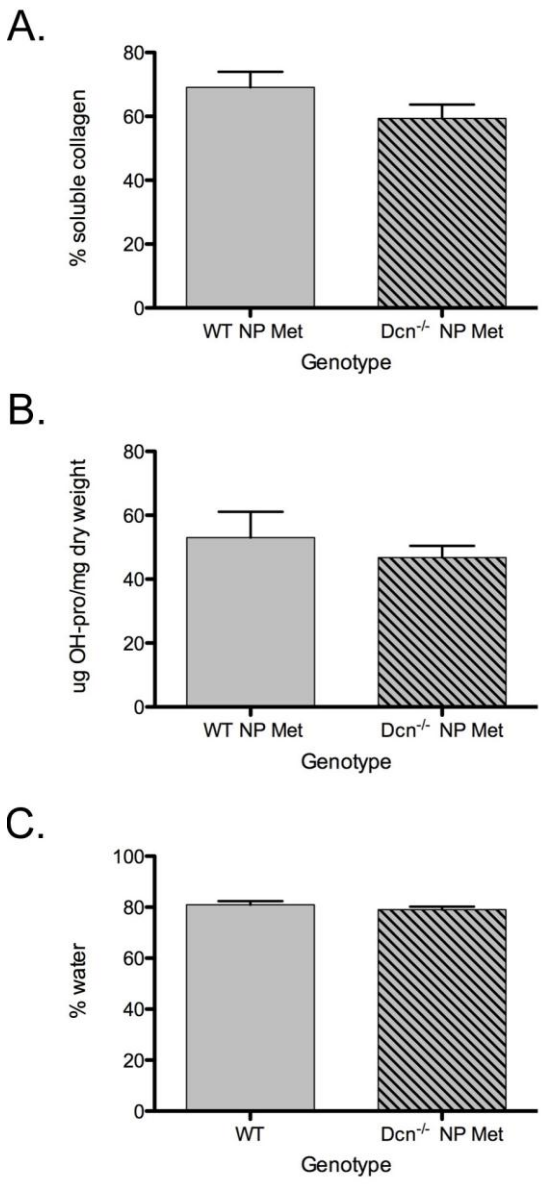

Figure 3-6. Loss of Decorin Does Not Change Collagen Content, Collagen Solubility, or Water Content in the Nonpregnant Cervix A) Collagen solubility B) collagen content and C) water content was assessed by hydroxyproline assay in WT and *Dcn*$^{-/-}$ NP metestrus cervices. No significance was seen between WT and *Dcn*$^{-/-}$ n=6 for WT and n=5 for *Dcn*$^{-/-}$ Error bars represent standard error of the mean.

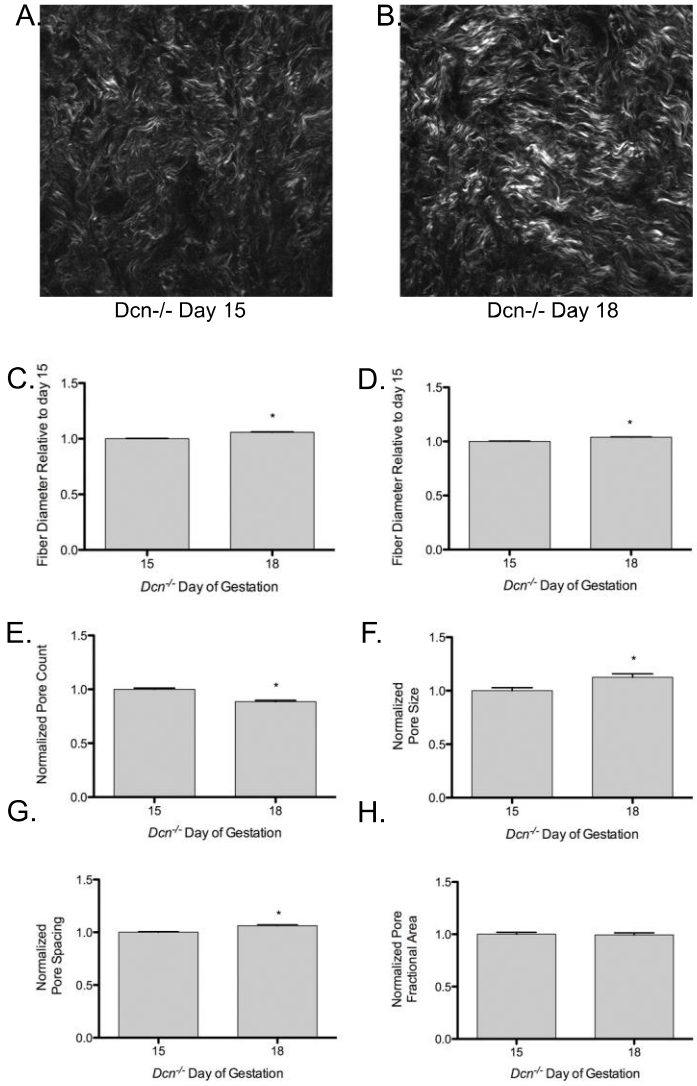

Figure 3-7. Changes in Morphological Structure of Collagen from Gestation Days 15 and 18 in *Dcn*$^{-/-}$ Cervices are Indistinguishable from Wildtype. Visual inspection of images from (A) gestation day 15 *Dcn*$^{-/-}$ cervices and (B) gestation day 18 *Dcn*$^{-/-}$. Fiber diameter of day 15 and day 18 *Dcn*$^{-/-}$ cervices was assessed in both C) Forward and D) Backward directions. Fiber diameter increased significantly in both directions ($P<0.0001$). The number of pores in images declined in *Dcn*$^{-/-}$ cervices from day 15 to day 18 (E, $P<0.001$). Pores were significantly larger in diameter (F, $P=0.0041$) and spaced farther apart

(G, P<0.0001). Pore fractional area did not significantly change between day 15 and day 18 in *Dcn*$^{-/-}$ cervices. Error bars represent standard error of the mean of 100 images for day 15 and 95 images for day 18. n=3 animals/time point.

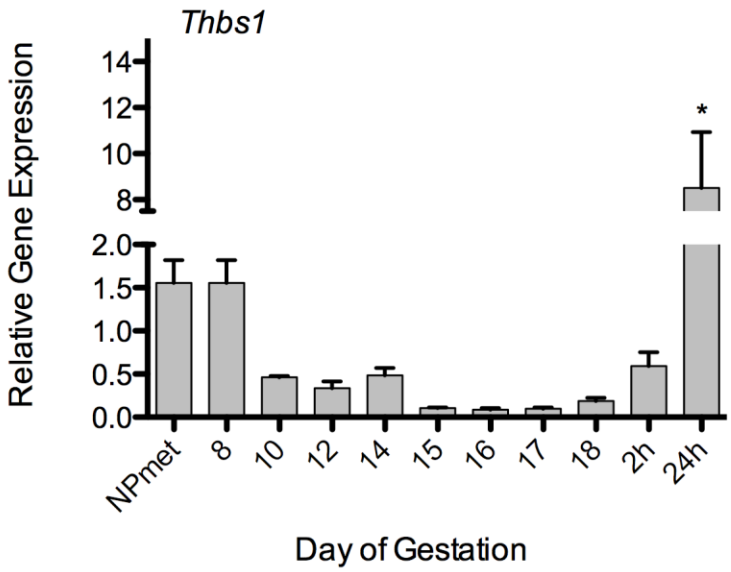

Figure 3-8. Thrombospondin 1 mRNA Levels Decline During Pregnancy and Parturition. Thrombospondin 1 levels were measured via QPCR in NP, gestation days 8, 10, 12, 14, 15, 16, 17, 18, and 2 and 24 hours postpartum. Samples were normalized to day 8. n= 4-6 cervices per time point. Error bars represent standard error of the mean. * Indicates significance at $p<0.0001$.

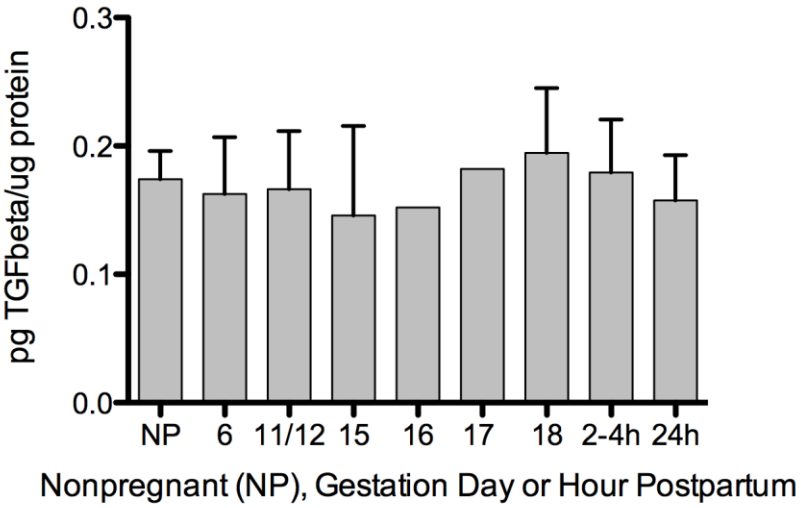

Figure 3-9. Activated TGFβ levels in the Cervix During Gestation. 300μg of cervical protein was assessed for activated TGFβ levels via ELISA in NP, gestation days 6, 11/12, 15, 16, 17, 18, and 2 and 24 hours postpartum. Samples were normalized for pg TGFβ per ug protein. n= 3 for NP, 11/12, 15, 18, and 2 and 24 hours postpartum. n=1 for day 16 and day 17. Error bars represent standard error of the mean.

Table 3-1 QUANTITATIVE SHG MEASUREMENTS OF DECORIN KNOCKOUT CERVICAL COLLAGEN

Gestation Day/Treatment	**Fiber Diameter (um ± SEM)**		**Number of Pores (± SEM)**		**Pore Diameter (um ± SEM)**		**Pore Spacing (um± SEM)**		**Pore Fractional Area (% ± SEM)**	
	Forward	Backward	Forward	Backward	Forward	Backward	Forward	Backward	Forward	Backward
***Dcn*$^{-/-}$ Day 15**	2.31 ±0.008	2.96 ±0.009	898 ±10.5	522 ±9.8	18.6 ±0.51	27.7 ±0.9	7.73 ±0.045	10.24 ±0.1	30.5 ±0.56	25.8 ±0.51
***Dcn*$^{-/-}$ Day 18**	2.45 ±0.008	3.08 ±0.008	796 ±11.1	471 ±7.6	20.9 ±0.62	26.8 ±0.63	8.22 ±0.05	10.71 ±0.08	30.3 ±0.60	23.2 ±0.46

Chapter 4 -Second Harmonic Generation Imaging for Distinguishing Cervical Collagen during Pregnancy

4.1 Introduction

As discussed in chapter 1, better understanding of the normal birth process and development of improved clinical tools to identify women at risk for preterm birth are keys to solving this global problem. Synchronized uterine contractions and the successful remodeling of the cervix are required for natural labor and delivery to occur. The cervix is comprised of a stroma containing fibroblasts embedded in extracellular matrix (ECM) made up of primarily of type I and to a lesser extent type III fibrillar collagen, proteoglycans and hyaluronan. In preparation for birth the cervix undergoes an extensive transformation changing from a closed rigid structure to one that can allow passage of a term fetus through the birth canal (Leppert, 1995; Read et al., 2007; Word et al., 2007). Biomechanical studies in mouse and human cervix reveal that changes in cervical compliance begin early in pregnancy and continue progressively thereafter; culminating in dramatic loss of tensile strength at the end of gestation (Figure 1-2) (Read et al., 2007; Mahendroo et.al., 1999; Myers et al., 2008). Current evidence suggests that changes in the extracellular matrix composition of the cervix underlie the progressive increase in cervical compliance and that these processes are well conserved between human and mouse (Straach et al., 2005; House et al.,

2009; Timmons et al., 2010). In early pregnancy alteration in fibril collagen assembly and processing are initiated. Soluble collagen, a marker of immature or unprocessed collagen, is increased in the murine cervix as early as day 7 of pregnancy (Read et al., 2007). Additionally, a decline in collagen cross-links due to reduced expression and activity of lysyl oxidase as well as expression of lysyl hydroxylase is implicated in the alteration of cervical collagen structure during pregnancy (Ozasa et al., 1981; Drewes et al., 2007; Akins et. al., 2011). Similarly in humans, increases in collagen solubility correlate with an increase in cervical malleability preceding birth (Danforth et al., 1974; Maillot and Zimmermann, 1976; Kleissl et al., 1978; Ito et al., 1979; Rechberger et al., 1988; Myers et al., 2008; Myers et al., 2009). The importance of collagen structure to cervical competency in highlighted by the fact that, women with defects in genes involved in collagen assembly or metabolism have a greater incidence of preterm birth due to cervical insufficiency (Warren et al., 2007; Warren and Silver, 2009; Anum et al., 2009a). Despite numerous reports suggesting there is a decline in cervical collagen concentration prior to birth, recent studies report no decrease in collagen content, further highlighting the importance of changes in other properties of the collagen matrix (Leppert, 1991; Read et al., 2007; Myers et al., 2008). Taken all together, there is compelling evidence to suggest that progressive changes in collagen structure accompany cervical remodeling in both women and animal models.

Second harmonic generation (SHG) imaging has recently emerged as a non-invasive tool for high resolution imaging of fibrillar type I collagen in tissues. Simultaneous interaction of two near infrared (NIR) photons with non-centrosymmetric structures can result in emission of a single photon at exactly half the wavelength of the excitation light. In particular, collagen type I produces a very robust SHG signal with a nonlinear excitation wavelength between 700 and 1064 nm, allowing a window of detection from 350-532 nm (Cox et al., 2003; Friedl et al., 2007). Because individual collagen fibrils are the source of the SHG signal, this method has the potential to spatially resolve collagen organization at the sub-micrometer level and provide information regarding physiological changes in collagen structure that correlate with tissue function. When visualizing collagen SHG signal in tissue sections, signals (photons) are emitted in all directions. This allows us to collect two different types of data, termed forward and backward signal. Forward signal is collected from a detector placed on the opposite side of the tissue from the excitation source, and backward signal is reflected back up to a detector on the same side of the tissue as the excitation laser. The greater anisotropy of collagen in the tissue the greater the forward directed signal, while conversely the more disordered the collagen matrix, the more backward directed signal (Lacomb et al., 2008b). Looking at both forward and backward images of a section provides more complete information about the properties of the studied tissue.

A recent SHG study of artificial hydrogels of collagen type I, shows that image features such as pore size and fiber size correlate well with measurements of collagen morphology by other methods such as scanning electron microscopy. These studies also demonstrate that changes in these features reflect the varying biomechanical properties of the collagen gels (Raub et al., 2008). In the present study, we apply SHG microscopy on frozen sections of mouse cervical tissue to characterize quantitatively the changes in collagen structure during cervical remodeling and show that SHG imaging provides a valuable tool to evaluate the progressive changes of collagen structure in the cervical ECM throughout normal pregnancy and in a mouse model of aberrant cervical remodeling. These studies demonstrate that pending the development of suitable endoscopes, SHG imaging has great potential as a tool for staging pregnancy and aberrant remodeling in the obstetrics clinic.

4.2 Results

4.2.1 Collagen Imaging

A robust signal with the appearance of fibrillar collagen was observed in both the forward and backward direction when 50 μm frozen sections of mouse cervix were imaged with nonlinear excitation. To verify that the signals are due to SHG, and not collagen autofluorescence, emission spectra of regions in the cervical stroma from a day 15 sample were obtained at two different excitation wavelengths. SHG signal is approximately ½ the wavelength of the excitation

wavelength, while collagen autofluorescence would have much broader peaks of 465 or 520 nm. Back scattered emission spectra from 382 to 596 nm were obtained from the same field of view with excitation at either 800 nm or 900 nm. In both cases, the emission spectrum had a single narrow peak that shifted from 400 nm to 450 nm with the change in excitation wavelength, as expected for an SHG signal. Two-photon excited fluorescence was not detected with either excitation wavelength (Figure 4-1). When sections were incubated with collagenase B (Sigma, St. Louis) (50 U/mL), the SHG signal rapidly disappeared, confirming that collagen was the primary source of the signal (unpublished result).

4.2.2 Changes in Collagen Morphology during Pregnancy

Cervical collagen organization during pregnancy was evaluated using an excitation wavelength of 900 nm. Forward and back-scattered SHG images were collected from cervical frozen sections in the transverse orientation from nonpregnant mice (NP), and from mice at day 6, 12, 15 and 18 of gestation. Visual inspection of the images revealed numerous striking qualitative differences in morphology at different time points during pregnancy (Figure 4-2). In samples from animals that were NP or day 6 of pregnancy, the cervical stroma exhibited two distinct domains: a prominent circumferential ring of long, straight, highly aligned fibers surrounding a narrower zone immediately adjacent to the lumen where the fibers appear more randomly arranged. The band of circumferentially

oriented fibers was especially evident in the backward SHG images because the SHG signal intensity along the length of the fibers was more uniform compared to the forward direction (Figure 4-2A,B). A similar circumferential band of SHG positive fibers was also observed in some samples from day 12 of pregnancy but was absent from samples taken at day 15 and later in gestation (unpublished results). In the more isotropically organized region adjacent to the lumen, the persistence length of collagen fibers appeared to differ at each stage of pregnancy, with fibers in NP (unpublished result) and day 6 samples appearing relatively straight, while those in samples from later in gestation exhibited a more kinked or undulating appearance (compare Figure 4- 2C,D with Fig. 4-2I,J). In addition, the collagen fiber bundles in samples from late in gestation appeared thicker compared to NP and early gestation, and were laterally associated in broad, loose clusters not seen in the earlier time points. The overall intensity of the SHG signal from NP and early pregnancy (day 6 and 12) samples appeared very low compared to days 15 and 18, and was barely detectable at acquisition settings where the signal from samples at later time points was close to saturation (Figure 4-3). Comparison of the forward and backward images for a given field of view revealed additional features of collagen organization. Backward images revealed clusters of punctate structures that were not always visible in the forward channel (Figure 4-4B arrowhead). The abundance of these structures increased greatly in samples from late in gestation. The punctate features were often aligned next to

fiber bundles visible in both the forward and the backward directions (Figure 4-4). xz and yz projections of the z stacks revealed that the puncta are not cross sections of collagen fibers extending along the optical axis (Figure 4-4C).

4.2.3 Quantitative Analysis of Collagen Structure

Application of relatively simple image analysis tools allows quantification of the morphological differences to be observed. Mean intensity of the SHG signal was measured from images of mouse cervix as described in Methods section 4.4.4. Mean signal intensity in both the forward (F) and backward (B) directions was found to increase significantly from day 6 to day 15 of pregnancy (Table 4-2). Total SHG signal (F+B) increased more than two fold between day 6 and day 12 and another 35% from day 12 to day 15 (Figure 4-3C). F+B on day 18 was not significantly different from day 15 ($p<0.0001$). The ratio of forward to backward detected SHG signal intensity (F/B) decreased two-fold from day 6 to day 12 and then remained unchanged through day 18 (Figure 4-3D). Due to the low sensitivity of the forward detector in our system, we were unable to calibrate the F/B ratio using a fluorescent standard, which is assumed to have F/B = 1. Instead, we used the F/B ratio measured from 10 μm frozen sections of mouse Achilles tendon excited at 830 nm, which is reported to be 24.9 to 1 (Legare et al., 2007). From images of the Achilles tendon sections taken with the same detector settings we used for the intensity measurements of cervix, and using a laser power of 30 mW at the specimen plane, we obtained F/B of 0.45, allowing us to correct

our intensity measurements for the relative sensitivity of the forward and backward detectors using a correction factor of 24.9/0.45 = 55.33. The results show that absolute F/B declines from 130:1 to 56:1 between day 6 and day 12 of pregnancy. However, we note that the SHG signal was greater than 99% forward directed at all stages of pregnancy, which allowed us to acquire images in the forward direction despite the insensitivity of the detector.

The characteristic fiber size and porosity of the collagen matrix as revealed by SHG of serial transverse sections from mouse cervices obtained from NP, and gestation days 6, 12, 15 and late 18 were determined as described in section 4.4.4. We observed no consistent differences in these morphological features as a function of location in the cervix. Inspection of longitudinal sections where the whole length of the cervix can be seen also revealed no obvious location-specific differences in morphology. The results summarized in Table 4-1 represent mean values measured from images taken throughout the length of the cervix. We consistently observed a somewhat larger fiber size in the backward detected images compared with the forward detected images at each time point. Systematic differences in fine detail between forward and backward collected SHG have been observed previously and ascribed to the intrinsically superior spatial resolution of the coherent forward-propagating SHG signal as opposed to the backward signal, which arises almost exclusively from incoherent, isotropic scattering of initially forward directed photons (Theodossiou et al., 2006). In both

sets of images, collagen fiber size compared with NP increased progressively 30 to 40% from early pregnancy (day 6) to late in pregnancy (day 18). The increase at each time point was statistically significant for all conditions (Figure 4-5). The average number of pores decreased modestly from NP to day 6 followed by a further significant decrease from day 6 to day 12 with numbers staying constant for the remainder of gestation. Pore-to-pore spacing increased from day 6 to day 18. In contrast, pore diameter decreased significantly from NP to day 6 and then progressively increased throughout pregnancy reaching significance between day 12 and 15. Pore fractional area decreased significantly from NP to day 6 and remained at the day 6 levels throughout pregnancy. Thus, the trend is toward fewer, larger pores with no significant change in fractional area of the pores during pregnancy (Table 1 and Figure 4-6).

4.2.4 SHG evaluation of Aberrant Cervical Remodeling

Mice deficient in the steroid hormone 5alpha reductase type 1 (5aR1) are unable to metabolize progesterone. Since a withdrawal of progesterone is essential at the end of pregnancy, these mice do not undergo cervical remodeling and do not deliver their pups (Mahendroo et al., 1999). SHG analysis was carried out on gestation day 15 and gestation day 18 cervical sections from mice that lack the steroid hormone 5aR1. Given the lack of cervical remodeling, we anticipated no change in collagen structure from gestation day 15 to day 18 by SHG analysis. As expected, there was no change in fiber diameter, pore size, pore area or total

intensity between day 15 and day 18 in *5aR1*$^{-/-}$ animals (Figure 4-7). A 10% decrease was seen in pore number, where in normal gestation a 16% decline in pore number is observed (Compare Figure 4-6A and 4-7A). Pore spacing in *5aR1*$^{-/-}$ animals also increased by 5% compared to a 21% increase between normal days 15 and 18 (Figure 4-7).

4.3 Discussion

We report the application of SHG microscopy for imaging collagen modifications that begin early in pregnancy and progress to birth. Key findings from this study are the identification of quantifiable changes in SHG signal intensity, collagen fiber size and matrix porosity that accompany progressive changes in collagen organization during normal cervical remodeling. This is accompanied by the finding that SHG morphological measurements can distinguish between normal and aberrant cervical remodeling.

Previous studies utilize autofluorescence spectroscopy of collagen or picrosirius red staining to evaluate changes in collagen ultrastructure during pregnancy and labor (Yu et al., 1995; Maul et al., 2003; Maul et al., 2005; Schlembach et al., 2009). SHG has distinct advantages over both these methods as it allows the visualization of collagen ultrastructure at submicrometer resolution without exogenous staining. Secondly, multiparametric quantitative analysis of SHG images taken from mouse cervix at various stages of pregnancy provides novel insight into collagen matrix reorganization during pregnancy and labor.

Three features of collagen are quantified from SHG images: signal intensity, fiber size and porosity. Total SHG signal intensity (F+B) increased progressively from day 6 to day 15 of gestation, with a more than two-fold increase between day 6 and day 12. In biological tissues, the primary source of SHG signal is reported to be type I collagen (Cox et al., 2003). Because the strength of the overall SHG signal is expected to scale as the square of the number of scattering domains, increased signal intensity can be explained by increased collagen concentration (Moreaux et al., 2001). However, there is no significant change in total collagen content in mouse cervix during gestation (Read et al., 2007). Another possible source of increased SHG signal strength could be an increase in the relative proportion of type I collagen to collagen type III which is not strongly susceptible to SHG (Cox et al., 2003). Protein blots of urea-extractable collagen using antibodies specific for collagen I or III (Abcam, Cambridge) showed no change in the relative amount of collagen type I or type III during gestation in the mouse cervix (Figure 2-1A) and confirmed previous reports that total collagen does not change significantly during pregnancy (Read et al., 2007; Akins et al., 2011). Immunofluorescence staining of frozen sections also revealed no significant changes in the relative amounts or proportions of collagen I and collagen III throughout gestation (Figure 2-1G&H). In biological tissues, changes in SHG signal intensity may also reflect changes in collagen organization that take place along the optical axis on a length scale comparable to

the SHG wavelength and thus provide information on collagen features that are at or below the limit of resolution of the objective lens. In general, an increase in overall SHG intensity may reflect increased fibril diameter, higher packing density of fibrils in fibers or higher packing order (Williams et al., 2005; Lacomb et al., 2008a).

Due to the coherent nature of SHG generation, SHG signals are intrinsically forward propagating. Backward signal can arise in cases where quasi-phase matching occurs due to periodicity of structures along the optical axis. In thick specimens such as the 50 μm frozen sections used here, forward emitted photons may also contribute to the backward signal through incoherent scattering within the tissue (Lacomb et al., 2008b). Changes in the ratio of forward to backward SHG signal intensity are indicative of changes in tissue properties at a length scale on the order of the excitation and emission wavelengths, which are at or below the resolution of the microscope. The more than two-fold decrease we observed in F/B ratio from day 6 to day 12 suggests there may be changes in fibril size and packing, and/or an increase in the scattering coefficient of the tissue during this time period (Lacomb et al., 2008b).

Collagen fibrils are laterally associated into bundles that can be resolved in SHG images and are referred to here as fibers. Quantitative assessment of the characteristic size of these fibers in SHG images shows that characteristic fiber size increases progressively through the course of pregnancy. The increase in

fiber size is accompanied by a transition from relatively straight fibers to kinked or wavy fibers. In general, shorter persistence length of a polymer is associated with reduced bending rigidity. Thus the change in morphology of the bundles is consistent with decreased tensile strength of the collagen matrix as pregnancy progresses toward term. Studies of collagen morphology in tendon and in the skin of a mouse model for osteogenesis imperfecta suggest that waviness correlates with loss of strength (Gutsmann et al., 2003; Williams et al., 2005; Nadiarnykh et al., 2010). Bending or kinking of collagen may reflect the decreased abundance of cross-links in cervical collagen fibrils during the course of pregnancy as has been reported in breast tumor ECM (Levental et.al., 2009; Akins et al., 2011)(see also Chapter 2).

Porosity measurements identify areas where collagen is absent or in a form that does not generate SHG signal, such as soluble collagen or collagen III. These "pores" most likely include spaces occupied by cells or blood vessels, as well as extracellular areas lacking insoluble type I collagen. During pregnancy, we observed that a decline in the number of pores was balanced by an increase in pore diameter, resulting in no net change in pore fractional area. This is consistent with the idea that changes in the collagen organization during normal term pregnancy reflect rearrangement rather than degradation of collagen.

Two additional features of the cervical collagen matrix change during the course of pregnancy. First is the circumferential ring of fibers prominent in day 6

and day 12 specimens that disappear by day 15. A similar region of circumferential collagen fibers, interspersed with smooth muscle cells and fibroblasts, is identified in the cervix of pregnant rat by picosirius red staining and by polarization microscopy (Yu et al., 1995). In rat, the disappearance of this ring of collagen at later stages of pregnancy is accompanied by apoptosis of both smooth muscle cells and fibroblasts (Leppert, 1998). In addition, we observed an accumulation of punctate SHG signal in the backward detected images as pregnancy progressed. Studies of collagen in other tissues report punctate signal in the backward channel and attribute it to unfused segments of immature collagen (Williams et al., 2005). This interpretation is consistent with extensive collagen remodeling during pregnancy and also with a reduced abundance of collagen cross-links at term. In contrast, a recent paper demonstrates that punctate patterns can arise from destructive interference in the backscattered SHG signal, similar to the case of speckle in confocal reflectance imaging, making a fiber that appears continuous in the forward image appear discontinuous in the backward direction (Goodman, 1985; Lacomb et al., 2008b). We note that the punctate structures in the backward channel of cervical images often do not overlap with fibers detectable in the forward direction and in fact tend to interdigitate with fibers visible in the forward direction (Figure 4-4). This suggests that a dramatically different collagen microstructure in these regions produces SHG

with a greatly reduced F/B ratio. Further study will be required to understand the origin of the punctate structures in SHG images of cervical tissue.

The power of SHG imaging as a tool to investigate collagen remodeling is shown in the ability for SHG to distinguish between days of normal pregnancy. This is augmented by the fact that SHG morphological measurements show limited change in a mouse model that is known to have impaired cervical remodeling (Mahendroo et al., 1999). As expected, there was no change between day 15 and 18, a critical time of collagen reorganization, in 4 of the 6 morphological measurements performed. The two parameters that did show significant differences were minimal when compared to normal changes that occur between these time points.

Collagen reorganization during normal pregnancy in mice is characterized by two overlapping regimes. Submicroscopic changes resulting in increased SHG intensity and decreased F/B ratio are complete by day 15. Meanwhile, several macroscopic features change progressively throughout pregnancy, resulting in increased fiber size and pore size, accompanied by a transition from straight to kinked fibers and accumulation of punctate signal in the backward images. While the relationship of these changes to the biomechanical changes occurring over the same time period is not yet clear, we note that increased fiber size and pore size in SHG images of artificial collagen gels correlated with decreased stiffness of the material (Raub et al., 2007; Raub et al., 2008; Raub et al., 2010). Even without a

detailed understanding of the molecular origin of the changes in SHG images during pregnancy, the information obtained by SHG imaging may have value as a diagnostic tool for detecting premature cervical ripening and impending preterm birth in women earlier and with greater accuracy than current measurements of cervical length by sonography (Iams et al., 2001). Application of SHG endoscopes and more sophisticated image analysis algorithms to distinguish the stages of gestation will be required to utilize backscattered SHG as a clinical tool in the obstetrics clinic (Bao et al., 2008; Wu et al., 2009). The ability to better identify women at risk for preterm birth along with improved therapies could have a significant impact in reducing the incidence of prematurity.

4.4 Materials and Methods

4.4.1 Animals and Tissue Collection

Mice used for normal pregnancy studies were of C57B6/129Sv mixed strain. Female mice were housed overnight with male mice and separated the following morning. The presence of a vaginal plug was checked every morning and mice with plugs were considered to be day 0 of their pregnancy with birth occurring early on gestation day 19. Cervices were collected from nonpregnant mice (NP) as well as mice on day 6, 12, 15 and 18.75 of gestation. In general, cervices were collected at noon for all time points except day 18 for which cervices were collected between 6-7 PM in order to collect cervices a few hours

prior to onset of labor. Cervices were dissected with uterus and vaginal tissue still attached in order to control for orientation of tissue during cutting and imaging.

All studies were conducted in accordance with the standards of humane animal care described in the National Institutes of Health Guide for the Care and Use of Laboratory Animals using protocols approved by an institutional animal care and research advisory committee (Committee for the Update of the Guide for the Care and Use of Laboratory Animals, 2011).

4.4.2 Tissue Processing

Cervices were obtained from 2 nonpregnant mice and 3 mice at each gestation time point or treatment group, and the tissue was snap frozen at liquid nitrogen temperature in OCT (Tissue Tek, Indiana). The entire length of the cervix was cut transversely into 50 μm serial sections. In general, 18 to 20 sections (approx. 1mm total thickness) were obtained from nonpregnant, and gestation day 6 and 12 cervix, while 36 to 40 sections (approx. 2mm total thickness) could be obtained from cervices at gestation days 15 and 18, reflecting the growth of the cervix during late pregnancy. Sections were mounted in 0.1 M PBS on glass slides under #1.5 glass coverslips (Corning, Corning, NY).

4.4.3 SHG Microscopy

Frozen sections were imaged on a Zeiss LSM510 META NLO configured with an Axiovert 200M inverted microscope and using an Achroplan 40x/0.8 W objective lens. A Chameleon XR pulsed Ti:sapphire laser (Coherent, California)

tuned to 900nm was focused onto stroma of the cervix and the resulting SHG signal was detected at 450nm. Forward scattered signal was detected with the transmitted light detector of the microscope after excitation light was removed by a HQ 450 sp-2p filter (Chroma Technology, Vermont). Backward scattered signal was detected with a non-descanned detector placed at the illumination port of the wide-field epifluorescence light path. Backscattered excitation light was removed using a 680nm short-pass dichroic mirror. Z-stacks of each frozen section were generated by acquiring images at 5um intervals through the thickness of the tissue. For intensity comparisons, the laser power, and the gain and offset of the detectors was set for optimal imaging of day 18 cervix, and these settings were used for images at all time points. Laser power measured at the focal plane of the specimen was 62 mW. The forward detector gain and amplifier offset were 558 V and -0.64, respectively. The backward detector gain and amplifier offset were 636 V and -0.46, respectively. For fiber size and porosity measurements the forward detector gain was varied over the range 586 to 636 V to optimize signal to noise within the linear range of the detectors for each day of pregnancy. For consistency between samples, we imaged the same general region of the cervix in each section. Images were taken in the stromal matrix between exocervix/vaginal epithelium and endocervix epithelium (Figure 4-9). The number of images collected for each experiment is indicated in the figure legends. Emission spectra were obtained in lambda scan mode with excitation at either

800nm or 900nm. Images were collected from 382-596nm using the META detector at its maximum spectral resolution of 10.7nm per detection channel.

4.4.4 Quantitative Measurements

Images were analyzed using ImageJ 1.41k (http://rsbweb.nih.gov/ij/). To avoid edge effects (attenuation of the SHG signal at the top and bottom of the section), only the central five images of each z-stack were included in the measurements. To quantify image intensity, images were filtered using a Gaussian blur with a kernel radius of 0.5 pixels to reduce shot noise and a minimum intensity threshold was set interactively to exclude the spaces between collagen fibers. Mean gray value limited to threshold of each image was calculated. Total SHG intensity for each z-slice was taken as the sum of the mean intensities of the forward and backward channels. The algorithms used to measure fiber size and porosity were adapted from previous SHG studies (Raub et al., 2008). In brief, characteristic fiber size was ascertained using the FD Math function of ImageJ to obtain the intensity autocorrelation of each image. A 2-D Gaussian was fit to a region of interest with a diameter of 32 pixels at the center of the autocorrelation image, omitting the central pixel (which represents shot noise), and two times the standard deviation of the mean was taken as fiber size (Raub et al., 2008). Data were collected in four 256 X 256 pixel regions of interest in each image and averaged to obtain the mean fiber size per image. For measurements of porosity, a minimum intensity threshold was set based on the

average of five measurements of the mean gray value of interactively chosen regions of interest lacking collagen fibers. A value of 1.25 times the threshold value was used to generate a binary mask. Interactive comparison of the binary masks with the original images showed that this method reliably segments the images into pores and fibers. The particle analysis tool of ImageJ was used to determine the number, mean Feret's diameter in μm, mean spacing and the fractional area in μm^2 covered by the pores in the binary mask. Particles less than 0.2 μm^2 were excluded from the analysis.

4.4.5 Statistics

For intensity, fiber size and porosity measurements of normal pregnancy means of images were compared using a one-way ANOVA followed by Tukey method. For $5aR1^{-/-}$ experiments means of images for intensity and porosity were compared using a student T-test.

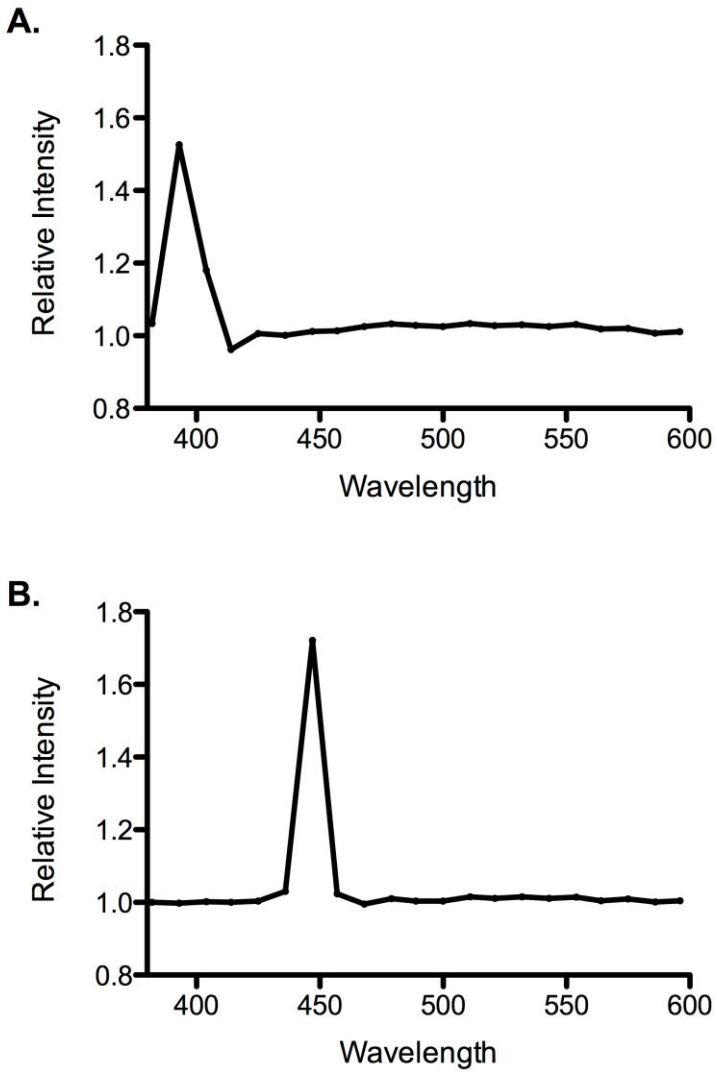

Figure 4-1. Signal Obtained From 900nm Excitation is SHG Not Autofluorescence. Emission spectra was obtained at A) 800nm and B) 900nm on day 18 cervical section. A) A sharp peak of signal intensity is seen at 400nm when excited with 800nm. B) The sharp signal peak moves to 450nm when excitation is changed to 900nm. No other signal is seen with either wavelength. With permission from Akins et.al. (2010) *Journal of Biomedical Optics*. 15(2):0260201-02602010.

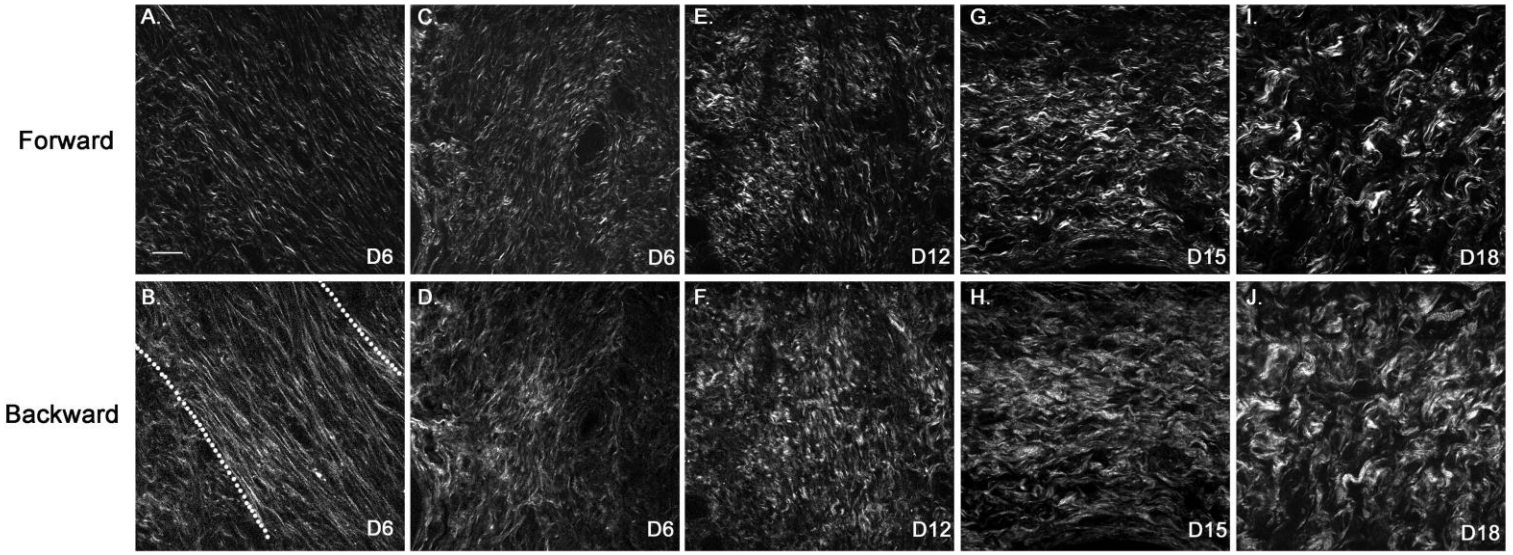

Figure 4-2. SHG Signal of Collagen Reveals Dramatic Changes in Collagen Morphology. Images were taken from gestation days 6 (A-D), 12 (E-F), 15 (G-H), 18 (I-J) cervices in both forward (A,C,E,G,I) and backward (B,D,F,H,J) directions. A and B show an example of a portion of the circumferential band of fibers prominent in samples from days 6 and 12 (demarcated by dotted lines, B). C and D show a region closer to the cervical lumen where the fibers appear more randomly oriented. In general collagen fibers appear thicker and more kinked as gestation progresses. Brightness and contrast for each panel were manipulated individually for optimal visualization of morphology at each time point. Scale bar represents 25um. With permission from Akins et.al. (2010) *Journal of Biomedical Optics*. 15(2):0260201-02602010.

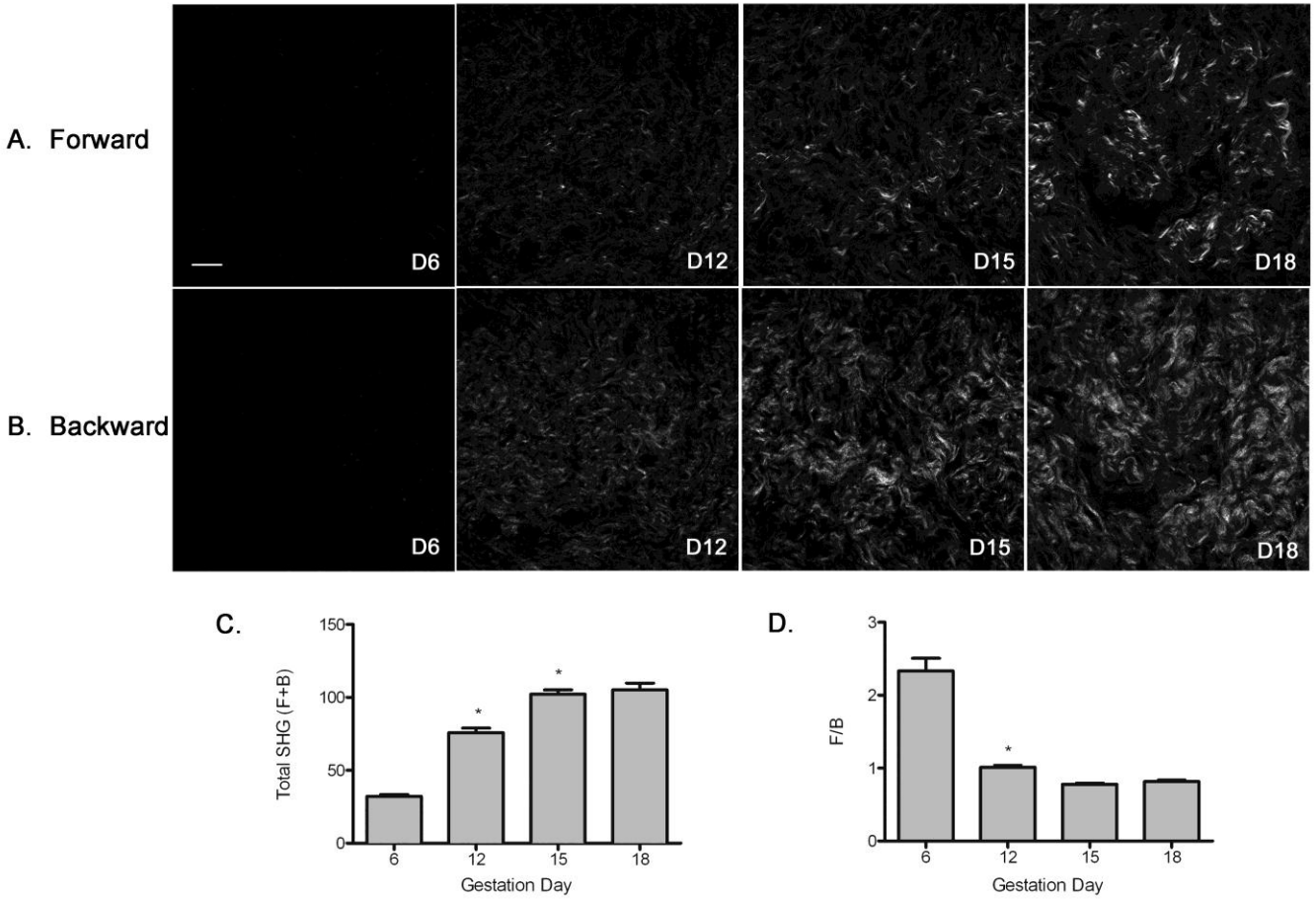
A. Forward
B. Backward
D6
D12
D15
D18
C.
Total SHG (F+B)
150
100
50
0
6
12
15
18
Gestation Day
D.
F/B
3
2
1
0
6
12
15
18
Gestation Day

Figure 4-3. **Absolute SHG Signal Intensity Changes During Pregnancy.** Representative forward (A) and backward (B) SHG images taken at gestation days 6, 12, 15, 18 using identical image acquisition parameters. Brightness and contrast adjustments were identical for all panels shown in A and B to preserve intensity relationships between the forward and backward channels and between time points. Quantitative comparison of signal intensity (C,D): Total SHG intensity (F+B) increases from day 6 to 15 (C). F/B ratio decreases more than two-fold from day 6 to day 12 and then remains constant for the remainder of gestation (D). * Difference from previous time point is statistically significant with $P < 0.0001$. Error bars represent standard error of the mean of 20 images. n=2 animals for each time point. Scale bar represents 25um. With permission from Akins et.al. (2010) *Journal of Biomedical Optics*. 15(2):0260201-02602010.

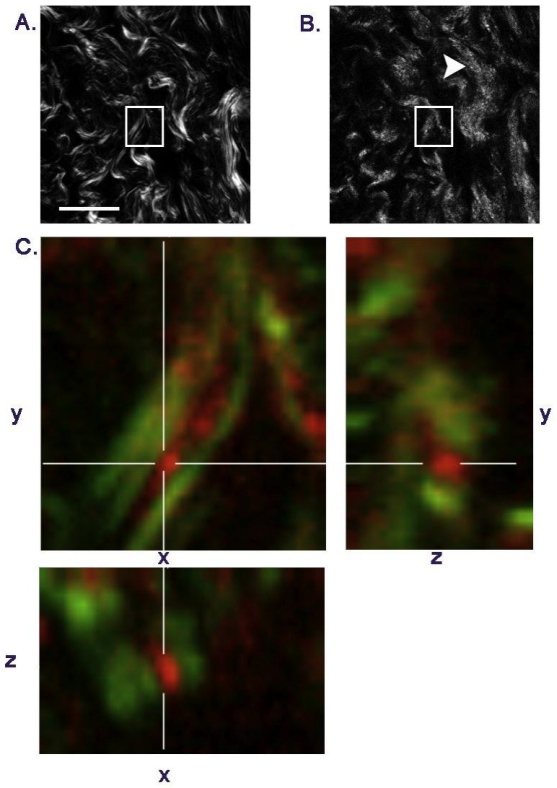

Figure 4-4. Punctate Features in the Backscattered Images are Abundant at Later Stages of Gestation. A. Forward image of d18 cervix. B. Backward image of same field of view. Arrowhead denotes a large cluster of punctae not visible in the forward image. xy, xz,and yz maximum intensity projections of the region inside the box show that punctae in the backward image (red) align adjacent to filaments visible in the forward direction (green) and are not cross sections of long filaments extending along the optic axis. Scale bar reprents 25um. With permission from Akins et.al. (2010) *Journal of Biomedical Optics*. 15(2):0260201-02602010.

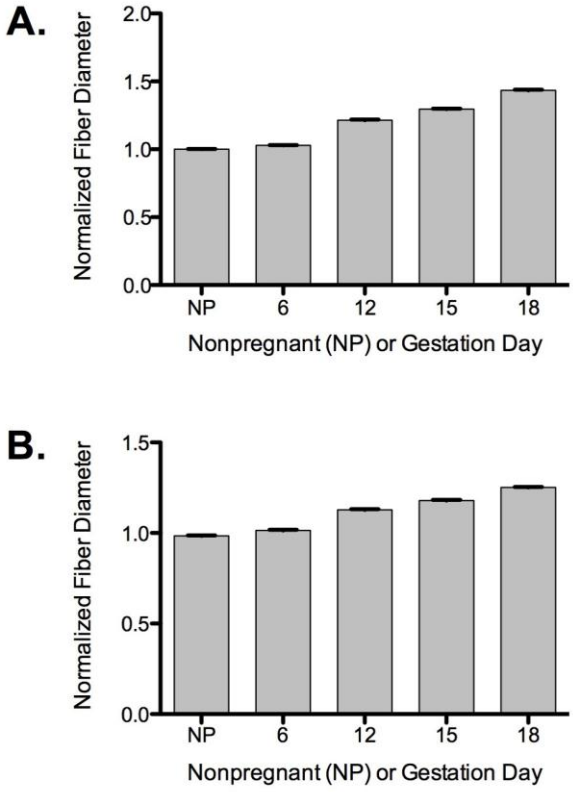

Figure 4-5. Fiber Size Increases with the Progression of Pregnancy. Fiber size was measured from forward (A) and backward (B) images and normalized to the value for non-pregnant samples (NP). Differences between all time points are statistically significant with $P<0.0001$. Bars represent the mean value of measurements from images of transverse sections collected throughout the longitudinal extent of the cervix. Error bars represent standard error of the mean of 94 (NP), 133 (d6), 134 (d12), 91 (d15) and 126 (d18) images. n=2 animals for NP; n=3 animals for pregnant time points. With permission from Akins et.al. (2010) *Journal of Biomedical Optics*. 15(2):0260201-02602010.

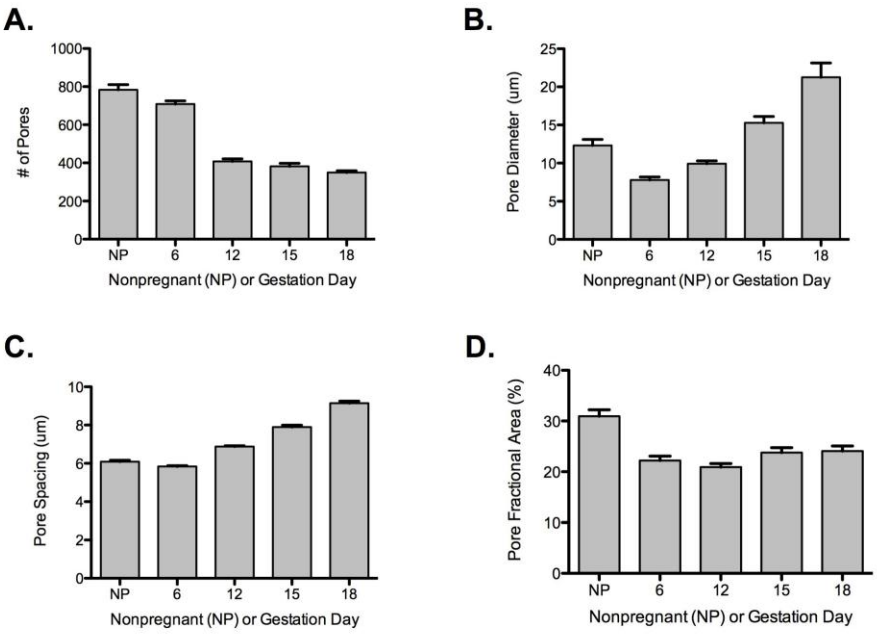

Figure 4-6 Evaluation of Changes in Spaces (Pores) Between Collagen Fibers. SHG images collected in the forward direction were evaluated for the number of pores (A), pore diameter (B), distance between pores (C) and pore fractional area (D). Pore number later in pregnancy was significantly less than non-pregnant and day 6 with $P<0.0001$. Pore diameter declined significantly between non-pregnant and day 6 samples and then increased progressively throughout gestation, becoming significant between day 12 and day 15 ($P< 0.0001$). Pore to pore spacing increased significantly beginning at day 12 ($P<0.0001$). Pore fractional area decreased by day 6 and showed no significant change thereafter ($P< 0.0001$). Bars represent the mean of measurements from images of transverse sections collected throughout the longitudinal extent of the cervix. Error bars represent standard error of the mean of 94 (NP), 133 (d6), 134 (d12), 91 (d15) and 126 (d18) images. n=2 animals for NP; n=3 animals for pregnant time points. With permission from Akins et.al. (2010) *Journal of Biomedical Optics*. 15(2):0260201-02602010.

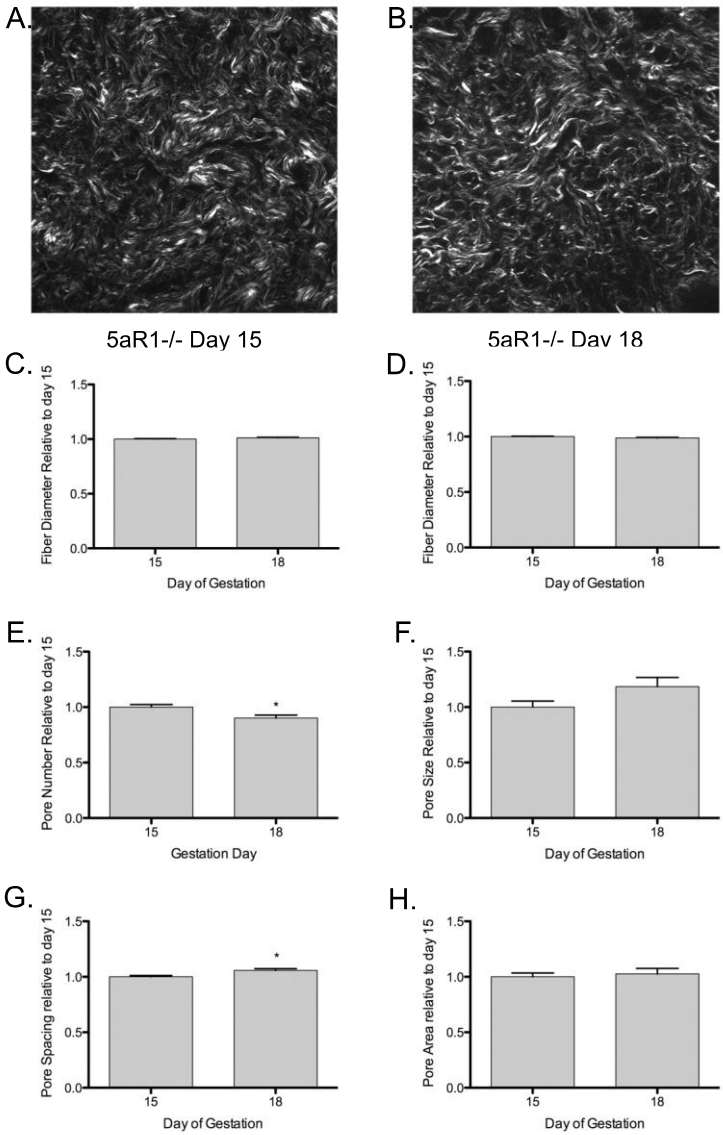

Figure 4-7. Second Harmonic Generation Morphological Assessment of the *5aR1*$^{-/-}$ Cervix. Visual inspection of images from (A) gestation day 15 *5aR1*$^{-/-}$ cervices and (B) gestation day 18 *5aR1*$^{-/-}$. Fiber diameter of day 15 and day 18 *Dcn*$^{-/-}$ cervices was assessed in both C) Forward and D) Backward directions. Fiber diameter showed no significant change in either direction. The number of pores in images declined in *5aR1*$^{-/-}$ cervices from day 15 to day 18 (E, P=0.0014). F) Pores size did not significantly change between day 15 and 18, but spacing

increased (G, P=0.0014). Pore fractional area did not significantly change between day 15 and day 18 in *5aR1*$^{-/-}$ cervices. Error bars represent standard error of the mean of 50 images for day 15 and 50 images for day 18. n=3 animals/time point.

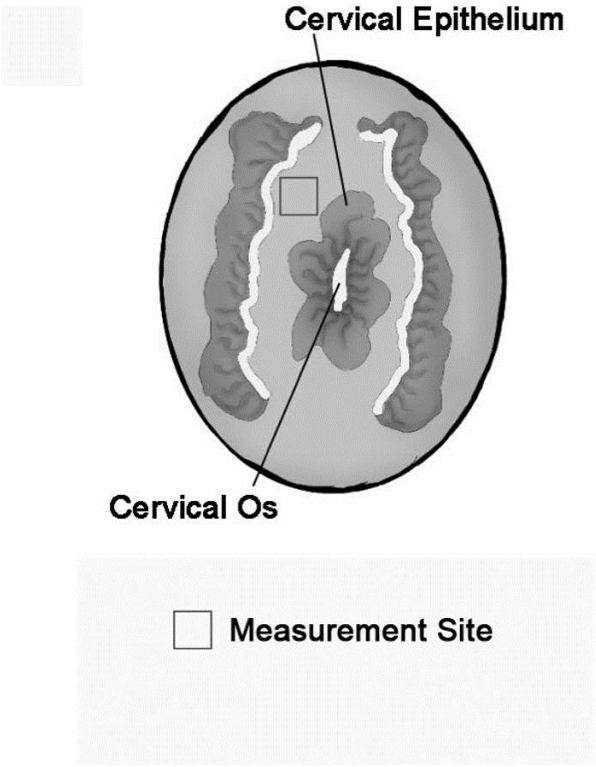

Figure 4-8. Illustration of Sample Orientation for SHG Detection. Cervices were dissected, frozen in OCT medium, and sectioned transversely in 50 um increments. SHG image Z-stacks were collected from each section in a cervical stroma region adjacent to cervical os as indicated by blue box. Modified with permission from Akins et.al. (2010) *Journal of Biomedical Optics*. 15(2):0260201-02602010.

Table 4-1 QUANTITATIVE SHG MEASUREMENTS THROUGHOUT GESTATION

Gestation Day/Treatment	**Fiber Diameter (um ± SEM)**		**Number of Pores (± SEM)**		**Pore Size (um ± SEM)**		**Pore Spacing (um± SEM)**		**Pore Fractional Area (% ± SEM)**	
	Forward	Backward	Forward	Backward	Forward	Backward	Forward	Backward	Forward	Backward
NP	1.42 ±0.004	1.85 ±0.004	783 ±26.7	514 ±24.2	12.3 ±0.79	21.5 ±1.8	6.1 ±0.07	7.4 ±0.12	30.9 ±1.3	34.6 ±1.4
Day 6	1.46 ±0.003	1.87 ±0.007	709 ±15.9	402 ±15.0	7.8 ±0.38	29.1 ±3.0	5.8 ±0.03	7.5 ±0.17	22.2 ±0.9	38.8 ±1.5
Day 12	1.72 ±0.006	2.08 ±0.007	408 ±12.9	295 ±18.2	9.9 ±0.36	20.3 ±1.2	6.9 ±0.04	8.2 ±0.14	20.9 ±0.7	27.4 ±0.9
Day 15	1.84 ±0.006	2.17 ±0.006	382 ±15.6	282 ±14.3	15.3 ±0.85	25.7 ±1.8	7.9 ±0.10	8.9 ±0.12	23.8 ±1.0	30.1 ±1.0
Day 18	2.04 ±0.006	2.31 ±0.005	349 ±10.4	280 ±9.9	21.3 ±1.89	30.0 ±1.6	9.1 ±0.11	9.7 ±0.12	24.1 ±1.0	29.4 ±1.0
5αR1$^{-/-}$ Day 15	1.90 ±0.008	2.13 ±0.008	1082 ±24.6	794 ±22.8	15.7 ±0.84	31.6 ±2.9	7.08 ±0.08	8.7 ±0.24	30.3 ±1.0	37.4 ±1.3
5αR1$^{-/-}$ Day 18	1.92 ±0.009	2.08 ±0.001	967 ±28.05	798 ±33.5	18.66 ±1.3	30.79 ±2.1	7.5 ±0.10	8.5 ±0.17	31.1 ±1.4	39.8 ±1.4

Table 4-2 SHG SIGNAL INTENSITY

Gestation Day	Signal Intensity (±SEM)	
	Forward	Backward
Day 6	22.09 ±1.11	10.12 ±0.59
Day 12	37.41 ±0.76	38.46 ±2.36
Day 15	44.33 ±0.85	57.90 ±2.24
Day 18	46.35 ±1.12	58.89 ±3.55

Chapter 5 Collagen and Preterm Birth- A Potential Biomarker?

5.1 Introduction

As discussed in Chapter 1, preterm birth affects 1 in every 8 babies in the United States. With countless risk factors and unknown etiologies in many patients, understanding exact mechanisms of preterm birth have remained elusive. Animal models have become very useful in pinpointing pathways and mechanisms of preterm birth that have been shown to be pertinent in humans.

5.1.1 Mouse Models of Preterm Birth

To better predict and prevent preterm birth a detailed understanding of the mechanisms involved are necessary. Animal models provide an inexpensive, relatively quick and physiologically relevant way to study mechanisms of preterm labor. Two well-established mouse models of preterm birth that mimic infection mediated and progesterone withdrawal mediated pathways are used by many investigators to understand mechanisms involved in initiating premature labor. The "progesterone-withdrawal" model mimics the functional loss of progesterone at the end of both the mouse and human pregnancies while; the "infection" model of preterm birth mimics an intrauterine infection, a known initiator of preterm labor.

Progesterone-Withdrawal Model

Progesterone receptor antagonists have been identified to bind the progesterone receptor resulting in loss of progesterone function. Mifepristone, a

well-studied progesterone receptor antagonist, blocks the progesterone receptor mimicking the fall of progesterone that occurs at the end of gestation (Kovacs et al., 1984; Chwalisz, 1994). It is used clinically to induce cessation of pregnancy, in the first trimester. Pregnant mice administered mifepristone will deliver their young prematurely within 12-24 hours after injection (Dudley et al., 1996).

Infection Model

Lipopolysaccharide (LPS) is a sugar chain found on the coat of gram-negative bacteria. Recognition of LPS by toll-like receptors instigates activation of pro-inflammatory responses to fight infection. It is well established that systemic infection can cause preterm birth. Systemic or intra-uterine injection of LPS will initiate preterm birth within 6 hours of injection (Elovitz et al., 2003). Intra-uterine injection of LPS is an established model of preterm birth with localized activation of inflammatory responses within the reproductive tract.

5.1.2 Insights from Murine Studies

While preterm birth was originally thought to be a accelerated progression of normal pregnancy, insight from recent studies confirms that premature cervical ripening due to infection or progesterone withdrawal have different pathways of action not only from the mechanisms of normal ripening but from each other as well (Hirsch et.al. 2002; Hirsch and Muhle, 2006; Gonzalez et al., 2009; Holt et al., 2011). This suggests that different etiologies of preterm

birth have independent mechanisms action and do not mimic the progressive normal labor process.

Gonzalez *et. al*. reports that while term ripening shows a marked increase in epithelial cell proliferation and associated gene expression, neither the infection (LPS) nor the non-infection (mifepristone) pathways of preterm birth had a similar pattern of gene expression. In fact, several genes that are upregulated at term are downregulated in preterm birth models (Gonzalez et al., 2009). As expected, inflammatory pathways were upregulated in the infection model of preterm birth (Gonzalez et al., 2009; Holt et al., 2011). Proinflammatory genes such as *Ptgs-2, Il-6, Mip2, Tnf-alpha, and Il-1* and their associated proteases, *Adamts1, Adamts4* and *Mmp8*, are all upregulated in the LPS model of preterm birth (Holt et al., 2011). Excluding upregulated *Adamts* 1 and 4 expressions, none of these other markers are upregulated during term cervical ripening (Gonzalez et al., 2009; Holt et al., 2011). Immune cell populations identified by flow cytometry identify increased infiltration of neutrophils in cervix of infection preterm birth models, which is not evident in term parturition or mifepristone induced preterm birth. Conversely, monocytes infiltrate the cervix during term and mifepristone induced ripening, but are not increased with infection induced preterm birth (Timmons et al., 2009; Holt et al., 2011).

Mifepristone treated animals seem to follow a mechanism more similar but not identical to normal pregnancy. Animals treated with mifepristone show a

marked increase in tissue wet weight. Changes in wet weight are similar to changes seen between gestation day 15 and day 18 in normal pregnancy, but occur just within 12 hours (Holt et al., 2011). There is also increased expression of the oxytocin receptor, connexin-26 similar to normal ripening. Unlike normal cervical ripening, proteases such as *Adamts1*, *Adamts4* and *Mmp8* are upregulated, these are normally seen upregulated during postpartum repair (Holt et al., 2011). In contrast to term ripening, gene expression of mifepristone treated animals have a marked increase in *Ptgs1* expression (where LPS model showed upregulation of *Ptgs2*) suggesting a role of prostaglandins in both preterm models. These studies strengthen the hypotheses that infection and inflammation is sufficient for preterm birth but not necessary for normal cervical remodeling and that preterm birth can occur via different mechanistic pathways.

With current evidence that mechanisms during preterm birth differ in regard to inflammatory pathways and timing of immune infiltration and protease expression, it is still unclear how collagen and the ECM are affected in these models. Mifepristone administration has been shown to have conflicting affects on cervical collagen. Studies looking at effects of mifepristone on human cervix following first trimester abortions, showed no change in collagen content (Bokstrom and Norstrom, 1995). In contrast, Clark found a decrease in collagen in rat cervices treated with mifepristone (Clark et al., 2006). Collagen cross-links measured by light-induced autofluorescence, showed a slight decline in

fluorescent signal in the rat when treated with mifepristone (Glassman et al., 1995). However, this is not necessarily an indication of collagen loss, as loss of signal could be seen from loss of collagen crosslinking or reorganization of the matrix. There are very few studies that correlate changes in collagen to LPS treatement. However, Maradny saw a decline in collagen in LPS treated rabbits as assessed by picrosirius red staining (Maradny et al., 1995). Most recently, Holt and Timmons showed that while levels of the collagenase *Mmp8* were upregulated post-LPS or mifepristone injection, collagen levels remained constant (Holt et al., 2011). In this same study, trichrome staining of LPS and mifepristone treated cervical sections indicates a clear decline in collagen organization from controls, but doesn't give an indication of collagen degradation (Figure5-1) (Holt et al., 2011). In mifepristone treated cervical stroma, collagen bundles appear very spaced and disjointed, similar to the postpartum cervix. However, in the LPS treated samples collagen remains dense and the morphology appears to resemble an intermediate between gestation day 15 and day 18 samples (Figure 5-1) (Holt et al., 2011).

The goal of this study is to better understand how cervical collagen structure and organization is changing during infection and non-infection mediated preterm birth, and to test if SHG can be used to distinguish these models from each other and from normal pregnancy. We find that collagen content does

not change in either preterm birth model, however structure and organization of collagen varies dramatically.

5.2 Results

5.2.1 Infection and Mifepristone Treatment

Delivery of 150 μg LPS is given with an intra-uterine injection during the early morning of gestation day 15. Mice deliver approximately 7-10 hours post injection. For all studies mice are sacrificed 6 hours post-injection. 0.5 mg mifepristone is administered subcutaneously on the night of gestation day 14. With this dosage mice begin delivering approximately 16-24 hours after injection. In these studies tissue is collected 12 hours post-administration of mifepristone. It is important to note that the experimental endpoint in mifepristone or LPS treated mice is at a similar time as the untreated gestation day 15 samples. Samples have been compared to vehicle treated controls as well as normal gestation day 15 and gestation day 18 (Figure 5-2).

5.2.2 Collagen Content

Several methods were applied to evaluate collagen content in cervices treated with LPS or mifepristone. Collagen content was directly assessed by a hydroxyproline assay comparing both LPS and mifepristone treatments to normal day 15 (day of drug administration) and day 18 (during cervical ripening). No significant changes were observed in hydroxyproline content in either treatment group indication that collagen content does not decline (Figure 5-3).

To determine if these were changes in collagen structure that may result in increased extractability of collagen I western blotting was performed. Collagen I is normally not soluble due to heavy crosslinking. As tissue properties change, collagen can become more or less extractible. By extracting collagen from tissue in 7M urea, we can assess the relative solubility or extractability of the collagen. Cervices from LPS and mifepristone treated animals and their vehicle controls, along with day 15 and day 18 of normal gestation, were extracted in 7M urea, and 10 μg of protein used for western blotting. A rabbit polyclonal anti-mouse collagen I (MD Biosciences, St. Paul MN, MD20151) was used to probe for collagen I alpha1. Blots showed equal amount of collagen extractability for all treatment groups and time points, indicating that changes in collagen properties in both preterm birth models does not alter extractability (Figure 5-3).

Collagen III is known to affect collagen I fibrillogenesis and subsequent tissue strength depending on changes in I/III ratio (Romanic et al., 1991; Liu et al., 1997; Lui et al., 2010) (Discussed in Chapter 1 and 2). To assess collagen content and collagen I/collagen III ratio, collagen I and collagen III immunofluorescence was performed. The collagen I/III ratio was approximately 2.0 for all treatment groups and gestation days (Figure 5-4). This indicates that there is no change in content or ratio of either collagen I or III. Interestingly, collagen I fluorescence images indicate a marked difference in collagen structure between LPS and mifepristone treatment groups and normal gestation. During

normal gestation between day 15 and day 18 there is a change in the pattern of collagen I staining. Wide spaces appear between collagen bundles in the normal day 18 cervices. Collagen I structure in mifepristone treated cervices shows an increased spacing between collagen I signal; this pattern is even more dramatic than what is seen in gestation day 18. However, LPS treated cervices remain indistinguishable from the day 15 pattern of collagen staining (Figure 5-4).

5.2.3 ECM and Collagen Ultrastructure

Given the observation that collagen loss is not appreciable in either of the preterm birth models, it is hypothesized that changes in collagen structure or ECM composition can account for changes in the cervix that allow for preterm birth. Immunofluorescence staining for collagen I and collagen III in both preterm birth models suggested differences in collagen and ECM structure between both preterm birth models and term ripening. Electron microscopy was utilized to observe collagen and ECM ultrastructure in premature cervical ripening. Electron micrographs from normal day 15, normal day 18, mifepristone treated and LPS treated were compared (Figure 5-5).

Similar to findings of collagen I and III immunofluorescence, collagen ultrastructure in gestation day 15 LPS treated cervices closely resembled untreated gestation day 15 controls. Furthermore, fibril diameter measurements in LPS treated cervices were similar to day 15 controls. Fibril diameter of treated collagen measured 63.4 nm whereas the control measured 61.4 nm. Normal day

15 collagen fibrils measure 63.7 nm. Frequency distribution of fibril size also revealed similar patterns between control, treated, and normal (Figure 5-6). Mifepristone treated collagen fibrils were unable to be analyzed for fibril diameter due to the increased amount of dispersion seen in TEM micrographs.

5.2.4 Collagen SHG in Preterm Birth Models

In the next series of studies, forward SHG microscopy of frozen sections was performed to further compare structural changes in collagen in preterm birth models with term ripening (Figures 5-7 and 5-8). Animals were treated with mifepristone or LPS (or vehicle) as described in Methods. Consistent with other findings, neither mifepristone nor LPS induced changes in collagen structure are similar to changes observed during the natural progression of gestation from day 15 to day 18. During normal ripening, fiber diameter increases in both directions (Figure 4-5). Pore number declines during ripening by the diameter and spacing of pores increases, resulting in no net changes in fractional pore area (Figure 4-6).

In mifepristone treated animals, F+B intensity declined in treated samples when compared to the control (Figure 5-7C), while no significant change was observed between day 15 and day 18 during normal ripening (Figure 4-3). No difference was seen in F/B ratio between treatment and vehicle (Figure 5-7). Cervices of mifepristone treated animals exhibited only modest differences in collagen fiber size and pore-to-pore spacing compared with vehicle controls (Table 5-1). In contrast, we observed a two-fold increase in mean pore diameter

along with a 13% increase in the mean number of pores in tissue from treated animals relative to the vehicle controls, resulting in a 55% overall increase in pore fractional area measured in the forward direction (Figure 5-7E-H).

In LPS treated animals, fiber diameter remained constant in treated animals in both forward and backward directions (Figure 5-8). Pore number increased modestly by 5% in LPS treated samples compared to sham surgery, whereas in normal term pregnancy number of pores decreases (compare Figure 5-8E to Figure 4-6A). Modest declines in pore spacing (3%) and pore size (13%) was seen in LPS treated animals. While the pattern of pore spacing and size are similar to patterns seen in term ripening, the declines are more pronounced at term. Pore fractional area declines in the LPS model by 9% (Figure 5-8).

Interestingly, changes in pore fractional area differ dramatically between preterm birth models and term ripening. In term animals fractional area remains constant throughout pregnancy. However, in mifepristone treated animals it increases dramatically (by 54%) and in LPS treated animals it declines by 9%. While we don't understand the physiological meanings behind the changes seen in collagen SHG signal, these parameters may allow us to distinguish not only cervical tissue destined for preterm birth, but different pathways of preterm birth.

5.3 Discussion

In this study, we investigated how cervical collagen structure is mediated in two preterm birth models as compared to term ripening. Our findings support

previous work that indicates the presence of multiple mechanisms and pathways of preterm cervical ripening that do not recapitulate pathways in normal term cervical ripening. We also show the power of SHG as a tool to distinguish different types of preterm birth based on morphological features of collagen.

Here we show that in the two preterm birth models studied cervical collagen content and extractability is not altered. However, the organization of collagen in the ECM changes dramatically as visualized by immunofluorescence. Factors that influence collagen solubility or extractability affect collagen as it is forming new fibrils and being laid down into the matrix. Since our treatments only lasted for 6-12 hours, it is unlikely that these would change. However, changes in supporting proteins, such as matricellular proteins and SLRP family members need to be assessed in order to understand if the ECM environment that the collagen is occupying differs between preterm birth models and term ripening.

The power of SHG imaging as a tool to investigate collagen remodeling is illustrated in the ability to distinguish collagen reorganization in preterm ripening induced with mifepristone or LPS from normal remodeling. Compared to term ripening we found a decrease in overall intensity in samples from the mifepristone treated animals and an increase in the number and size of pores; resulting in a 54% increase in pore fractional area in cervices from mifepristone treated mice. In contrast to term ripening, a increase in pore number and modest decline in size and spacing accounts for a 9% decline in pore fractional area in LPS treated mice.

While the functional significance of differences of morphological features of collagen remains to be elucidated, these findings confirm that premature cervical ripening in the progesterone withdrawal model occurs via different mechanisms from LPS model and normal cervical ripening. This conclusion is supported by both biomechanical and gene expression studies which report that cervical ripening induced in mifepristone treated rats or mice respectively does not reach the degree of ripening or harbor the same gene expression patterns characteristic of normal term cervix (Buhimschi et al., 2004; Clark et al., 2006; Gonzalez et al., 2009). The increased pore fractional area could be indicative of increased collagen degradation, increased cellularity, or increases in hydration and hyaluronan content. The decrease in overall SHG signal intensity observed with mifepristone treatment suggests increased clipping of collagen type I fibers or that collagen structure undergoes a different transformation as compared to term ripening in mouse cervix. Studies in term pregnant women treated with mifepristone suggest a decline in collagen synthesis with little change in collagen abundance (Buhimschi et al., 2004). However, in the rat there is a report of increased collagen degradation with mifepristone treatment (Clark et al., 2006). The observation that pore fractional area increased in mifepristone treated cervices and declined in LPS treated cervices is also supported by the collagen I immunofluorescence. The affect of LPS on collagen I is not well studied. A study in rabbits has shown that collagen concentration declined in cervical tissue

with administration of LPS, however, the quantification of collagen was measured only by picrosirius red staining (Maradny et al., 1995). Our findings together with trichrome analysis performed by Holt and Timmon suggests that cervical collagen is incompletely remodeled in LPS treated animals (Holt et al., 2011). LPS treatment does cause increased uterine contractility; this increase in uterine activity may be able to overcompensate for a cervix that is incompletely remodeled (Ross et al., 2004). Biomechanical comparison of cervices from both preterm models is required to address changes and differences in tissue strength and viscoelasticity.

5.4 Methods

5.4.1 Animals

Mice used for these studies were of C57B6/129Sv mixed strain. Cervical tissue was dissected out of the reproductive tract and vaginal tissue was carefully removed from cervical tissue. Cervices were flash-frozen in liquid nitrogen immediately following their extraction. All studies were conducted in accordance with the standards of humane animal care described in the National Institutes of Health Guide for the Care and Use of Laboratory Animals using protocols approved by an institutional animal care and research advisory committee.

Mifepristone Treatment

Administration of the progesterone receptor antagonist, mifepristone, results in premature cervical ripening and preterm birth 15-18 hours after

injection (Dudley et al., 1996; Clark et al., 2006). Mice were given 0.5mg of mifepristone (Sigma) in Triolene oil (Sigma, St Louis) or vehicle control (Triolene only) by subcutaneous injection at 1900-2000 hours on the late evening of gestation day 14. Mice were sacrificed and cervices collected 12 hours later on gestation day 15.

LPS Treatment

Administration of intrauterine LPS results in preterm delivery approximately 6 hours post injection (Elovitz et al., 2003). Mice were anesthetized using avertin on gestation day 15. Using sterile surgical practices a small incision was made in the left upper quadrant of the abdominal cavity. Once uterus was visualized, injection of 150 μg of LPS was placed intrauterine with care to avoid fetal membranes. Mice were then sewn up using silk nonabsorbable sterile (5-0 1.0 metric) (Ethicon, Somerville, New Jersey) sutures and 0.1ug/kg buprenorphine (Hospira, Lake Forest, Illinios) was given for pain management. Mice were observed post-surgery and all mice used for experiments woke from surgery with no obvious complications. Mice were sacrificed and cervices collected 6 hours post surgery.

Immunoblotting:

Collagen was extracted with 7M urea (Sigma, St. Louis), 0.1M sodium phosphate with 1% protease inhibitor (Sigma), overnight at 4°C. The protein concentration was determined by a Bradford protein assay (Pierce, Thermo

Scientific, Rockford, Il). Ten micrograms of protein was loaded on a 4-20% Tris-HCL polyacrylamide gel and electrophoresed at 100V. After overnight transfer to nitrocellulose membrane and Ponceu S (Sigma) staining to assess equal loading of protein, immunoblotting was performed using rabbit polyclonal anti-mouse collagen I (MD Biosciences, St. Paul MN, MD20151).

Collagen Content

Cervices were lyophilized and dry weight was obtained. Dry samples were digested in 0.5mg/mL proteinase K (Roche, Basal, Switzerland) in 100mM ammonium acetate pH 7.0 at 60°C for 4 hours. The equivalent of 1mg of tissue was hydrolyzed in 6M HCL overnight at 110°C. Samples were dried and dissolved in water. Hydroxyproline assay was carried out as previously described (Chapter 3 Section 3.4.5) (Stegemann and Stalder, 1967; Read et al., 2007).

Immunofluorescence:

Cervical tissue was collected at 12 hours post injection of mifepristone and 6 hours post injection of LPS and frozen in OCT medium (Tissue Tek, Indiana). Five-micrometer cervical sections were cut from tissue blocks. Sections were fixed for 10 minutes in acetone at -20°C. Tissue was rehydrated in PBS, blocked in 10% normal goat serum (Invitrogen, California, catalog # 01-6201) and incubated with collagen I or collagen III rabbit polyclonal antibodies (Abcam, Cambridge, ab34710 and ab7778). Sections were then washed in PBS and incubated with goat α rabbit IgG antibodies coupled to Alexa 488

(Invitrogen/Molecular Probes, California, A11008). Slides were viewed on a Zeiss LSM510 META NLO confocal microscope using an Acroplan 40x/0.8 W objective lens. Fluorescence signal intensity was measured using ImageJ 1.41k (http://rsbweb.nih.gov/ij/).

Electron Microscopy:

Mifepristone or LPS treatd mice were perfused with 1% glutaraldehyde, 2% paraformaldehyde fixative in 0.1M phosphate buffer. Cervical and uterine tissue was removed and fixed in 2.5% glutaraldehyde in 0.1M cacodylate buffer containing 0.1% ruthenium red overnight at 4^0C. Tissue was then cut into 250 μm longitudinal sections using a Vibratome Series 3000 Sectioning System (The Vibratome Company, St. Louis). Vaginal and uterine tissue was removed from the cervix and the cervix was rinsed for 30 minutes with cacodylate buffer. The tissue was post-fixed with 1% osmium in 0.1M cacodylate buffer containing 0.1% ruthenium red for 90 minutes. Specimens were dehydrated through a graded series of ethanols (50%, 70%, 95%, 100%) followed by propylene oxide and embedded in Epon. Thin sections were stained with uranyl acetate and lead citrate. Sections were viewed on a TEM Tecnai microscope (FEI Company, Hillsboro, Oregon) and images captured at 4200x or 20500x with a Morada 11 1 megapixel CCD camera.

Collagen Fibril Measurements

Electron microscope images of transversely sectioned collagen fibrils taken at 20,500x were analyzed with Image J 1.41k (http://rsb.info.nih.gov/ij/). An intensity threshold was interactively determined for optimal segmentation of fibril from background. Segmented images were converted to a binary mask, and erode, open, dilation and fill holes binary operations were used to separate merged fibrils. Particles were analyzed using the Particle Analysis function of Image J with parameters set for size, 1000-10000 and circularity 0-1. Ellipses were fit to all particles and the minor angle of the ellipse was taken as the fibril diameter.

Second Harmonic Generation and Image analysis

Cervices were snap frozen at liquid nitrogen temperature in OCT (Tissue Tek, Indiana). The entire length of the cervix was cut transversely into 50 µm serial sections. Sections were mounted in 0.1 M PBS on glass slides under #1.5 glass coverslips (Corning, Corning, NY). Frozen sections were imaged on a Zeiss LSM510 META NLO configured with an Axiovert 200M inverted microscope and using an Achroplan 40x/0.8 W objective lens. A Chameleon XR pulsed Ti:sapphire laser (Coherent, California) tuned to 900 nm was focused onto stroma of the cervix and the resulting SHG signal was detected at 450 nm. Forward scattered signal was detected with the transmitted light detector of the microscope after excitation light was removed by a HQ 450 sp-2p filter (Chroma Technology, Vermont). Backward scattered signal was detected with a non-descanned detector placed at the illumination port of the wide-field epifluorescence light path.

Backscattered excitation light was removed using a 680nm short-pass dichroic mirror. For consistency between samples, we imaged the same general region of the cervix in each section. The number of images collected for each experiment is indicated in the figure legends.

Images were analyzed using ImageJ 1.41k (http://rsbweb.nih.gov/ij/), to quantify image intensity, fiber diameter and porosity as described in Chapter 4 methods.

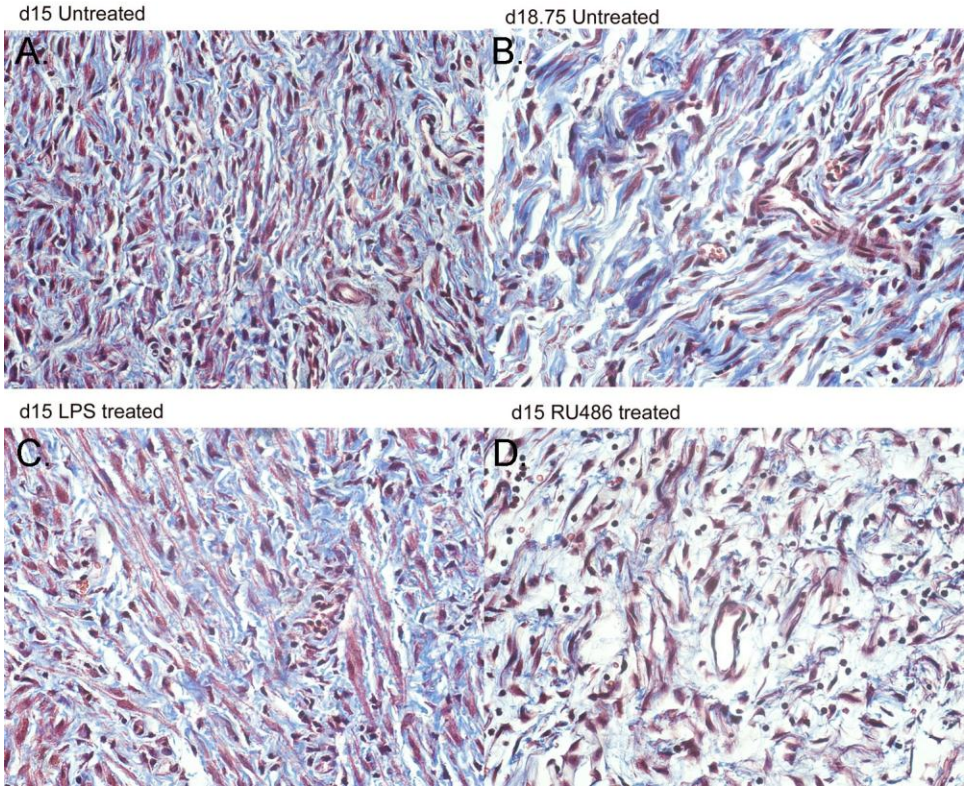

Figure 5-1. Trichrome Assessment of Preterm Birth Models. Sections of A) gestation day 15 and B) day 18 along with C) LPS treated and D) mifepristone treated cervices were stained with Masson's Trichrome Stain. Fibrillar collagen appears (blue) while nuclei stain dark red and cytoplasm stains pink. Modified with permission from Holt *et.al.*(2011) *Endocrinology* 152(3):1036-1046.

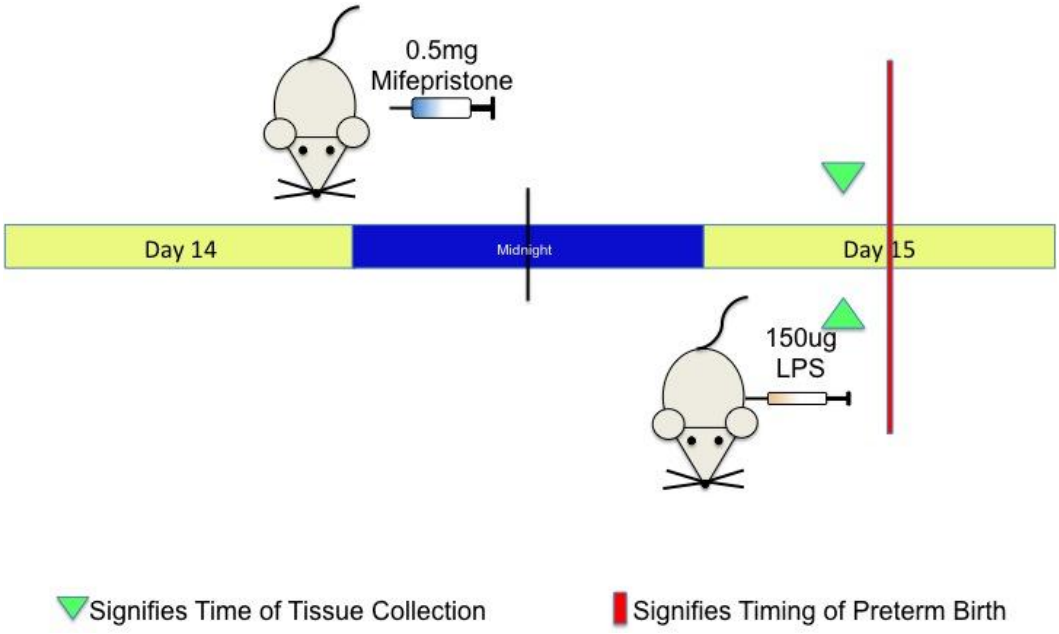

Figure 5-2. Timescale for Preterm Treatments. Mifepristone (top) and LPS (bottom) are administered to mice to cause preterm birth. Subcutaneous injection of 0.5mg of mifepristone is given on the night of gestation day 14. Mice will deliver approximately 18 hours post-injection (Red line), so mice are sacrificed 12 hours post-injection (Green triangle) on day 15). 150ug LPS is administered via intrauterine injection early on day 15. Mice will deliver after 7 hours of LPS treatment (Red line). Mice are sacrificed 6 hours post-injection (Green triangle). Both models are sacrificed in the early afternoon of what would be gestation day 15.

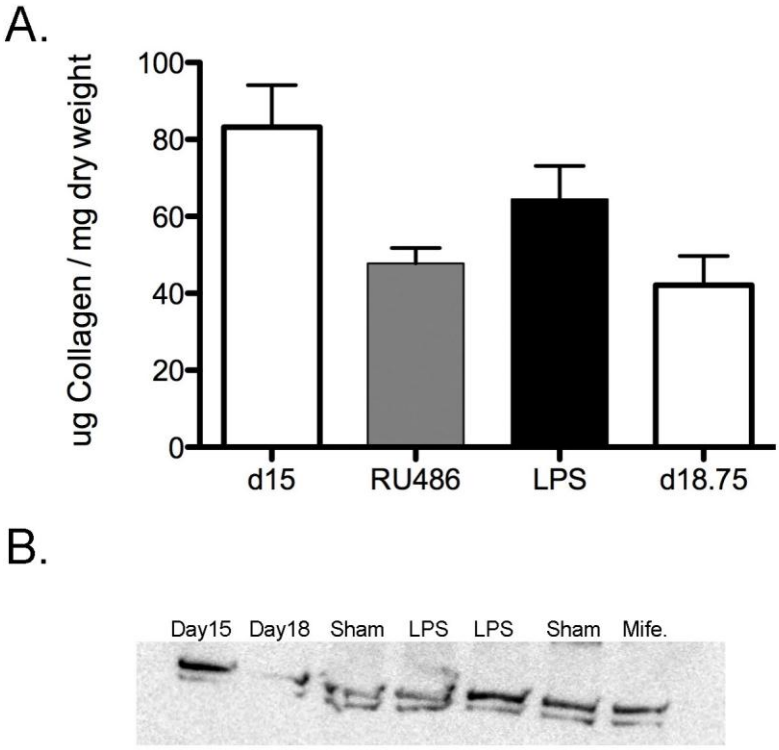

Figure 5-3. Collagen Content Does Not Decline in Mice Treated with Preterm Agents. A) Collagen content was measured via hydroxyproline assay in gestation day 15, mifepristone-treated, LPS-treated and gestation day 18 cervices. No significant difference was seen between any of the groups. Error bars represent standard error mean. B) Collagen extractability was assessed via western blotting in time points listed in A).

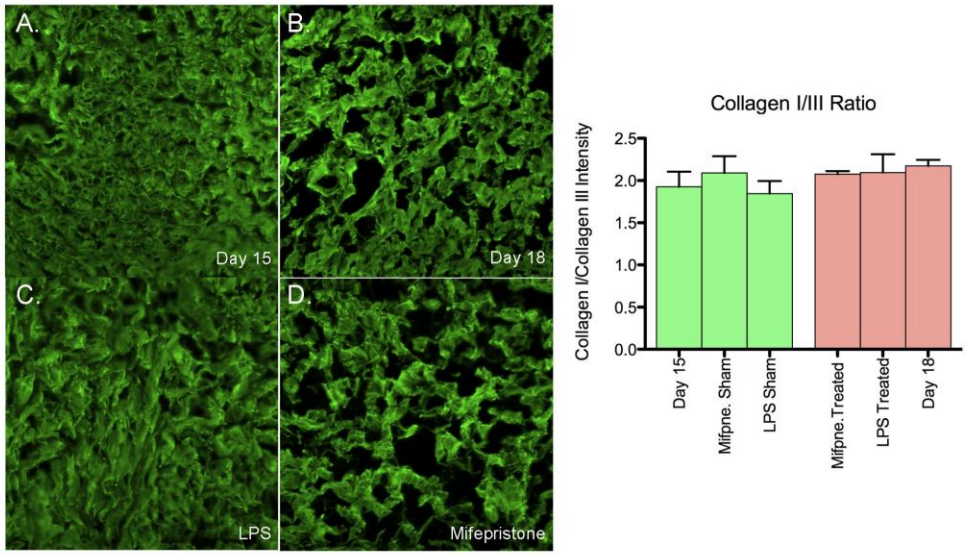

Figure 5-4. Collagen Structure and I/III Ratio in Preterm Birth Models. Immunofluorescence of Collagen I in A) gestation day 15, B) gestation day 18, C) LPS treated and D) mifepristone treated cervices reveals cervical collagen structure. Immunofluorescence intensity of collagen I and collagen III intensity was measured and collagen I/III ratio was determined for gestation day 15, day 18, LPS and mifepristone treatement, and LPS and mifepristone sham treatments. Ratio of collagen I/III was approximately 2.0 for all time points and treatments. Error bars represent standard error mean. n= 3 animals per time point/ 12 images per time point.

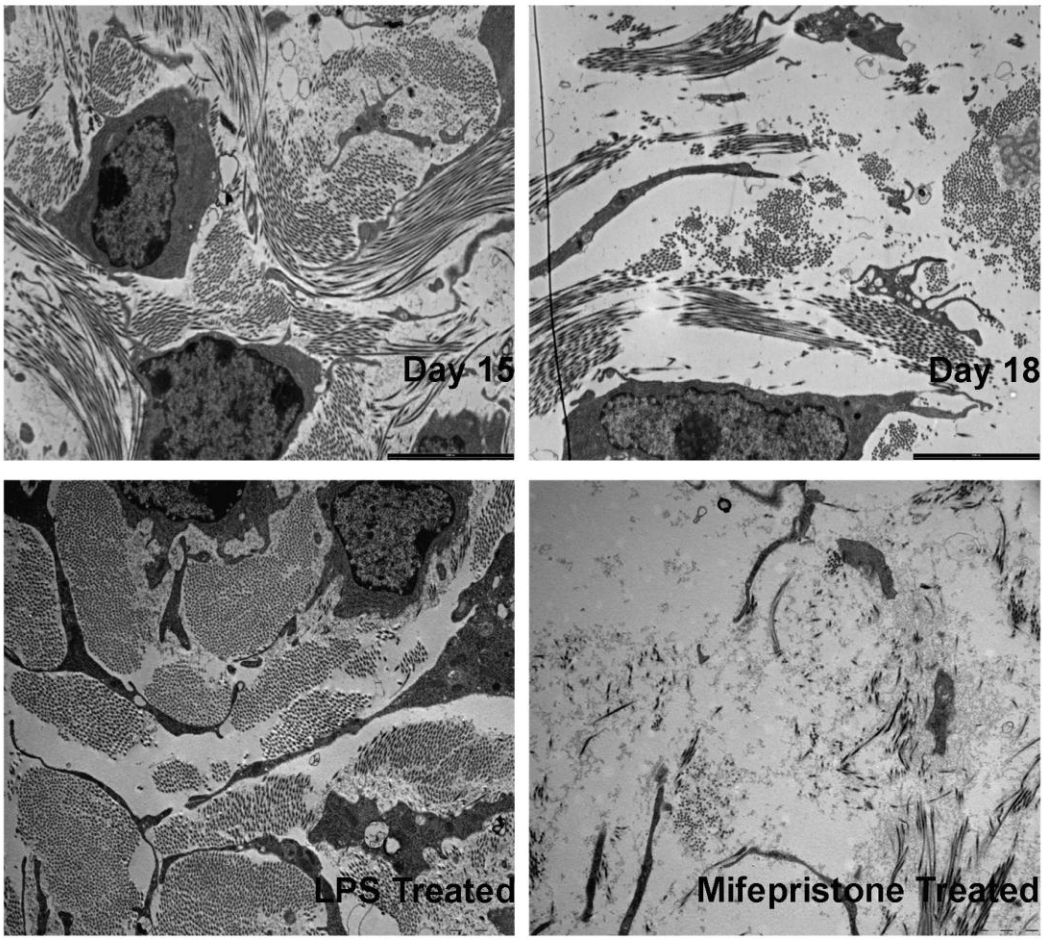

Figure 5-5. Ultrastructural Assessment of Cervical Collagen in Preterm Models. Electron micrographs of cervical ECM taken at 4200x on gestation day 15, day 18 and in LPS and mifepristone treatment. Bar = 5μm.

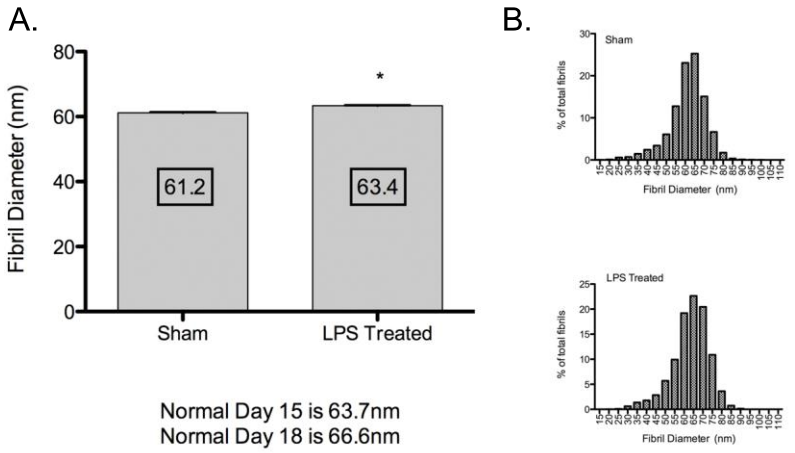

Figure 5-6. Collagen Fibril Diameter is Not Altered in the LPS Treated Cervix. Electron micrographs taken at 20500x of LPS treated and sham treated cervical collagen were analyzed for fibril diameter frequency A) LPS treatement does not cause an in crease in collagen fibril diameter or a change in fibril frequency (B). n= 2922 fibrils for sham treatment and n=4231 fibrils for LPS treated. n=3 animals per treatment group.

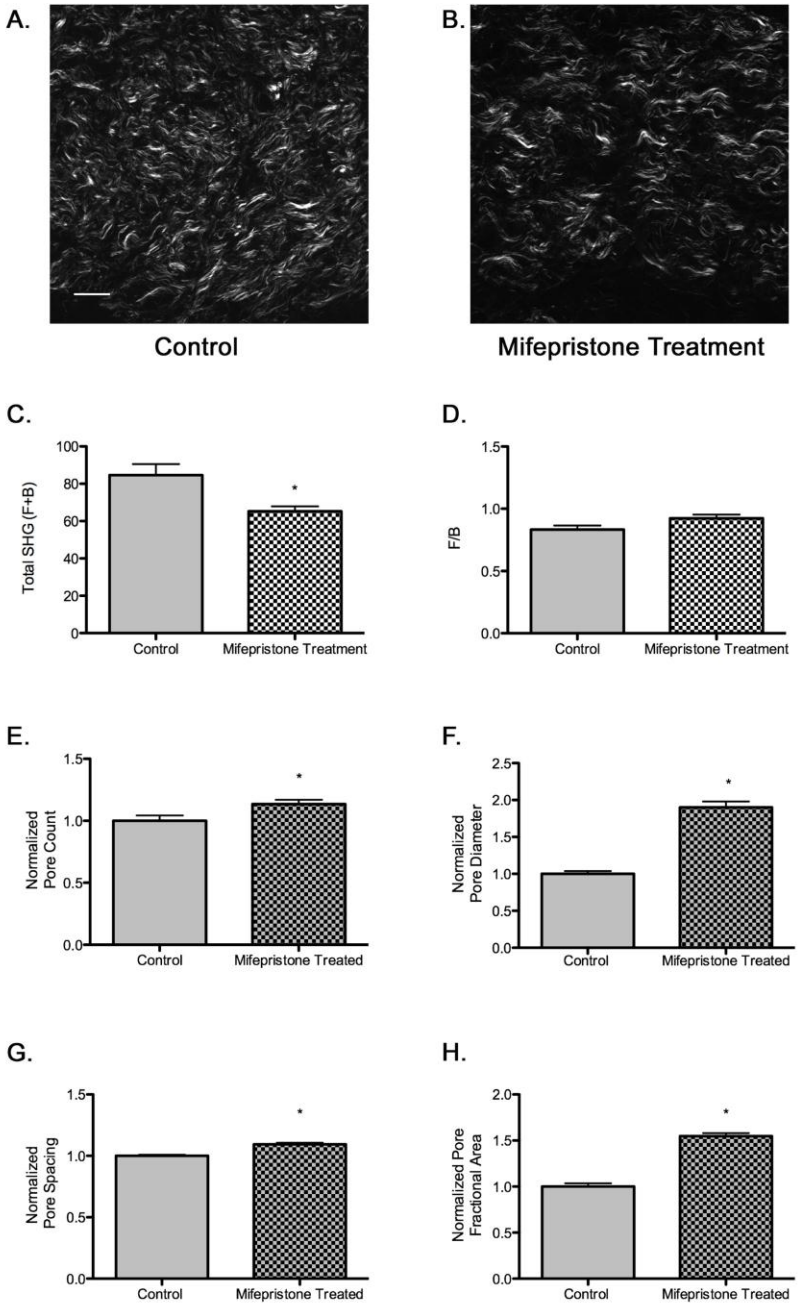
A.
B.
Control
Mifepristone Treatment
C.
Total SHG (F+B)
100
80
60
40
20
0
*
Control
Mifepristone Treatment
D.
F/B
1.5
1.0
0.5
0.0
Control
Mifepristone Treatment
E.
Normalized Pore Count
1.5
1.0
0.5
0.0
*
Control
Mifepristone Treated
F.
Normalized Pore Diameter
2.5
2.0
1.5
1.0
0.5
0.0
*
Control
Mifepristone Treated
G.
Normalized Pore Spacing
1.5
1.0
0.5
0.0
*
Control
Mifepristone Treated
H.
Normalized Pore Fractional Area
2.0
1.5
1.0
0.5
0.0
*
Control
Mifepristone Treated

Figure 5-7. Changes in Collagen Structure with Mifepristone Treatment Do Not Mimic Normal Cervical Ripening. Visual inspection of images from vehicle (A) or mifepristone (B) treated samples reveals a change in spacing between collagen fibers. Quantitative measurement of total signal intensity (F+B) (C) and F/B ratio (D) reveals a decline in SHG intensity in samples from treated animals compared with untreated controls (C, $P=0.0064$; D, $P=0.0038$). The number of pores in cervices from treated animals is increased relative to the vehicle control (E, $P=0.0215$). Pores are significantly larger in diameter (F, $P<0.0001$) and spaced farther apart (G, $P<0.0001$). Pore fractional area increases significantly upon treatment (H, $P<0.0001$). Bars represent the mean of measurements from images of transverse sections collected throughout the longitudinal extent of the cervix. Error bars represent standard error of the mean of 62 images for control and 52 images for treatment. n=4 animals/treatment group. Scale bar represents 25um. Modified with permission from Akins et.al. (2010) *Journal of Biomedical Optics*. 15(2):0260201-02602010.

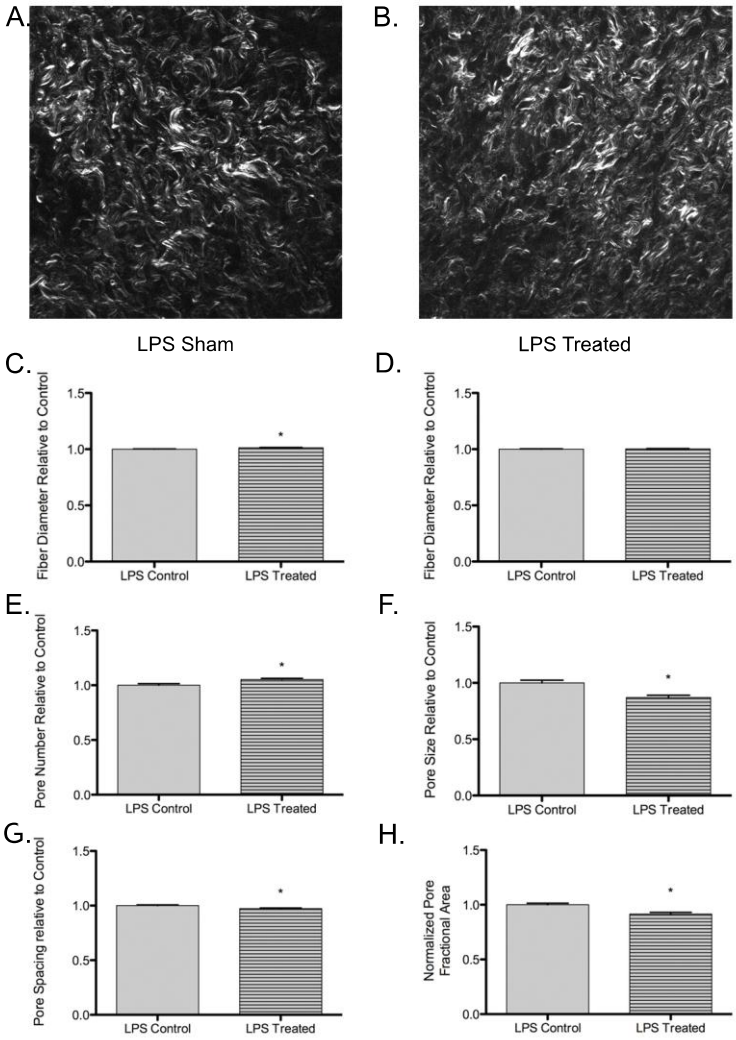

Figure 5-8. Changes in Collagen Structure with LPS Treatment Do Not Mimic Normal Cervical Ripening or Mifepristone Treatment. Visual inspection of images from (A) LPS Sham and (B) LPS treated cervices. Fiber diameter increased in the forward direction (C) (P=0.0024), but showed no significant change in the D) backward direction. The number of pores in images declined in LPS treated cervices increased (E, P=0.0026). Pores were significantly larger in diameter (F, P=0.0009) and spaced farther apart (G, P<0.0001). Pore fractional area significantly declined in LPS treated animals (P=0.0002). Error bars represent standard error of the mean of 100 images for sham and 110 images for day treated. n=3 animals/time point.

Table 5-1 QUANTITATIVE SHG MEASUREMENTS IN PRETERM BIRTH MODELS

Gestation Day/Treatment	**Fiber Diameter (um ± SEM)**		**Number of Pores (± SEM)**		**Pore Diameter (um ± SEM)**		**Pore Spacing (um± SEM)**		**Pore Fractional Area (% ± SEM)**	
	Forward	Backward	Forward	Backward	Forward	Backward	Forward	Backward	Forward	Backward
Day 15 + 0.5mg Mifepristone	1.93 ±0.009	2.16 ±0.007	553 ±16.9	370 ±12.2	21.2 ±0.86	45.5 ±2.6	7.7 ±0.08	9.8 ±0.17	34.0 ±0.72	45.0 ±0.94
Day 15 +Vehicle	1.83 ±0.007	2.12 ±0.007	488 ±21.6	414 ±33.4	11.1 ±0.41	20.3 ±1.14	7.1 ±0.07	7.8 ±0.14	22.0 ±0.77	31.7 ±0.97
Day 15 + 150µg LPS	2.38 ±0.006	2.81 ±0.006	827.8 ±8.37	597 ±8.45	20.7 ±0.5	27.7 ±0.64	8.05 ±0.04	9.53 ±0.07	31.4 ±0.53	29.9 ±0.4
Day 15 + Vehicle	2.35 ±0.007	2.79 ± 0.008	786 ±10.9	578 ±13.6	23.8 ±0.6	32.3 ±1.3	8.3 ±0.06	9.8 ±0.11	34.3 ±0.5	32.3 ±0.56

Chapter 6 Discussion and Future Directions

Cervical remodeling is essential for successful birth. It has long been appreciated that dynamic changes in the ECM must orchestrate remodeling of the connective tissue rich cervix, which allows for the progressive loss of tensile strength observed during gestation. Over the last 35 years two major paradigms have dominated the cervical biology field. The first is the concept that the majority of changes in the cervix occur at the end of pregnancy when there is a functional loss of the pregnancy-maintaining hormone, progesterone. Secondly, that immune cells are recruited to the cervix and orchestrate changes in ECM structure that allow cervical ripening and dilation at birth. In recent years work from our laboratory and others has determined that cervical changes begin shortly after pregnancy and continue progressively thereafter and secondly that immune cells are not activated during term ripening to cause ECM breakdown. Read observed an increase in collagen solubility and a decline in tissue stiffness as early as day 12 of the 19 day mouse gestation. This work highlighted the fact that ECM changes, in particular collagen changes, begin long before the withdrawal of progesterone occurs (Read et al., 2007). Subsequent work in our lab has shown that myeloid derived cells populate the cervix during term cervical ripening, the activation of the immune system does not occur until postpartum repair of the cervix, rather than remodeling the cervix at term (Timmons et al., 2009). The finding that ECM transformations begin early, coupled with the fact that collagen

degradation by immune cell proteases is not a key process in remodeling, leads to the critical question as to how ECM and collagen structures are modulated to allow the cervix to become more compliant and dilate sufficiently at birth. Work in our laboratory and the aforementioned query set the stage for the work described in this thesis, which is based on the hypothesis that changes in collagen processing and assembly or changes in collagen modulating molecules contribute to the progressive decline in tensile strength over gestation.

Studies described in this thesis have determined that a decline in expression of collagen cross-linking enzymes as well as a decline in the matricellular proteins, tenascin C and thrombospondin 2 are the earliest described changes in the pregnant cervix. These changes contribute to a change in the type and degree of collagen cross-links, an increase in collagen fibril diameter and progressive changes in collagen fiber microstructure. Equally important in this study were the findings that: 1) many enzymes involved in collagen processing are expressed at constant levels throughout gestation 2) changes in the proteoglycan decorin do not appear important for term ripening, and 3) changes in the ratio of fibrillar collagen I to III does not contribute to changes in biomechanical properties of the cervix. Finally, these studies provide evidence that modifications in collagen structure occur by diverse mechanisms in two preterm birth models as compared to term pregnancy. These studies provide novel insights into mechanisms of term and preterm remodeling as well as provide

evidence to suggest that quantitative assessment of collagen microstructure by SHG harbors potential as a clinical tool to stage pregnancy and risk of prematurity. These findings in turn lead to a number of new questions and suggest further studies required to complete our understanding of the cervical remodeling process.

One important area of investigation will be the elucidation of hormonal factors that regulate early pregnancy changes in the cervical ECM. Matricelluar proteins, THBS2 and TNC, as well enzymes important in collagen cross-linking (PLOD and LOX) were all shown to decline early in pregnancy, long before a change in the local hormone environment. While LOX levels have been shown to be in part induced by estrogen, a link between matricellular proteins and PLOD family enzymes with pregnancy hormones has yet to be studied (Ozasa et al., 1981). *Plod2* has been shown to be regulated by thyroid stimulating hormone, and to be induced by the pituitary hormone *Pitx2* but it is not clear if these pathways are implicated in the cervix during pregnancy (Hjalt et al., 2001; Saha et al., 2005). Understanding the hormonal control (if any) of these ECM regulating factors will provide a foundation for understanding the mechanisms that control cervical softening and may identify factors whose misregulation could predispose women to cervical insufficiency.

The reduction in collagen cross-links during cervical remodeling is likely due to the reduction in lysyl hydroxylases in the ER (PLOD family) and lysyl

oxidase (LOX) in the extracellular space, as both these enzymes are key in forming non-reducible HP and LP crosslinks. While mRNA levels of these enzymes decline during pregnancy, the enzyme activity of the lysyl hydroxylases have not been measured in the mouse cervix. Enzyme activity should be quantified to confirm the relationship between enzyme mRNA and the decline in cervical collagen cross-links. Understanding how a decline in cross-links affects the biomechanical strength of the cervix would help us comprehend the contribution crosslinks play in the decline of cervical tensile strength. Beta-aminopropionitrile (BAPN) is a lathyrogen that irreversibly blocks LOX activity and therefore decreases collagen cross-links. By administering BAPN to NP mice we may be able to recapitulate a pregnancy cervical collagen phenotype. Recent work by Leventhal *et.al.* has demonstrated that a reduction in collagen cross-links via BAPN can contribute to an SHG signal, in which collagen fibers have a curly and thick in appearance, similar to what is seen on day 18 of mouse gestation (Figure 4-3) (Levental et al., 2009). BAPN treatment of NP mice may allow us to elucidate the contribution that a reduction in cross-linking plays in altering cervical biomechanical strength and SHG collagen signal.

We have shown that collagen organization is dramatically altered during pregnancy. Collagens and cells interact via cell surface receptors such as integrins and DDRs (discoid domain receptors) to modulate cell adhesion, migration, proliferation and cell death. These interactions can dramatically change collagen

properties. Integrins are localized to both epithelia and fibroblasts in the cervix (Zutter and Santoro, 1990). However, changes in localization and resulting signaling cascades have not been carefully studied in the cervix. Studies focusing on understanding interactions of collagen and cell surface receptors are needed to understand the cellular cues and signaling cascades in the cervix at the time of cervical remodeling.

A greater understanding of the molecular mechanisms regulating cervical remodeling will require investigations focused on other collagens that can affect collagen fibrillogensis. Collagen V is a fibril collagen that associates with collagen I and has widespread distribution in the body (Aszodi et al., 2006; Kadler et al., 2008). It is required for collagen fibrillogenesis as seen in knockout mice of *Col5a1,* which have virtually no collagen I fibril formation and die on embryonic day ten. *Col5a1* heterozygous mice live and show abnormal and reduced collagen (Wenstrup et al., 2004). Collagen V and collagen XI (structurally similar to collagen V) are defined as a fibril collagen nucleator. These molecules incorporate with collagen I molecules and nucleate the resulting fibril. Collagen V and XI have their c-terminal triple helical domain in the center of the collagen fibril, while their N-terminus extends to the fibril surface, this configuration is thought to allow collagen V and XI to control lateral fusion and fibril size (Holmes and Kadler, 2006; Kadler et al., 2008). A reduction in collagens V and XI may cause collagen I fibrils to self aggregate unchecked,

causing abnormalities in fibril size (Wenstrup et al., 2004; Wenstrup et al., 2011). Collagen V and XI levels in the cervix have not been directly measured. However, preliminary data show that Col5a1, Col5a3 and ColXIa1 levels all decline at term and are upregulated postpartum. Understanding the affect of a decline in both collagen nucleators during cervical remodeling would be a beneficial area of study.

Non-fibrillar collagens called FACITS (fibril-associated collagens with interrupted triple helices) can also bind to fibrillar collagens and affect their fibrillogenesis (Gordon and Hahn, 2010). Collagen XIV has been shown to bind collagen I and is found in tissues that have high mechanical stress (Walchli et al., 1994; Niyibizi et al., 1995; Berthod et al., 1997; Gerecke et al., 2004). In collagen XIV knockout mice, tissue has a decreased elasticity and the maximum stress the tissue can withstand is greatly reduced. Fibril diameter increased in collagen XIV deficient mice but more interestingly the distribution of collagen fibril diameter broadened in a similar pattern to the broadening seen in progressive normal pregnancy (Figure 2-7) (Ansorge et al., 2009). Collagen XIV has not been studied in the cervix, however, preliminary microarray data shows that mRNA levels decline from gestation day 15 to day 18 and further decline immediately postpartum. Further study will be needed to understand the regulation and roles of this and other FACITs in the cervix during pregnancy and parturition.

While direct changes in collagen organization and morphology are present in the cervix during pregnancy changes in other ECM components also affect the organization of the ECM, tissue strength and cell signaling cascades. Matricellular proteins, SLRPs, and GAGs all play essential roles in maintaining or altering ECM environments. Previous work in the cervix, suggested that decorin increased during gestation and was responsible for dispersion of the matrix (Leppert et al., 2000). However, insights from knockout mice have shown that a loss of decorin rather than an excess allows for dispersion of collagen and can affect fibrillogenesis by increasing lateral fusion of collagen fibrils (Danielson et al., 1997). Here we show that SLRPs, specifically decorin, are not regulated during cervical ripening and mice lacking decorin have aberrantly shaped cervical collagen fibrils. Even though decorin and other SLRPS are not altered during cervical remodeling it is important to understand how each of these factors interact within the changing cervical matrix at this time and their contributions to the total tensile strength of the tissue. Decorin misregulation occurs in Ehlers-Danlos Syndrome patients, who are at higher risk for preterm birth (via PPROM and cervical insufficiency), understanding how decorin and other SLRPs function and interact in the matrix may shine light on potential therapies. SLRPs are regulated during postpartum repair, which is essential to allow recovery of the cervix to the NP state. GAG composition of decorin and other PGs may be altered during gestation. GAG concentration has been previously shown to decline in the

cervix at term (Danforth et al., 1974; Osmers et al., 1993). GAGs are vital in organizing the ECM. In tendon, the concentration of GAGs is the single highest prediction factor for biomechanical strength (Robinson et al., 2004). Analysis of SLRP GAG chains and free GAGs is essential in understanding the viscoelastic properties of the cervix during pregnancy.

While collagen content does not appear to change in the mouse models of preterm birth, collagen structure assessed via TEM and immunofluorescence appears dramatically altered with mifepristone treatment. Collagen structure and fibril diameter are not significantly altered with LPS treatment, however passage of pups still occur. This further confirms that preterm birth can occur with multiple mechanisms. Biomechanical assessment of preterm birth models is crucial to understand the degree of remodeling that occurs in both models of preterm birth. Previous work has suggested that mifepristone and LPS treatment partially activates proinflammatory pathways (Gonzalez et al., 2009; Holt et al., 2011). To assess the contribution of immune cell proteases to mifepristone and/or LPS induced preterm birth, future investigations using collagenase resistant mice may be informative. Collagenase resistant mice have been created with site-directed mutagenesis to the collagen I alpha1 MMP cleavage site (Wu et al., 1990). The fact that these mice have normal delivery implies that collagenase is not essential for successful birth to occur. However, if increased collagenase is

part of the mechanism involved in either mifepristone or LPS mediated preterm birth models, we anticipate the treated mice will not deliver preterm.

Collagen SHG has remarkable potential to act as a means to stage pregnancy and diagnose preterm birth early enough for preventative measures to be taken. As shown in chapter 4, changes in collagen ultrastructure can be observed as early as day 6 in normal pregnancy, long before any measurable biomechanical changes have occurred. SHG can also distinguish differences in collagen morphology in preterm birth images as compared to gestation matched controls and shows no change in morphological measurements in a model that fails to undergo cervical ripening (Chapter 4 and 5).

Classification algorithm and acquisition techniques must be resolved to allow for optimal procurement of quantifiable and comparable images in the clinic along with development of an SHG endoscope. Development of an SHG endoscope will allow us to first follow SHG signal during pregnancy of a single mouse, and to watch changes when treating mice with preterm-causing agents. SHG endoscopes are currently in development and their application to identification of women at risk for impending preterm birth has great potential to improve diagnostic tools in the obstetrics clinic (Bao et al., 2008; Wu et al., 2009).

Bibliography

2008 Assisted Reproductive Technology Success Rates: National Summary and Fertility Clinic Reports (2010). Center for Disease Control and Prevention. Atlanta, Georgia.

Adams, M. M., L. D. Elam-Evans, et al., 2000. Rates of and factors associated with recurrence of preterm delivery. JAMA 283(12): 1591-6.

Akins, M. L., K. Luby-Phelps, et al., 2010. Second harmonic generation imaging as a potential tool for staging pregnancy and predicting preterm birth. J Biomed Opt 15(2): 0260201 - 02602010.

Akins, M. L., K. Luby-Phelps, et al., 2011. Cervical Softening During Pregnancy-Regulated Changes in Collagen Cross-Linking and Composition of Matricellular Proteins in the Mouse. Biology of Reproduction. 84(5): 1053-62.

Akins, M. L., K. Luby-Phelps, et al., 2010. Second harmonic generation imaging as a potential tool for staging pregnancy and predicting preterm birth. J Biomed Opt 15(2): 0260201 - 02602010.

Ameye, L. and M. F. Young, 2002. Mice deficient in small leucine-rich proteoglycans: novel in vivo models for osteoporosis, osteoarthritis, Ehlers-Danlos syndrome, muscular dystrophy, and corneal diseases. Glycobiology 12(9): 107R-16R.

Andersson, S., D. Minjarez, et al., 2008. Estrogen and progesterone metabolism in the cervix during pregnancy and parturition. J Clin Endocrinol Metab 93(6): 2366-74.

Andres, R. L. and M. C. Day, 2000. Perinatal complications associated with maternal tobacco use. Semin Neonatol 5(3): 231-41.

Ansorge, H. L., X. Meng, et al., 2009. Type XIV Collagen Regulates Fibrillogenesis: PREMATURE COLLAGEN FIBRIL GROWTH AND TISSUE DYSFUNCTION IN NULL MICE. The Journal of biological chemistry 284(13): 8427-38.

Anum, E. A., L. D. Hill, et al., 2009a. Connective tissue and related disorders and preterm birth: clues to genes contributing to prematurity. Placenta 30(3): 207-15.

Anum, E. A., E. H. Springel, et al., 2009b. Genetic contributions to disparities in preterm birth. Pediatr Res 65(1): 1-9.

Aszodi, A., K. R. Legate, et al., 2006. What mouse mutants teach us about extracellular matrix function. Annu Rev Cell Dev Biol 22: 591-621.

Bank, R. A., B. Beekman, et al., 1997. Sensitive fluorimetric quantitation of pyridinium and pentosidine crosslinks in biological samples in a single high-performance liquid chromatographic run. J Chromatogr B Biomed Sci Appl 703(1-2): 37-44.

Bao, H., J. Allen, et al., 2008. Fast handheld two-photon fluorescence microendoscope with a 475 microm x 475 microm field of view for in vivo imaging. Opt Lett 33(12): 1333-5.

Berghella, V., T. J. Rafael, et al., 2011. Cerclage for short cervix on ultrasonography in women with singleton gestations and previous preterm birth : a meta-analysis. Obstet Gynecol 117(3): 663-71.

Berthod, F., L. Germain, et al., 1997. Differential expression of collagens XII and XIV in human skin and in reconstructed skin. The Journal of investigative dermatology 108(5): 737-42.

Bi, Y., C. H. Stuelten, et al., 2005. Extracellular matrix proteoglycans control the fate of bone marrow stromal cells. The Journal of biological chemistry 280(34): 30481-9.

Bokstrom, H. and A. Norstrom, 1995. Effects of mifepristone and progesterone on collagen synthesis in the human uterine cervix. Contraception 51(4): 249-54.

Border, W. A., N. A. Noble, et al., 1992. Natural inhibitor of transforming growth factor-beta protects against scarring in experimental kidney disease. Nature 360(6402): 361-4.

Bornstein, P., 2009. Matricellular proteins: an overview. J Cell Commun Signal 3(3-4): 163-5.

Bornstein, P. and E. H. Sage, 2002. Matricellular proteins: extracellular modulators of cell function. Curr Opin Cell Biol 14(5): 608-16.

Bradshaw, A. D., P. Puolakkainen, et al., 2003. SPARC-null mice display abnormalities in the dermis characterized by decreased collagen fibril diameter and reduced tensile strength. J Invest Dermatol 120(6): 949-55.

Breeveld-Dwarkasing, V. N., J. M. te Koppele, et al., 2003. Changes in water content, collagen degradation, collagen content, and concentration in repeated biopsies of the cervix of pregnant cows. Biol Reprod 69(5): 1608-14.

Briery, C. M., E. W. Veillon, et al., 2011. Women with preterm premature rupture of the membranes do not benefit from weekly progesterone. American journal of obstetrics and gynecology 204(1): 54 e1-5.

Buhimschi, I. A., L. Dussably, et al., 2004. Physical and biomechanical characteristics of rat cervical ripening are not consistent with increased collagenase activity. Am J Obstet Gynecol 191(5): 1695-704.

Calmus, M. L., E. E. Macksoud, et al., 2011. A Mouse Model of Spontaneous Preterm Birth Based on the Genetic Ablation of Biglycan and Decorin. Reproduction.

Canty, E. G. and K. E. Kadler, 2005. Procollagen trafficking, processing and fibrillogenesis. J Cell Sci 118(Pt 7): 1341-53.

Caritis, S. N., D. J. Rouse, et al., 2009. Prevention of preterm birth in triplets using 17 alpha-hydroxyprogesterone caproate: a randomized controlled trial. Obstetrics and gynecology 113(2 Pt 1): 285-92.

Celik, E., M. To, et al., 2008. Cervical length and obstetric history predict spontaneous preterm birth: development and validation of a model to provide individualized risk assessment. Ultrasound Obstet Gynecol 31(5): 549-54.

Chwalisz, K., 1994. The use of progesterone antagonists for cervical ripening and as an adjunct to labour and delivery. Hum Reprod 9 Suppl 1: 131-61.

Clark, K., H. Ji, et al., 2006. Mifepristone-induced cervical ripening: structural, biomechanical, and molecular events. Am J Obstet Gynecol 194(5): 1391-8.

Cleary, B. J., J. M. Donnelly, et al., 2011. Methadone and perinatal outcomes: a retrospective cohort study. American journal of obstetrics and gynecology 204(2): 139 e1-9.

Committee for the Update of the Guide for the Care and Use of Laboratory Animals, Institute of Laboratory Animal Research, Division on Earth and Life Studies (2011). Guide for the Care and Use of Laboratory Animals. The National Academies Press, Washington D.C.

Conde-Agudelo, A., A. Rosas-Bermudez, et al., 2006. Birth spacing and risk of adverse perinatal outcomes: a meta-analysis. JAMA : the journal of the American Medical Association 295(15): 1809-23.

Condon, J. C., P. Jeyasuria, et al., 2003. A decline in the levels of progesterone receptor coactivators in the pregnant uterus at term may antagonize progesterone receptor function and contribute to the initiation of parturition. Proceedings of the National Academy of Sciences of the United States of America 100(16): 9518-23.

Condon, J. C., D. B. Hardy, et al., 2006. Up-regulation of the progesterone receptor (PR)-C isoform in laboring myometrium by activation of nuclear factor-kappaB may contribute to the onset of labor through inhibition of PR function. Molecular endocrinology 20(4): 764-75.

Costa, L. M. and A. I. Csapo, 1959. Asymmetrical delivery in rabbits. Nature 184(4681): 144-146.

Cox, G., E. Kable, et al., 2003. 3-dimensional imaging of collagen using second harmonic generation. J Struct Biol 141(1): 53-62.

Csapo, A. I. and M. A. Lloyd-Jacob, 1961. Effect of progesterone on pregnancy. Method of administration and effect of progesterone. Nature 192: 329-30.

Cunningham, F. G., K. J. Leveno, et al. (2010a). Chapter 6-Parturition. Williams Obstetrics, McGraw-Hill.

Cunningham, F. G., K. J. Leveno, et al. (2010b). Chapter 9- Abortion. Williams Obstetrics, McGraw-Hill.

Cunningham, F. G., K. J. Leveno, et al. (2010c). Chapter 36-Preterm Birth. Williams Obstetrics, McGraw-Hill.

da Fonseca, E. B., R. E. Bittar, et al., 2003. Prophylactic administration of progesterone by vaginal suppository to reduce the incidence of spontaneous preterm birth in women at increased risk: a randomized placebo-controlled double-blind study. American journal of obstetrics and gynecology 188(2): 419-24.

Dailey, T., H. Ji, et al., 2009. The role of transforming growth factor beta in cervical remodeling within the rat cervix. Am J Obstet Gynecol 201(3): 322 e1-6.

Danforth, D. N., A. Veis, et al., 1974. The effect of pregnancy and labor on the human cervix: changes in collagen, glycoproteins, and glycosaminoglycans. Am J Obstet Gynecol 120(5): 641-51.

Danielson, K. G., H. Baribault, et al., 1997. Targeted disruption of decorin leads to abnormal collagen fibril morphology and skin fragility. J Cell Biol 136(3): 729-43.

de Carvalho, M. H., R. E. Bittar, et al., 2005. Prediction of preterm delivery in the second trimester. Obstetrics and gynecology 105(3): 532-6.

Dietz, P. M., L. J. England, et al., 2010. Infant morbidity and mortality attributable to prenatal smoking in the U.S. Am J Prev Med 39(1): 45-52.

Drewes, P. G., H. Yanagisawa, et al., 2007. Pelvic organ prolapse in fibulin-5 knockout mice: pregnancy-induced changes in elastic fiber homeostasis in mouse vagina. Am J Pathol 170(2): 578-89.

Dudley, D. J., D. W. Branch, et al., 1996. Induction of preterm birth in mice by RU486. Biol Reprod 55(5): 992-5.

Elovitz, M. A., Z. Wang, et al., 2003. A new model for inflammation-induced preterm birth: the role of platelet-activating factor and Toll-like receptor-4. The American journal of pathology 163(5): 2103-11.

Eyre, D. R., M. A. Paz, et al., 1984. Cross-linking in collagen and elastin. Annu Rev Biochem 53: 717-48.

Feltovich, H., H. Ji, et al., 2005. Effects of selective and nonselective PGE2 receptor agonists on cervical tensile strength and collagen organization and microstructure in the pregnant rat at term. Am J Obstet Gynecol 192(3): 753-60.

Fleischmajer, R., E. D. MacDonald, et al., 1990a. Dermal collagen fibrils are hybrids of type I and type III collagen molecules. Journal of structural biology 105(1-3): 162-9.

Fleischmajer, R., J. S. Perlish, et al., 1990b. Type I and type III collagen interactions during fibrillogenesis. Annals of the New York Academy of Sciences 580: 161-75.

Fleischmajer, R., J. S. Perlish, et al., 1987. Amino and carboxyl propeptides in bone collagen fibrils during embryogenesis. Cell and tissue research 247(1): 105-9.

Fonseca, E. B., E. Celik, et al., 2007. Progesterone and the risk of preterm birth among women with a short cervix. N Engl J Med 357(5): 462-9.

Friedl, P., K. Wolf, et al., 2007. Biological second and third harmonic generation microscopy. Curr Protoc Cell Biol Chapter 4: Unit 4 15.

Ge, G., Y. Zhang, et al., 2006. Mammalian tolloid-like 1 binds procollagen C-proteinase enhancer protein 1 and differs from bone morphogenetic protein 1 in the functional roles of homologous protein domains. J Biol Chem 281(16): 10786-98.

Geng, Y., D. McQuillan, et al., 2006. SLRP interaction can protect collagen fibrils from cleavage by collagenases. Matrix Biol 25(8): 484-91.

Gerecke, D. R., X. Meng, et al., 2004. Complete primary structure and genomic organization of the mouse Col14a1 gene. Matrix biology : journal of the International Society for Matrix Biology 22(7): 595-601.

Glassman, W., M. Byam-Smith, et al., 1995. Changes in rat cervical collagen during gestation and after antiprogesterone treatment as measured in vivo with light-induced autofluorescence. American journal of obstetrics and gynecology 173(5): 1550-6.

Goldenberg, R. L., J. F. Culhane, et al., 2008. Epidemiology and causes of preterm birth. Lancet 371(9606): 75-84.

Goldenberg, R. L., J. D. Iams, et al., 2000. The Preterm Prediction Study: sequential cervical length and fetal fibronectin testing for the prediction of spontaneous preterm birth. National Institute of Child Health and Human Development Maternal-Fetal Medicine Units Network. Am J Obstet Gynecol 182(3): 636-43.

Goldenberg, R. L., M. A. Klebanoff, et al., 1996a. Bacterial colonization of the vagina during pregnancy in four ethnic groups. Vaginal Infections and Prematurity Study Group. Am J Obstet Gynecol 174(5): 1618-21.

Goldenberg, R. L., B. M. Mercer, et al., 1996b. The preterm prediction study: fetal fibronectin testing and spontaneous preterm birth. NICHD Maternal Fetal Medicine Units Network. Obstetrics and gynecology 87(5 Pt 1): 643-8.

Gonzalez, J. M., H. Xu, et al., 2009. Preterm and term cervical ripening in CD1 Mice (Mus musculus): similar or divergent molecular mechanisms? Biol Reprod 81(6): 1226-32.

Goodman, J. W. (1985). Statistical Optics. Wiley-Interscience, Stanford.

Gordon, M. K. and R. A. Hahn, 2010. Collagens. Cell Tissue Res 339(1): 247-57.

Gutsmann, T., G. E. Fantner, et al., 2003. Evidence that collagen fibrils in tendons are inhomogeneously structured in a tubelike manner. Biophys J 84(4): 2593-8.

Ha-Vinh, R., Y. Alanay, et al., 2004. Phenotypic and molecular characterization of Bruck syndrome (osteogenesis imperfecta with contractures of the large joints) caused by a recessive mutation in PLOD2. Am J Med Genet A 131(2): 115-20.

Han, Z., S. Mulla, et al., 2011. Maternal underweight and the risk of preterm birth and low birth weight: a systematic review and meta-analyses. Int J Epidemiol 40(1): 65-101.

Hassan, S. S., R. Romero, et al., 2006. The transcriptome of the uterine cervix before and after spontaneous term parturition. American journal of obstetrics and gynecology 195(3): 778-86.

Hassan, S. S., R. Romero, et al., 2009. The transcriptome of cervical ripening in human pregnancy before the onset of labor at term: identification of novel molecular functions involved in this process. J Matern Fetal Neonatal Med 22(12): 1183-93.

Hassan, S. S., R. Romero, et al., 2011. Vaginal progesterone reduces the rate of preterm birth in women with a sonographic short cervix: a multicenter, randomized, double-blind, placebo-controlled trial. Ultrasound Obstet Gynecol.

Hausser, H., A. Groning, et al., 1994. Selective inactivity of TGF-beta/decorin complexes. FEBS letters 353(3): 243-5.

Heaps, B. R., M. House, et al. 2007. Matrix Biology and Preterm Birth. Preterm Birth: Mechanisms, Mediators, Prediction, Prevention, and Intervention F. Petraglia, J. F. Strauss, 3rd, S. Gabbe and G. Weiss. Informa. London.

Hegar, A., 1895. Diagnose der fruhesten Shwangerschaftsperiode Dtsch. Med. Wochenschr. 21: 565-567.

Heino, J., R. A. Ignotz, et al., 1989a. Regulation of cell adhesion receptors by transforming growth factor-beta. Concomitant regulation of integrins that share a common beta 1 subunit. The Journal of biological chemistry 264(1): 380-8.

Heino, J. and J. Massague, 1989b. Transforming growth factor-beta switches the pattern of integrins expressed in MG-63 human osteosarcoma cells and causes a selective loss of cell adhesion to laminin. The Journal of biological chemistry 264(36): 21806-11.

Hendershot, L. M. and N. J. Bulleid, 2000. Protein-specific chaperones: the role of hsp47 begins to gel. Curr Biol 10(24): R912-5.

Hildebrand, A., M. Romaris, et al., 1994. Interaction of the small interstitial proteoglycans biglycan, decorin and fibromodulin with transforming growth factor beta. The Biochemical journal 302 (Pt 2): 527-34.

Hirsch, E. and R. Muhle, 2002. Intrauterine bacterial inoculation induces labor in the mouse by mechanisms other than progesterone withdrawal. Biology of reproduction 67(4): 1337-41.

Hirsch, E., Y. Filipovich, et al., 2006. Signaling via the type I IL-1 and TNF receptors is necessary for bacterially induced preterm labor in a murine model. Am J Obstet Gynecol 194(5): 1334-40.

Hjalt, T. A., B. A. Amendt, et al., 2001. PITX2 regulates procollagen lysyl hydroxylase (PLOD) gene expression: implications for the pathology of Rieger syndrome. The Journal of cell biology 152(3): 545-52.

Holmes, D. F. and K. E. Kadler, 2006. The 10+4 microfibril structure of thin cartilage fibrils. Proceedings of the National Academy of Sciences of the United States of America 103(46): 17249-54.

Holt, R., B. C. Timmons, et al., 2011. The Molecular Mechanisms of Cervical Ripening Differ between Term and Preterm Birth. Endocrinology 152(3): 1036-46.

Honest, H., C. A. Forbes, et al., 2009. Screening to prevent spontaneous preterm birth: systematic reviews of accuracy and effectiveness literature with economic modelling. Health Technol Assess 13(43): 1-627.

House, M., D. L. Kaplan, et al., 2009. Relationships between mechanical properties and extracellular matrix constituents of the cervical stroma during pregnancy. Semin Perinatol 33(5): 300-7.

House, M. and S. Socrate, 2006. The cervix as a biomechanical structure. Ultrasound Obstet Gynecol 28(6): 745-9.

Hulmes, D. J., K. E. Kadler, et al., 1989. Pleomorphism in type I collagen fibrils produced by persistence of the procollagen N-propeptide. J Mol Biol 210(2): 337-45.

Hyry, M., J. Lantto, et al., 2009. Missense mutations that cause Bruck syndrome affect enzymatic activity, folding, and oligomerization of lysyl hydroxylase 2. J Biol Chem 284(45): 30917-24.

Hyytiainen, M., C. Penttinen, et al., 2004. Latent TGF-beta binding proteins: extracellular matrix association and roles in TGF-beta activation. Crit Rev Clin Lab Sci 41(3): 233-64.

Iams, J. D., 2003. The epidemiology of preterm birth. Clin Perinatol 30(4): 651-64.

Iams, J. D., R. L. Goldenberg, et al., 1996. The length of the cervix and the risk of spontaneous premature delivery. National Institute of Child Health and Human Development Maternal Fetal Medicine Unit Network. N Engl J Med 334(9): 567-72.

Iams, J. D., R. L. Goldenberg, et al., 2001. The preterm prediction study: can low-risk women destined for spontaneous preterm birth be identified? Am J Obstet Gynecol 184(4): 652-5.

Iams, J. D., R. Romero, et al., 2008. Primary, secondary, and tertiary interventions to reduce the morbidity and mortality of preterm birth. Lancet 371(9607): 164-75.

Iozzo, R. V., 1998. Matrix proteoglycans: from molecular design to cellular function. Annu Rev Biochem 67: 609-52.

Iozzo, R. V., 1999. The biology of the small leucine-rich proteoglycans. Functional network of interactive proteins. J Biol Chem 274(27): 18843-6.

Ishida, Y., H. Kubota, et al., 2006. Type I collagen in Hsp47-null cells is aggregated in endoplasmic reticulum and deficient in N-propeptide processing and fibrillogenesis. Mol Biol Cell 17(5): 2346-55.

Ito, A., K. Kitamura, et al., 1979. The change in solubility of type I collagen in human uterine cervix in pregnancy at term. Biochem Med 21(3): 262-70.

Jones, P. L. and F. S. Jones, 2000. Tenascin-C in development and disease: gene regulation and cell function. Matrix Biol 19(7): 581-96.

Kadler, K. E., C. Baldock, et al., 2007. Collagens at a glance. J Cell Sci 120(Pt 12): 1955-8.

Kadler, K. E., A. Hill, et al., 2008. Collagen fibrillogenesis: fibronectin, integrins, and minor collagens as organizers and nucleators. Curr Opin Cell Biol 20(5): 495-501.

Kadler, K. E., Y. Hojima, et al., 1987. Assembly of collagen fibrils de novo by cleavage of the type I pC-collagen with procollagen C-proteinase. Assay of critical concentration demonstrates that collagen self-assembly is a classical example of an entropy-driven process. The Journal of biological chemistry 262(32): 15696-701.

Kadler, K. E., Y. Hojima, et al., 1990a. Collagen fibrils in vitro grow from pointed tips in the C- to N-terminal direction. Biochem J 268(2): 339-43.

Kadler, K. E., D. F. Holmes, et al., 1996. Collagen fibril formation. Biochem J 316 (Pt 1): 1-11.

Kadler, K. E., D. J. Hulmes, et al., 1990b. Assembly of type I collagen fibrils de novo by the specific enzymic cleavage of pC collagen. The fibrils formed at about 37 degrees C are similar in diameter, roundness, and apparent flexibility to the collagen fibrils seen in connective tissue. Ann N Y Acad Sci 580: 214-24.

Kagan, K. O., M. To, et al., 2006. Preterm birth: the value of sonographic measurement of cervical length. BJOG 113 Suppl 3: 52-6.

Kalamajski, S. and A. Oldberg, 2010. The role of small leucine-rich proteoglycans in collagen fibrillogenesis. Matrix Biol 29(4): 248-53.

Kao, K. Y. and J. G. Leslie, 1977. Polymorphism in human uterine collagen. Connect Tissue Res 5(2): 127-9.

Keene, D. R., L. Y. Sakai, et al., 1987a. Type III collagen can be present on banded collagen fibrils regardless of fibril diameter. The Journal of cell biology 105(5): 2393-402.

Keene, D. R., L. Y. Sakai, et al., 1987b. Direct visualization of IgM antibodies bound to tissue antigens using a monoclonal anti-type III collagen IgM as a model system. The journal of histochemistry and cytochemistry : official journal of the Histochemistry Society 35(3): 311-8.

Kershaw, C. M., R. J. Scaramuzzi, et al., 2007. The expression of prostaglandin endoperoxide synthase 2 messenger RNA and the proportion of smooth muscle and collagen in the sheep cervix during the estrous cycle. Biol Reprod 76(1): 124-9.

Kleissl, H. P., M. van der Rest, et al., 1978. Collagen changes in the human uterine cervix at parturition. Am J Obstet Gynecol 130(7): 748-53.

Kokenyesi, R., L. C. Armstrong, et al., 2004. Thrombospondin 2 deficiency in pregnant mice results in premature softening of the uterine cervix. Biol Reprod 70(2): 385-90.

Kokenyesi, R. and J. F. Woessner, Jr., 1990. Relationship between dilatation of the rat uterine cervix and a small dermatan sulfate proteoglycan. Biol Reprod 42(1): 87-97.

Kovacs, L., M. Sas, et al., 1984. Termination of very early pregnancy by RU 486--an antiprogestational compound. Contraception 29(5): 399-410.

Kuc, I. M. and P. G. Scott, 1997. Increased diameters of collagen fibrils precipitated in vitro in the presence of decorin from various connective tissues. Connective tissue research 36(4): 287-96.

Kyriakides, T. R., K. J. Leach, et al., 1999. Mice that lack the angiogenesis inhibitor, thrombospondin 2, mount an altered foreign body reaction characterized by increased vascularity. Proc Natl Acad Sci U S A 96(8): 4449-54.

Kyriakides, T. R., Y. H. Zhu, et al., 1998a. Mice that lack thrombospondin 2 display connective tissue abnormalities that are associated with disordered collagen fibrillogenesis, an increased vascular density, and a bleeding diathesis. J Cell Biol 140(2): 419-30.

Kyriakides, T. R., Y. H. Zhu, et al., 1998b. The distribution of the matricellular protein thrombospondin 2 in tissues of embryonic and adult mice. J Histochem Cytochem 46(9): 1007-15.

Lacomb, R., O. Nadiarnykh, et al., 2008a. Quantitative second harmonic generation imaging of the diseased state osteogenesis imperfecta: experiment and simulation. Biophys J 94(11): 4504-14.

Lacomb, R., O. Nadiarnykh, et al., 2008b. Phase Matching considerations in Second Harmonic Generation from tissues: Effects on emission

directionality, conversion efficiency and observed morphology. Opt Commun 281(7): 1823-1832.

Lamande, S. R. and J. F. Bateman, 1999. Procollagen folding and assembly: the role of endoplasmic reticulum enzymes and molecular chaperones. Semin Cell Dev Biol 10(5): 455-64.

Legare, F., C. Pfeffer, et al., 2007. The role of backscattering in SHG tissue imaging. Biophys J 93(4): 1312-20.

Leppert, P. C., 1995. Anatomy and physiology of cervical ripening. Clin Obstet Gynecol 38(2): 267-79.

Leppert, P. C., 1998. Proliferation and apoptosis of fibroblasts and smooth muscle cells in rat uterine cervix throughout gestation and the effect of the antiprogesterone onapristone. Am J Obstet Gynecol 178(4): 713-25.

Leppert, P. C., R. Kokenyesi, et al., 2000. Further evidence of a decorin-collagen interaction in the disruption of cervical collagen fibers during rat gestation. Am J Obstet Gynecol 182(4): 805-11; discussion 811-2.

Leppert, P. C., Yu S.Y., 1991. In Chapter 5: elastin and collagen in the human uterus and cervix. The extracellular matrix of the uterus, cervix, and fetal membranes: Synthesis, degradation, and hormonal regulation. . P. Leppert, Wessner JF. Perinatology Press.

Leung, M. K., L. I. Fessler, et al., 1979. Separate amino and carboxyl procollagen peptidases in chick embryo tendon. J Biol Chem 254(1): 224-32.

Leveno, K. J., D. D. McIntire, et al., 2009. Decreased preterm births in an inner-city public hospital. Obstetrics and gynecology 113(3): 578-84.

Levental, K. R., H. Yu, et al., 2009. Matrix crosslinking forces tumor progression by enhancing integrin signaling. Cell 139(5): 891-906.

Liggins, G. C. 1981. Cervical ripening as an inflammatory reaction. The Cervix in Pregnancy and Labour, Clinical and Biochemical Investigation. D. Ellwood, Anderson ,ABM. Churchill Livingston Edinburgh

Liu, X., H. Wu, et al., 1997. Type III collagen is crucial for collagen I fibrillogenesis and for normal cardiovascular development. Proc Natl Acad Sci U S A 94(5): 1852-6.

Lockwood, C. J., A. E. Senyei, et al., 1991. Fetal fibronectin in cervical and vaginal secretions as a predictor of preterm delivery. N Engl J Med 325(10): 669-74.

Lui, P. P., L. S. Chan, et al., 2010. Sustained expression of proteoglycans and collagen type III/type I ratio in a calcified tendinopathy model. Rheumatology (Oxford) 49(2): 231-9.

Mahendroo, M. S., K. M. Cala, et al., 1997. Fetal death in mice lacking 5alpha-reductase type 1 caused by estrogen excess. Mol Endocrinol 11(7): 917-27.

Mahendroo, M. S., K. M. Cala, et al., 1996. 5 alpha-reduced androgens play a key role in murine parturition. Molecular endocrinology 10(4): 380-92.

Mahendroo, M. S., A. Porter, et al., 1999. The parturition defect in steroid 5alpha-reductase type 1 knockout mice is due to impaired cervical ripening. Mol Endocrinol 13(6): 981-92.

Maillot, K. V. and B. K. Zimmermann, 1976. The solubility of collagen of the uterine cervix during pregnancy and labour. Arch Gynakol 220(4): 275-80.

Maloni, J. A., 2010. Antepartum bed rest for pregnancy complications: efficacy and safety for preventing preterm birth. Biol Res Nurs 12(2): 106-24.

Maradny, E. E., N. Kanayama, et al., 1995. Effects of neutrophil chemotactic factors on cervical ripening. Clin Exp Obstet Gynecol 22(1): 76-85.

Martin, J. A., 2011. Preterm births - United States, 2007. MMWR Surveill Summ 60 Suppl: 78-9.

Mathews, T. J. and M. F. MacDorman, 2010. Infant mortality statistics from the 2006 period linked birth/infant death data set. Natl Vital Stat Rep 58(17): 1-31.

Maul, H., G. Olson, et al., 2003. Cervical light-induced fluorescence in humans decreases throughout gestation and before delivery: Preliminary observations. Am J Obstet Gynecol 188(2): 537-41.

Maul, H., G. Saade, et al., 2005. Prediction of term and preterm parturition and treatment monitoring by measurement of cervical cross-linked collagen using light-induced fluorescence. Acta Obstet Gynecol Scand 84(6): 534-6.

McDonald, H. M., P. Brocklehurst, et al., 2007. Antibiotics for treating bacterial vaginosis in pregnancy. Cochrane Database Syst Rev(1): CD000262.

Meis, P. J., R. L. Goldenberg, et al., 1995. The preterm prediction study: significance of vaginal infections. National Institute of Child Health and Human Development Maternal-Fetal Medicine Units Network. Am J Obstet Gynecol 173(4): 1231-5.

Meis, P. J., R. L. Goldenberg, et al., 1998. The preterm prediction study: risk factors for indicated preterm births. Maternal-Fetal Medicine Units Network of the National Institute of Child Health and Human Development. American journal of obstetrics and gynecology 178(3): 562-7.

Meis, P. J., M. Klebanoff, et al., 2003. Prevention of recurrent preterm delivery by 17 alpha-hydroxyprogesterone caproate. N Engl J Med 348(24): 2379-85.

Mercer, B. M., R. L. Goldenberg, et al., 1996. The preterm prediction study: a clinical risk assessment system. American journal of obstetrics and gynecology 174(6): 1885-93; discussion 1893-5.

Minamoto, T., K. Arai, et al., 1987. Immunohistochemical studies on collagen types in the uterine cervix in pregnant and nonpregnant states. Am J Obstet Gynecol 156(1): 138-44.

Moreaux, L., O. Sandre, et al., 2001. Coherent scattering in multi-harmonic light microscopy. Biophys J 80(3): 1568-74.

Mowa, C. N., S. Jesmin, et al., 2004. Characterization of vascular endothelial growth factor (VEGF) in the uterine cervix over pregnancy: effects of denervation and implications for cervical ripening. J Histochem Cytochem 52(12): 1665-74.

Myers, K., S. Socrate, et al., 2009. Changes in the biochemical constituents and morphologic appearance of the human cervical stroma during pregnancy. Eur J Obstet Gynecol Reprod Biol 144 Suppl 1: S82-9.

Myers, K. M., A. P. Paskaleva, et al., 2008. Mechanical and biochemical properties of human cervical tissue. Acta Biomater 4(1): 104-16.

Myers, K. M., S. Socrate, et al., 2010. A study of the anisotropy and tension/compression behavior of human cervical tissue. J Biomech Eng 132(2): 0210031 - 02100315.

Myllyharju, J., 2003. Prolyl 4-hydroxylases, the key enzymes of collagen biosynthesis. Matrix Biol 22(1): 15-24.

Nadiarnykh, O., R. B. LaComb, et al., 2010. Alterations of the extracellular matrix in ovarian cancer studied by Second Harmonic Generation imaging microscopy. BMC Cancer 10: 94.

Nagai, N., M. Hosokawa, et al., 2000. Embryonic lethality of molecular chaperone hsp47 knockout mice is associated with defects in collagen biosynthesis. J Cell Biol 150(6): 1499-506.

Nageotte, M. P., D. Casal, et al., 1994. Fetal fibronectin in patients at increased risk for premature birth. Am J Obstet Gynecol 170(1 Pt 1): 20-5.

Niyibizi, C., C. S. Visconti, et al., 1995. Collagens in an adult bovine medial collateral ligament: immunofluorescence localization by confocal microscopy reveals that type XIV collagen predominates at the ligament-bone junction. Matrix biology : journal of the International Society for Matrix Biology 14(9): 743-51.

Norman, M., G. Ekman, et al., 1991. Proteoglycan metabolism in the connective tissue of pregnant and non-pregnant human cervix. An in vitro study. Biochem J 275 (Pt 2): 515-20.

Osmers, R., W. Rath, et al., 1990. Collagenase activity in the cervix of non-pregnant and pregnant women. Arch Gynecol Obstet 248(2): 75-80.

Osmers, R., W. Rath, et al., 1991. Collagenase activity in the human cervix uteri after prostaglandin E2 application during the first trimester. Eur J Obstet Gynecol Reprod Biol 42(1): 29-32.

Osmers, R., W. Rath, et al., 1993. Glycosaminoglycans in cervical connective tissue during pregnancy and parturition. Obstet Gynecol 81(1): 88-92.

Osmers, R., H. Tschesche, et al., 1994. Serum collagenase levels during pregnancy and parturition. Eur J Obstet Gynecol Reprod Biol 53(1): 55-7.

Owen, J., G. Hankins, et al., 2009. Multicenter randomized trial of cerclage for preterm birth prevention in high-risk women with shortened midtrimester cervical length. American journal of obstetrics and gynecology 201(4): 375 e1-8.

Owen, J., N. Yost, et al., 2001. Mid-trimester endovaginal sonography in women at high risk for spontaneous preterm birth. JAMA 286(11): 1340-8.

Ozasa, H., T. Tominaga, et al., 1981. Lysyl oxidase activity in the mouse uterine cervix is physiologically regulated by estrogen. Endocrinology 109(2): 618-21.

Platz-Christensen, J. J., P. Pernevi, et al., 1997. Prostaglandin E and F2 alpha concentration in the cervical mucus and mechanism of cervical ripening. Prostaglandins 53(4): 253-61.

Preterm Birth: Causes, Consequences, and Prevention (2007). National Academy of Sciences, Washington DC.

Prockop, D. J. and K. I. Kivirikko, 1995. Collagens: molecular biology, diseases, and potentials for therapy. Annu Rev Biochem 64: 403-34.

Rajabi, M. R., G. R. Dodge, et al., 1991. Immunochemical and immunohistochemical evidence of estrogen-mediated collagenolysis as a mechanism of cervical dilatation in the guinea pig at parturition. Endocrinology 128(1): 371-8.

Raspanti, M., M. Viola, et al., 2008. Glycosaminoglycans show a specific periodic interaction with type I collagen fibrils. J Struct Biol 164(1): 134-9.

Rath, W., R. Osmers, et al., 1993. Biochemical changes in human cervical connective tissue after intracervical application of prostaglandin E2. Prostaglandins 45(4): 375-84.

Raub, C. B., A. J. Putnam, et al., 2010. Predicting bulk mechanical properties of cellularized collagen gels using multiphoton microscopy. Acta Biomater.

Raub, C. B., V. Suresh, et al., 2007. Noninvasive assessment of collagen gel microstructure and mechanics using multiphoton microscopy. Biophys J 92(6): 2212-22.

Raub, C. B., J. Unruh, et al., 2008. Image correlation spectroscopy of multiphoton images correlates with collagen mechanical properties. Biophys J 94(6): 2361-73.

Read, C. P., R. A. Word, et al., 2007. Cervical remodeling during pregnancy and parturition: molecular characterization of the softening phase in mice. Reproduction 134(2): 327-40.

Rechberger, T., N. Uldbjerg, et al., 1988. Connective tissue changes in the cervix during normal pregnancy and pregnancy complicated by cervical incompetence. Obstet Gynecol 71(4): 563-7.

Reed, C. C. and R. V. Iozzo, 2002. The role of decorin in collagen fibrillogenesis and skin homeostasis. Glycoconj J 19(4-5): 249-55.

Rentz, T. J., F. Poobalarahi, et al., 2007. SPARC regulates processing of procollagen I and collagen fibrillogenesis in dermal fibroblasts. J Biol Chem 282(30): 22062-71.

Ricciotti, E. and G. A. FitzGerald, 2011. Prostaglandins and inflammation. Arterioscler Thromb Vasc Biol 31(5): 986-1000.

Riikonen, T., L. Koivisto, et al., 1995. Transforming growth factor-beta regulates collagen gel contraction by increasing alpha 2 beta 1 integrin expression in osteogenic cells. The Journal of biological chemistry 270(1): 376-82.

Robinson, P. S., T. W. Lin, et al., 2004. Investigating tendon fascicle structure-function relationships in a transgenic-age mouse model using multiple regression models. Ann Biomed Eng 32(7): 924-31.

Romanic, A. M., E. Adachi, et al., 1991. Copolymerization of pNcollagen III and collagen I. pNcollagen III decreases the rate of incorporation of collagen I into fibrils, the amount of collagen I incorporated, and the diameter of the fibrils formed. The Journal of biological chemistry 266(19): 12703-9.

Ross, R. G., K. Sathishkumar, et al., 2004. Mechanisms of lipopolysaccharide-induced changes in effects of contractile agonists on pregnant rat myometrium. American journal of obstetrics and gynecology 190(2): 532-40.

Rouse, D. J., S. N. Caritis, et al., 2007. A trial of 17 alpha-hydroxyprogesterone caproate to prevent prematurity in twins. N Engl J Med 357(5): 454-61.

Saha, S. K., P. Ghosh, et al., 2005. Differential expression of procollagen lysine 2-oxoglutarate 5-deoxygenase and matrix metalloproteinase isoforms in hypothyroid rat ovary and disintegration of extracellular matrix. Endocrinology 146(7): 2963-75.

Sakamoto, Y., P. Moran, et al., 2005. Macrophages and not granulocytes are involved in cervical ripening. J Reprod Immunol 66(2): 161-73.

Sakamoto, Y., P. Moran, et al., 2004. Interleukin-8 is involved in cervical dilatation but not in prelabour cervical ripening. Clin Exp Immunol 138(1): 151-7.

Savitz, D. A. and P. Murnane, 2010. Behavioral influences on preterm birth: a review. Epidemiology 21(3): 291-9.

Schaffir, J., 2006. Sexual intercourse at term and onset of labor. Obstetrics and gynecology 107(6): 1310-4.

Schlembach, D., L. Mackay, et al., 2009. Cervical ripening and insufficiency: from biochemical and molecular studies to in vivo clinical examination. Eur J Obstet Gynecol Reprod Biol 144 Suppl 1: S70-6.

Schonherr, E., P. Witsch-Prehm, et al., 1995. Interaction of biglycan with type I collagen. J Biol Chem 270(6): 2776-83.

Schultz-Cherry, S., H. Chen, et al., 1995. Regulation of transforming growth factor-beta activation by discrete sequences of thrombospondin 1. The Journal of biological chemistry 270(13): 7304-10.

Scott, J. E. and C. R. Orford, 1981. Dermatan sulphate-rich proteoglycan associates with rat tail-tendon collagen at the d band in the gap region. The Biochemical journal 197(1): 213-6.

Scott, J. E., C. R. Orford, et al., 1981. Proteoglycan-collagen arrangements in developing rat tail tendon. An electron microscopical and biochemical investigation. The Biochemical journal 195(3): 573-81.

Scott, J. E. and D. A. Parry, 1992. Control of collagen fibril diameters in tissues. Int J Biol Macromol 14(5): 292-3.

Sennstrom, M. B., G. Ekman, et al., 2000. Human cervical ripening, an inflammatory process mediated by cytokines. Mol Hum Reprod 6(4): 375-81.

Shelton, J. M., M. H. Lee, et al., 2000. Microsomal triglyceride transfer protein expression during mouse development. J Lipid Res 41(4): 532-7.

Sosa, C., F. Althabe, et al., 2004. Bed rest in singleton pregnancies for preventing preterm birth. Cochrane Database Syst Rev(1): CD003581.

Spong, C. Y., 2007. Prediction and prevention of recurrent spontaneous preterm birth. Obstet Gynecol 110(2 Pt 1): 405-15.

Stegemann, H. and K. Stalder, 1967. Determination of hydroxyproline. Clin Chim Acta 18(2): 267-73.

Steiglitz, B. M., D. R. Keene, et al., 2002. PCOLCE2 encodes a functional procollagen C-proteinase enhancer (PCPE2) that is a collagen-binding protein differing in distribution of expression and post-translational modification from the previously described PCPE1. J Biol Chem 277(51): 49820-30.

Straach, K. J., J. M. Shelton, et al., 2005. Regulation of hyaluronan expression during cervical ripening. Glycobiology 15(1): 55-65.

Taipale, J., K. Miyazono, et al., 1994. Latent transforming growth factor-beta 1 associates to fibroblast extracellular matrix via latent TGF-beta binding protein. The Journal of cell biology 124(1-2): 171-81.

Takaluoma, K., M. Hyry, et al., 2007. Tissue-specific changes in the hydroxylysine content and cross-links of collagens and alterations in fibril morphology in lysyl hydroxylase 1 knock-out mice. J Biol Chem 282(9): 6588-96.

Taylor, P. (1986). Practical Teratology. Academic Press, London.

Theodossiou, T. A., C. Thrasivoulou, et al., 2006. Second harmonic generation confocal microscopy of collagen type I from rat tendon cryosections. Biophysical journal 91(12): 4665-77.

Timmons, B., M. Akins, et al., 2010. Cervical remodeling during pregnancy and parturition. Trends Endocrinol Metab 21(6): 353-61.

Timmons, B. C., A. M. Fairhurst, et al., 2009. Temporal changes in myeloid cells in the cervix during pregnancy and parturition. J Immunol 182(5): 2700-7.

Timmons, B. C. and M. Mahendroo, 2007. Processes regulating cervical ripening differ from cervical dilation and postpartum repair: insights from gene expression studies. Reprod Sci 14(8 Suppl): 53-62.

Timmons, B. C. and M. S. Mahendroo, 2006. Timing of neutrophil activation and expression of proinflammatory markers do not support a role for neutrophils in cervical ripening in the mouse. Biol Reprod 74(2): 236-45.

Timmons, B. C., S. M. Mitchell, et al., 2007. Dynamic changes in the cervical epithelial tight junction complex and differentiation occur during cervical ripening and parturition. Endocrinology 148(3): 1278-87.

Uldbjerg, N., G. Ekman, et al., 1983. Human cervical connective tissue and its reaction to prostaglandin E2. Acta Obstet Gynecol Scand Suppl 113: 163-6.

Uldbjerg, N., A. Malmstrom, et al., 1983. Isolation and characterization of dermatan sulphate proteoglycan from human uterine cervix. The Biochemical journal 209(2): 497-503.

Uldbjerg, N., A. Malmstrom, et al., 1985. The integrity of cervical collagen during pregnancy and labor. Gynecol Obstet Invest 20(2): 68-73.

van der Slot, A. J., A. M. Zuurmond, et al., 2003. Identification of PLOD2 as telopeptide lysyl hydroxylase, an important enzyme in fibrosis. J Biol Chem 278(42): 40967-72.

Varner, M. W. and M. S. Esplin, 2005. Current understanding of genetic factors in preterm birth. BJOG 112 Suppl 1: 28-31.

Virgo, B. B. and G. D. Bellward, 1974. Serum progesterone levels in the pregnant and postpartum laboratory mouse. Endocrinology 95(5): 1486-90.

Vogel, K. G. and J. A. Trotter, 1987. The effect of proteoglycans on the morphology of collagen fibrils formed in vitro. Collagen and related research 7(2): 105-14.

von Marschall, Z. and L. W. Fisher, 2010. Decorin is processed by three isoforms of bone morphogenetic protein-1 (BMP1). Biochem Biophys Res Commun 391(3): 1374-8.

Walchli, C., M. Koch, et al., 1994. Tissue-specific expression of the fibril-associated collagens XII and XIV. Journal of cell science 107 (Pt 2): 669-81.

Warren, J. E. and R. M. Silver, 2009. Genetics of the cervix in relation to preterm birth. Semin Perinatol 33(5): 308-11.

Warren, J. E., R. M. Silver, et al., 2007. Collagen 1Alpha1 and transforming growth factor-beta polymorphisms in women with cervical insufficiency. Obstet Gynecol 110(3): 619-24.

Watson, R. B., D. F. Holmes, et al., 1998. Surface located procollagen N-propeptides on dermatosparactic collagen fibrils are not cleaved by procollagen N-proteinase and do not inhibit binding of decorin to the fibril surface. J Mol Biol 278(1): 195-204.

Wenstrup, R. J., J. B. Florer, et al., 2004. Type V collagen controls the initiation of collagen fibril assembly. The Journal of biological chemistry 279(51): 53331-7.

Wenstrup, R. J., S. M. Smith, et al., 2011. Regulation of Collagen Fibril Nucleation and Initial Fibril Assembly Involves Coordinate Interactions with Collagens V and XI in Developing Tendon. The Journal of biological chemistry 286(23): 20455-65.

Werner, E. F., C. S. Han, et al., 2010. Universal cervical length screening to prevent preterm birth: a cost-effectiveness analysis. Ultrasound Obstet Gynecol.

Westergren-Thorsson, G., M. Norman, et al., 1998. Differential expressions of mRNA for proteoglycans, collagens and transforming growth factor-beta in the human cervix during pregnancy and involution. Biochim Biophys Acta 1406(2): 203-13.

Williams, R. M., W. R. Zipfel, et al., 2005. Interpreting second-harmonic generation images of collagen I fibrils. Biophys J 88(2): 1377-86.

Winkler, M. and W. Rath, 1999. Changes in the cervical extracellular matrix during pregnancy and parturition. J Perinat Med 27(1): 45-60.

Word, R. A., X. H. Li, et al., 2007. Dynamics of cervical remodeling during pregnancy and parturition: mechanisms and current concepts. Semin Reprod Med 25(1): 69-79.

Wu, H., M. H. Byrne, et al., 1990. Generation of collagenase-resistant collagen by site-directed mutagenesis of murine pro alpha 1(I) collagen gene. Proceedings of the National Academy of Sciences of the United States of America 87(15): 5888-5892.

Wu, Y., Y. Leng, et al., 2009. Scanning all-fiber-optic endomicroscopy system for 3D nonlinear optical imaging of biological tissues. Opt Express 17(10): 7907-15.

Yamaguchi, Y., D. M. Mann, et al., 1990. Negative regulation of transforming growth factor-beta by the proteoglycan decorin. Nature 346(6281): 281-4.

Yan, Q. and E. H. Sage, 1999. SPARC, a matricellular glycoprotein with important biological functions. J Histochem Cytochem 47(12): 1495-506.

Yang, Z., T. R. Kyriakides, et al., 2000. Matricellular proteins as modulators of cell-matrix interactions: adhesive defect in thrombospondin 2-null fibroblasts is a consequence of increased levels of matrix metalloproteinase-2. Mol Biol Cell 11(10): 3353-64.

Yu, S. Y., C. A. Tozzi, et al., 1995. Collagen changes in rat cervix in pregnancy--polarized light microscopic and electron microscopic studies. Proc Soc Exp Biol Med 209(4): 360-8.

Zutter, M. M. and S. A. Santoro, 1990. Widespread histologic distribution of the alpha 2 beta 1 integrin cell-surface collagen receptor. The American journal of pathology 137(1): 113-20.